Neal Scheraga

Epigenetics of Marine Stickleback:

Gene Expression Across a Latitudinal Gradient

UNIVERSIDADE DO ALGARVE

Faculdade de Ciências e Tecnologia

2019

Neal Scheraga

Epigenetics of Marine Stickleback:

Gene Expression Across a Latitudinal Gradient

Mestrado em Biologia Marinha

Supervisors:

Dr. Lisa Shama, Alfred Wegener Institute (Germany)

Dr. Rita Castilho, Universidade do Algarve (Portugal)

UNIVERSIDADE DO ALGARVE

Faculdade de Ciências e Tecnologia

2019

Epigenetics of Marine Stickleback:

Gene Expression Across a Latitudinal Gradient

Declaração de autoria de trabalho

Declaração de autoria de trabalho. Declaro ser o autor deste trabalho, que é original e inédito. Autores e trabalhos consultados estão devidamente citados no texto e constam da listagem de referências incluída.

Assinado;

Neal Scheraga

Assinado;

Neal Scheraga

Abstract

Epigenetic mechanisms underlying phenotypic plasticity can be an important factor in the survival of a fish species through a changing climate or in migrating to a new habitat. The threespine stickleback (*Gasterosteus aculeatus*) is found throughout the northern hemisphere and can adapt via genetic change in relatively few generations to new environments. Epigenetic mechanisms work faster than genetic change, and have the potential to be passed on to future generations, possibly leading to population-wide changes in gene expression and phenotypic variation. To study genes involved in epigenetic mechanisms in stickleback, populations were selected for sampling between Northern Germany and northern Norway. Eleven populations of stickleback were successfully sampled across this latitudinal gradient, and four evenly distributed populations were selected for gene expression analyses in this research. Collected samples were dissected for gonads and pectoral fin muscle (in addition to other organs) and brought to the Alfred Wegener Institute where RNA was extracted. After converting RNA into cDNA, a targeted qPCR approach was performed to test for expression levels of a number of epigenetic actors; DNMT1, DNMT3ab, TET1, TET3, MacroH2A, and Sirtuin2. DNMTs are involved in promoting methylation, TETs actively demethylate cytosine, and MacroH2A and Sirtuin2 are actively involved in cold acclimation.

Results from the fieldwork sampling found that stickleback body size (measured as standard length) decreased as latitude increased, in opposition to Bergmann's rule of species increasing in size toward the poles. Additionally, there was evidence for slight sexual dimorphism in which males were significantly smaller than females across all populations. Furthermore, gravid females were found to be significantly larger than non-gravid females. Results from the target gene qPCR testing found Sirtuin2 to be more expressed in female gonads of northern populations than in southern populations. This is in line with Sirtuin´s role in cold acclimation which would be more beneficial to northern than southern populations. Male gonads showed higher expression of DNMTs and TETs, possibly indicating greater plasticity of epigenetic actors capable of change. This thesis project is the first to study epigenetic differences in fish populations across a latitudinal gradient. Future research could benefit from increasing the

sample size (number of individuals and populations) and/or investigating alternative organs that may also show differential gene expression of epigenetic actors.

Overall, epigenetic mechanisms are likely to be differentially expressed depending on factors of organ, sex, population, and local environmental factors, all of which can potentially allow greater adaptive potential under climate change.

Keywords: Epigenetics, Threespine Stickleback, Gene expression, Latitudinal variation

Resumo

O stickleback de três espinhos é um peixe teleósteo encontrado circunglobalmente e é uma espécie modelo em ecologia evolutiva, pois é conhecido por se adaptar em poucas gerações em relação a outras espécies de peixes. Um dos mecanismos usados para se adaptar a ambientes em mudança é através da plasticidade fenotípica por mecanismos epigenéticos. A adição de um grupo metilo à citosina é conhecida como metilação do ADN, e tem o potencial de causar mudanças rápidas em resposta a estímulos ambientais, tais como mudanças na temperatura ou salinidade. A metilação pode ser transmitida aos descendentes, dando a este mecanismo o potencial para produzir mudanças em toda a população de gerações sucessivas. A metilação pode ser criada por metiltransferases de DNA como DNMT1 e DNMT3ab, e removida por proteínas de translocação Ten-eleven como TET1 e TET3. A aclimatação a frio é a capacidade de um organismo de se adaptar a baixas temperaturas, uma característica particularmente útil na sobrevivência em altas latitudes, caracterizadas por temperaturas de água mais baixas. Os genes potencialmente envolvidos na aclimatação a frio incluem MacroH2A e Sirtuin2 que, além desta função, desempenham outras como a modificação da histona e o metabolismo regulador. A aclimatação térmica e a capacidade de um organismo de regular a temperatura é interessante porque cenários futuros de mudança climática prevêem aquecimento, e a capacidade de um organismo para se adaptar a esta mudança pode determinar a sobrevivência de uma população.

Para estudar o papel potencial dos mecanismos epigenéticos na adaptação local das populações de três espinhos de stickleback, foi realizado um trabalho de campo para recolher amostras de tecido de stickleback em 11 locais diferentes ao longo das costas do Mar do Norte e

da Noruega. A primeira metade do trabalho de campo foi um "loop sul" que ocorreu entre 6 e 28 de Maio de 2019, partindo e regressando ao Instituto Alfred Wegener em List auf Sylt, Alemanha. A rota seguida foi, sucessivamente: de List auf Sylt, Alemanha para Marianger, Dinamarca; Oslofjord, Haugesund, Bergen, Ålesund, Trondheim, Noruega; e finalmente de volta para List auf Sylt, Alemanha. O Stickleback foi capturado com sucesso por rede de cerco em Oslofjord, Haugesund, Bergen e Trondheim na Noruega, por armadilhas do tipo covo em Mariangerfjord, Dinamarca, e por puça em List auf Sylt, Alemanha. A segunda metade do trabalho de campo foi o "loop norte" que ocorreu entre 3 e 20 de junho de 2019, saindo e retornando da Universidade Nord em Bodø, Noruega. A rota geral seguida foi: de Bodø para Vesterålen, Tromsø, Alta, Mo i Rana (NO), e de volta para Bodø. O Stickleback foi capturado com sucesso por armadilhas do tipo covo em Bodø e Vesterålen, e por puça em Alta e Mo i Rana. Por último, foi feita uma curta viagem até Limfjord, Dinamarca, para amostragem de uma população de stickleback com rede de cerco. Finalmente, 305 indivíduos foram capturados, em 11 populações separadas, com cerca de 30 indivíduos capturados em cada local. O stickleback mostrou ser abundante no Atlântico nordeste e apenas dois dos locais, Ålesund e Tromsø, não computaram stickleback. Os resultados da amostragem de stickleback apresentaram uma tendência de diminuição do comprimento padrão com o aumento da latitude. Esta situação é contrária à regra de Bergmann, que afirma que os organismos aumentam de tamanho em altas latitudes. A tendência encontrada pode ser devido a uma variedade de fatores, como regimes térmicos, luz solar, disponibilidade de nutrientes e complexidade do ecossistema. O comprimento do dorso do stickleback diferiu por sexo e mostrou dimorfismo sexual, com os machos sendo consistentemente mais curtos que as fêmeas. Além disso, as fêmeas portadoras de ovos eram maiores do que as fêmeas sem ninhadas desenvolvidas.

O comprimento padrão do stickleback de três espinhos foi medido, fotografado e foram dissecados gônadas, músculo peitoral, pele, cérebro e brânquias. O dorso do stickleback foi classificado por gênero somente após a identificação visual de suas gônadas. O stickleback feminino foi designado "gravid female" se seus ovários contivessem óvulos totalmente desenvolvidos e esses óvulos fossem segurados frouxamente ou livremente suspensos na cavidade corporal. Todas as dissecações seguiram o procedimento idêntico de eutanásia por

corte preciso da medula espinhal, e amostras de órgãos foram colocadas em tubos Eppendorf contendo RNAlater, rotulados, armazenados em uma criobox, e levados de volta ao Alfred Wegener Institute. No laboratório, as amostras de gônadas e tecido muscular peitoral tiveram o seu RNA extraído utilizando um kit de ADN/RNA da Qiagen® AllPrep™ e as extrações foram normalizadas para conter pelo menos 10 nanogramas por microlitro de RNA. Onze populações tiveram amostras de tecido recuperadas, mas apenas quatro locais foram selecionados para serem usados na análise de expressão gênica para este estudo. Sylt (DE), Bergen, Mo i Rana, e Alta, (NO) foram selecionados porque representavam o comprimento total do gradiente latitudinal desde o Mar do Norte até o extremo norte do Oceano Atlântico. Isso foi feito para aumentar a probabilidade de detecção de diferenças de expressão gênica usando populações o mais afastadas possível.

Index

Abstract……i
Resumo……ii
Index……v
Index of Figures……vi
Index of Tables……ix
Abbreviations, acronyms, symbols……x
1 - Introduction……1
1.1 - Climate Change and the Future of Stickleback……1
1.2 - Marine and Freshwater Stickleback Ecotypes……3
1.3 Genetic Adaptations……6
1.3.1 - Lateral Plate Adaptations……6
1.3.2 - Pelvic Girdle and Spine Adaptations……8
1.4 - Threespine Stickleback Biogeography……9
1.5 - The North Sea and Norwegian Sea: Past, Present, and Future……11
1.6 - Epigenetic Mechanisms of Stickleback Divergence……14
1.7 - Temperature and Stickleback……18
1.8 - Epigenetic Actors Potentially Influencing Thermal Adaptation……22
1.8.1 DNMT……22
1.8.2 TET……23
1.8.3 MacroH2A……23
1.8.4 Sirtuin……24
2 - Materials and Methods……25
2.1 - Field Sampling in Germany, Denmark, and Norway……25
2.1.1 - Dissection of Samples……32
2.1.2 - RNA Extraction……35
2.2 - Gene Expression assays using Quantitative Real Time PCR……35
2.2.1 - Housekeeping Gene Validation Tests……36
2.2.2 - Target Genes Validation Tests……38
2.2.3 - qPCR of Target Genes……39
2.2.4 - Data analysis……41
3 - Results……42
3.1 - Field sampling of Temperate to Arctic Stickleback Populations……42
3.2 - Sea surface temperature and stickleback body size across a latitudinal gradient……47
3.3 - Target Gene Expression……49
3.3.1 - DNMT1……50
3.3.2 - DNMT3ab……52
3.3.3 - TET1……55
3.3.4 - TET3……58
3.3.5 - MacroH2A……61
3.3.6 - Sirt2……63
4 – Discussion……66

4.1 Stickleback Populations Across a Latitudinal Gradient……67
4.2 Sex-specific and Site-specific Expression of Epigenetic Genes……69
5 – Conclusion……73
6 – Acknowledgments……75
7 – References……75
8 – Annex……86
8.1 Housekeeping Gene Expression……86
8.2 Target Genes Site by Sex Plot ……89
8.3 Target Gene Sequences……96

Index of Figures

Figure 2.1. Map of the route of the “southern loop” of the stickleback sampling fieldwork.

Figure 2.2. Map of the route of the “northern loop” of the stickleback sampling fieldwork.

Figure 2.3. Location of the captured Sylt stickleback population.

Figure 2.4. Location of the captured Bergen stickleback population.

Figure 2.5. Location of the captured Mo i Rana stickleback population.

Figure 2.6. Location of the captured Alta stickleback population.

Figure 2.7. An image of a threespine stickleback immediately before dissection.

Figure 2.8. The cuts required for stickleback tissue dissection.

Figure 2.9. The V-shaped cuts required for dissecting the brain.

Figure 2.10. Box plot of median (and range) of Ct values for 18S and 18SRNA housekeeping gene validation tests prior to the experiment.

Figure 2.11. Example of a good melting curve showing that DNMT1_1 passed validation.

Figure 2.12. Example of a good amplification curve showing that DNMT1_1 passed validation.

Figure 3.1. Map of all threespine stickleback locations sampled.

Figure 3.2. The average February and August 2019 ocean temperatures at each sampled location.

Figure 3.3. Box plot of median standard length (and range) of all stickleback populations sampled in order of ascending latitude.

Figure 3.4. Mean standard length (± SD) of stickleback compared between sexes using 9 sampling sites arranged with ascending latitude.

Figure 3.5. Average Ct values of 18S and 18SRNA housekeeping genes obtained during the experiment.

Figure 3.6. Box plot of median (and range) DNMT1 expression in both female and gravid female gonads for each of the four sampled populations.

Figure 3.7. Box plot of median (and range) DNMT1 expression of male pectoral muscle averaged for each of the four sampled populations.

Figure 3.8. Box plot of median (and range) DNMT1 expression of pectoral muscle tissue averaged from all sampled populations for each of the three sexes.

Figure 3.9. Box plot of median (and range) DNMT3ab expression of gonad tissue averaged from the three sexes averaged for each the four sampled populations.

Figure 3.10. Box plot of median (and range) DNMT3ab expression of pectoral muscle tissue averaged from each of the three sexes and for each the four sampled populations.

Figure 3.11. Box plot of median (and range) DNMT3ab expression of male pectoral muscle for each of the four sampled populations.

Figure 3.12. Box plot of median (and range) TET1 expression of gonad tissue averaged from each of the three sexes for each the four sampled populations.

Figure 3.13. Box plot of median (and range) TET1 expression of gravid female gonads averaged for each of the four sampled populations.

Figure 3.14. Box plot of median (and range) TET1 expression of pectoral muscle tissue averaged from the three sexes and for each the four sampled populations.

Figure 3.15. Box plot of median (and range) TET1 expression of female pectoral muscle tissue averaged for each of the four sampled populations.

Figure 3.16. Box plot of median (and range) TET1 expression of male pectoral muscle tissue averaged for each of the four sampled populations.

Figure 3.17. Box plot of median (and range) TET3 expression of female gonads averaged for each of the four sampled populations.

Figure 3.18. Box plot of median (and range) TET3 expression of gravid female gonads averaged for each of the four sampled populations.

Figure 3.19. Box plot of median (and range) TET3 expression of pectoral muscle tissue averaged for all sexes for each of the four sampled populations.

Figure 3.20. Box plot of median (and range) TET3 expression of pectoral muscle tissue averaged from each of the three sexes for each the four sampled populations.

Figure 3.21. Box plot of median (and range) TET3 expression of female pectoral muscle averaged for each of the four sampled populations.

Figure 3.22. Box plot of median (and range) MacroH2A expression of gonads averaged from the four sampled populations for each of the three sexes.

Figure 3.23. Box plot of median (and range) MacroH2A expression of pectoral muscle tissue averaged from the four sampled populations for each of the three sexes.

Figure 3.24. Box plot of median (and range) Sirt2 expression of gonads from all sites for each of the three sexes.

Figure 3.25. Box plot of median (and range) Sirt2 expression of female gonads averaged for each the four sampled populations. Populations are ordered on the x-axis with increasing latitude.

Figure 3.26. Box plot of median (and range) Sirt2 expression of pectoral muscle tissue averaged from all four sampled populations for each of the three sexes.

Figure 3.27. Box plot of median (and range) Sirt2 expression of pectoral muscle tissue averaged from all sexes for each of the four sampled populations.

Figure 8.1. Box plot of median (and range) 18S expression averaged over gonads for all sexes across the four sampled populations.

Figure 8.2. Box plot of median (and range) 18S expression in gonads for all sampled populations between the three sexes.

Figure 8.3. Box plot of median (and range) 18SRNA expression averaged over pectoral muscle for all sexes across the four sampled populations.

Figure 8.4. Box plot of median (and range) 18SRNA expression in pectoral muscle tissue for all sampled populations between the three sexes.

Figure 8.5. Box plot of median (and range) DNMT1 expression averaged over gonads for all sexes for each of the four sampled populations.

Figure 8.6. Box plot of median (and range) DNMT1 expression averaged over pectoral muscle for all sexes for each of the four sampled populations.

Figure 8.7. Box plot of median (and range) DNMT3ab expression averaged over gonads for all sexes for each of the four sampled populations.

Figure 8.8. Box plot of median (and range) DNMT3ab expression averaged over pectoral muscle for all sexes for each of the four sampled populations.

Figure 8.9. Box plot of median (and range) TET1 expression averaged over gonads for all sexes for each of the four sampled populations.

Figure 8.10. Box plot of median (and range) TET1 expression averaged over pectoral muscle for all sexes for each of the four sampled populations.

Figure 8.11. Box plot of median (and range) TET3 expression averaged over gonads for all sexes for each of the four sampled populations.

Figure 8.12. Box plot of median (and range) TET3 expression averaged over pectoral muscle for all sexes for each of the four sampled populations.

Figure 8.13. Box plot of median (and range) MacroH2A expression averaged over gonads for all sexes for each of the four sampled populations.

Figure 8.14. Box plot of median (and range) MacroH2A expression averaged over pectoral muscle for all sexes for each of the four sampled populations.

Figure 8.15. Box plot of median (and range) Sirt2 expression averaged over gonads for all sexes for each of the four sampled populations.

Index of Tables

Table 2.1. Site and GPS coordinates of the “southern loop” fieldwork.

Table 2.2. Site and GPS coordinates of the “northern loop” fieldwork.

Table 2.3. Results of validation tests for 8 candidate housekeeping genes.

Table 2.4. Standard curve efficiencies of candidate target genes during the validation tests.

Table 3.1. Sampling site locations ordered by capture date.

Table 3.2. Water temperature data of sampled locations.

Table 3.3. Number of stickleback of each sex category caught at each sampling site.

Table 3.4. ANOVA results for standard length of threespine stickleback populations testing the effects of site and three sex categories.

Table 3.5. ANOVA results for expression of DNMT1 in gonad and pectoral muscle tissue across four threespine stickleback populations and three sex categories.

Table 3.6. ANOVA results for expression of DNMT3ab in gonad and pectoral muscle tissue across four threespine stickleback populations and three sex categories.

Table 3.7. ANOVA results for expression of TET1 gonad and pectoral muscle tissue across four threespine stickleback populations and three sex categories.

Table 3.8. ANOVA results for expression of TET3 gonad and pectoral muscle tissue across four threespine stickleback populations and three sex categories.

Table 3.9. ANOVA results for expression of MacroH2A gonad and pectoral muscle tissue across four threespine stickleback populations and three sex categories.

Table 3.10. ANOVA results for expression of Sirt2 gonad and pectoral muscle tissue across four threespine stickleback populations and three sex categories.

Table 8.1. ANOVA results for expression of the housekeeping gene 18S in gonad tissue across four threespine stickleback populations.

Table 8.2. ANOVA results for expression of the housekeeping gene 18S in gonad tissue across three threespine stickleback sexes.

Table 8.3. ANOVA results for expression of the housekeeping gene 18SRNA in pectoral muscle tissue across three threespine stickleback sexes.

Table 8.4. Tukey test contrasts, multiple comparisons of means for expression of the housekeeping gene 18SRNA in pectoral muscle tissue across threespine stickleback sexes

Table 8.5. ANOVA results for expression of the housekeeping gene 18SRNA in pectoral muscle tissue across four threespine stickleback populations

Table 8.6. Target Gene Sequences

Abbreviations, acronyms, symbols

DNMT - DNA methyltransferase

TET - Ten-eleven translocation

MacroH2A - Core histone macro-H2A.1

Sirt2 - NAD-dependent deacetylase sirtuin 2

DE – Germany

DK – Denmark

NO – Norway

C_t - Cycle Threshold

ΔC_t – the difference of cycle threshold between the target gene and the housekeeping gene

SD – Standard Deviation

1. Introduction

1.1 Climate Change and the Future of Stickleback

Earth's evolutionary history can be, in part, defined by cycles of climatic warming and cooling. In the present day, excessive carbon dioxide release by humans is creating a global 'greenhouse effect' whereby temperatures are rising and species are being impacted. As of 2018, global warming has contributed to approximately a 1.0^{o}C increase in global temperatures with the possibility of a 1.5^{o}C increase between the years 2030 and 2052 (IPCC 2018 Special Report). Near the poles, temperatures have risen at least 0.6^{o} C over the last thirty years, which is double the average for the rest of the planet (IPCC 2013). Climate change will undoubtedly have cascading effects on the environment, such as melting of polar permafrost which will, in turn, release more carbon dioxide into the atmosphere (Schuur *et al.,* 2015). Other negative outcomes due to climate change are sea levels rising 0.1 meters by 2100, glaciers and the polar ice caps melting, extreme temperature fluctuations, and increased risks of drought or flooding depending on the region (IPCC 2018 Special Report). Without climate change mitigation by humans, species extinctions and ultimately a global loss in biodiversity will occur (Martin *et al.,* 2019). One study by Warren *et al.* (2013) suggested that 34 ± 7% of animals will lose over 50% of their present-day range by 2080. Indeed, an earlier review predicted that 80% of the 434 species studied will have their range and abundance shift because of the effects of climate change. Using a meta-analysis of 99 species, it was shown that their range-boundaries will shift toward the poles at a rate of 6.1 kilometers per decade (Parmesan and Yohe 2003).

Fish are particularly vulnerable to the effects of climate change because of changes in water quality, such as temperature, salinity, oxygenation, acidity, and nutrient content. Warmer oceans will have higher sea levels, be more acidic and less oxygenated (due to lower solubility of gases in warm water), become more stratified because of less water mixing, and will have lower average salinity due to changes in precipitation patterns, run-off and melting (Frost *et al.,* 2012). These critical parameters will almost certainly affect at least some marine life with local extirpations and extinction events likely throughout the oceans. In one climate scenario model

used by the Intergovernmental Panel on Climate Change, a 1.5^{o}C increase in ocean temperature will decrease the annual global fish catch by 1.5 million tonnes (IPCC 2018 Special Report). Besides overall increased mortality and lower reproduction rates, fish populations in the Northern hemisphere are predicted to move northward toward the pole in order to persist in their ideal environmental and habitat conditions. Marine fish in general have higher mobility compared to terrestrial species due to a lack of constraints of their movement, but northward range expansion for marine fish will also have its limit. Different fish species will respond to climate change in different ways, but research by Perry *et al.* (2005) found that marine fish that are capable of shifting their distribution will be those species with a faster life history and a smaller overall body size than non-shifting species.

The Family Gasterosteidae, also known as the sticklebacks, are a family of 16 species most closely related to pipefish and seahorses (Bell 1994). This family contains five genera; *Apeltes* – the fourspine sticklebacks, Culaea – the brook sticklebacks, *Pungitius* – the ninespine sticklebacks, *Spinachia* – the fifteen-spine sticklebacks, and *Gasterosteus* – the threespine sticklebacks. There are six species within the genus *Gasterosteus*, with *G. aculeatus* representing the most commonly known and best studied threespine stickleback species (hereafter referred to simply as stickleback). Stickleback (*Gasterosteus aculeatus*, Linnaeus 1758) are commonly found in marine and freshwater habitats across Europe, Asia, and North America. The earliest known fossils of threespine stickleback were found in western California, date to about 13 million years ago, and have a morphology closely resembling modern marine and anadromous stickleback (Bell *et al.,* 2009). Today, stickleback grow to an average total length of 5 cm, and typically range between 3 and 8 cm (Fuller *et al.,* 2019). Stickleback have cryptic coloration, appearing with dark brown or green hues above the lateral line, and shining silver on their underside (Fuller *et al.* 2019). Sexually mature males, however, display red undersides and bright blue eyes (Frischknecht 1993). Stickleback are predated upon by at least 68 species worldwide since they are abundant in a wide range of habitats, and are usually targeted for their small size and comparatively slow swimming speed (Reimchen 1994). Stickleback have two pelvic and three dorsal spines (giving the species its name), and rather than scales, have bony lateral plates along both sides of their torso centered on the lateral line (Walker 1996). Three main lateral plate

morphs are recognized (complete, partial and low plated), with the number of lateral plates varying within and among populations and habitats (Song *et al.*, 2010). The amount of defensive plating per population is linked to tradeoffs with mobility to evade predators versus physical defenses to survive an attack (Bergstrom 2002).

Stickleback are one of the most widely used model species in ecology and evolution. Ancestral stickleback populations lived in the Pacific Ocean, spread to the Arctic and then the Atlantic Ocean during the last inter-glacial period (Fang et al., 2018). Throughout their range, ancestral marine populations colonized brackish and freshwater aquatic environments, resulting in one of the best natural experiments to investigate mechanisms of parallel evolution (Rundle *et al*., 2000). Stickleback are highly variable in morphology depending on the environment, and can be classified as separate ecotypes within certain habitats e.g. benthic or limnetic freshwater ecotypes (Willacker *et al.,* 2010). In addition to their abundance in nature, and hence, their suitability for eco-evolutionary studies of wild populations, stickleback are also often used as a model species in laboratory experiments. They are easy to maintain in aquaria, survive well under laboratory conditions, and can be bred without much difficulty. Genetic variation between populations can occur relatively quickly and can be easily recreated in a laboratory setting, with the added benefit of designing specific lineages in which the environment of a family tree can be strictly controlled (Jones *et al.,* 2012b). In 2006, the first whole genome assembly of the threespine stickleback was completed by the Broad Institute of Cambridge, Massachusetts (Jones *et al.,* 2012). This sequencing effort led to great strides within stickleback research which continues to the present day. In this way, stickleback are similar to zebrafish (*Danio rerio*), another important fish model species whose entire genome has also been sequenced (Jones *et al.,* 2012). In addition, stickleback are a model organism in behavioural ecology, as they show large variances in mating behavior and varying levels of cooperative behaviors amongst individuals (Huntingford *et al.* 1994; Millinski *et al.* 1992).

1.2 Marine and Freshwater Stickleback Ecotypes

After the retreat of glaciers in the northern hemisphere, marine stickleback colonized new habitats including freshwater lakes and rivers. More precisely, oceanic stickleback can either live

an entirely marine life or be anadromous, with spawning occurring either in marine or freshwater, respectively (Madsen et al. unpublished data). Marine stickleback will spawn in the shallow nearshore areas of the coasts, whereas the anadromous or migratory type will spawn in the lower parts of freshwater rivers and streams (Mäkinen *et al.* 2006). Some stickleback populations diverged and adapted to an entirely freshwater existence while other populations remained anadromous. Freshwater stickleback populations typically have a lower number of lateral plates, missing or reduced spines, a smaller body size, and a fewer number of gill rakers in comparison to oceanic forms (Wantanabe *et al.* 2003). The freshwater ecotype persists in the northern hemisphere because of parallel divergence through the continuous expansion of the core marine population into lakes and rivers (Raeymaekers *et al.* 2005).

In the Transporter Hypothesis, all freshwater stickleback populations diverged from core, highly genetically differentiated marine stickleback populations (Liu *et al.* 2016). In northern Europe and western Canada, stickleback populations in freshwater lakes and streams are only as old as the waterbodies themselves, e.g. since the glaciers melted (Reusch *et al.* 2001). Molecular evidence for freshwater ecotypes being the derived ecotype comes from analyses of their microsatellites and allozymes, which were found to have lower allelic richness than their marine counterparts, which is typical of a derived population (Reusch *et al.* 2001). Additionally, rare alleles with low frequency in the founding marine populations have a better chance of being positively selected for in a freshwater-divergent population (Liu *et al.* 2016). In some cases, freshwater stickleback evolved into different allopatric mitochondrial DNA lineages (mtDNA) which occurred after the Pleistocene. For instance, Scandinavian freshwater lineages can be grouped by western, eastern, and southern types, and likely arose from differing colonization routes from different refugium (Mäkinen *et al.* 2006). Between 9-8 Kya and 4 Kya, freshwater stickleback populations in Greenland and Northern Europe declined, possibly due to the other periods of glaciation. Contrasting results on the origins of different freshwater populations have found some with an origin of multiple marine populations (Raeymaekers *et al.* 2005), whereas another freshwater group was found to be monophyletic in origin (Reusch *et al.* 2001). In most cases, marine populations have more microsatellite diversity and less differentiation due to larger population sizes and a higher rate of gene flow than freshwater populations (Mäkinen *et*

al. 2006). The high adaptive potential and durability of stickleback has enabled it to successfully thrive in all marine and freshwater habitats in and around the Northern hemisphere.

When a marine stickleback enters freshwater, over 25% of its genome can diverge in just 50 years (Nelson *et al.* 2018). Typically, reduced gene flow and divergent selection should promote local adaptation. But a theory by Samuk *et al.* (2017) states that when gene flow and divergent selection occur in tandem, this can slow adaptation because of hybridization between the source and colonized populations. This happens due to a breakdown of positive linkage disequilibrium in which locally adapted alleles are tightly genetically linked on the same chromosome or occur in a site of low recombination (Samuk *et al.* 2017). Additionally, their results suggest that gene flow may cause the usable area of the threespine stickleback's genome to shrink, which could place a constraint on future adaptation (Samuk *et al.* 2017). Suppression of the number of genes recombining while a population is diverging can determine the pattern of genetic differentiation and divergence (Nelson *et al.* 2018). Indeed, Nelson *et al.* (2018) found a negative association between genetic divergence and recombination rate. This could help preserve freshwater haplotypes during a transition to a marine environment because of reduced recombination rates (Nelson *et al.*, 2018). Additionally, freshwater chromosome sequence diversity was found to be higher than their marine relatives. Nelson *et al.* (2018) concludes that these genomic patterns reflect the strong population structure of freshwater stickleback which fortifies them against recombination with marine chromosomes. While the freshwater ecotype is better adapted at preserving their individual genetic identity, marine stickleback appear more susceptible to genetic recombination, and can, theoretically, adapt to climate change in novel ways (Nelson *et al.*, 2018).

Gene flow is thought to homogenize most marine populations due to a higher frequency of migrants flowing between adjacent stickleback populations (Caldera and Bolnick 2008). Despite this uniformity, the genetic diversity of intermixing populations will increase over time as the frequency of allele exchange rises and more random mutations are passed on (Caldera and Bolnick 2008). This increased gene flow has also resulted in marine populations becoming the foundational stable genetic lineage from which freshwater populations have diverged (Reusch *et al.* 2001). In the "isolation by distance" theory, genetic isolation increases as distance to another

population increases because it creates reproductive isolation and a lack of gene flow (Reusch *et al.,* 2001). Through this model, brackish or estuarine stickleback have higher gene flow than freshwater populations because they will be closer to an ubiquitous marine population. Freshwater stickleback will only diverge once they are blocked by a barrier to dispersal that leads to reproductive isolation (Kristjánsson 2005). The rate of migration into a freshwater source depends on abiotic factors of the watershed such as the slope of the channel, flow rates, altitude, waterfalls, and man-made obstacles (Caldera and Bolnick 2008). Freshwater ecotypes suffer from the "founder effect": reduced genetic diversity because the population arose from a genetically limited number of stickleback. This can result in higher inbreeding, more genetic drift, and a higher risk of extirpation than that in marine populations.

1.3 Genetic Adaptations

1.3.1 Lateral Plates

Lateral dermal plates are a defensive adaptation that threespine stickleback developed to resist penetrating attacks, enlarge their body size, and increase the difficulty of being swallowed (Song *et al.* 2010). These plates are anisotropic, body conforming, porous, and comprised of acellular lamellar bone (Song *et al.* 2010). An interlocking mechanism links the armored plates to the pelvic girdle and the basal plate of the spines for added protection (Song *et al.* 2010). Marine stickleback typically have over 30 plates while freshwater stickleback have less than 10, including some ecotypes that lack plates completely (Hansson *et al.* 2016). There are also partial plate morphs, often residing in brackish water, where fish have an intermediary set of between 10 and 30 lateral plates (Hansson *et al.* 2016). The number of lateral plates is highly heritable in all three morphological variations, and each variation of plate number can arise independently in geographically isolated populations (Loehr *et al.* 2012). Hypotheses for the reduction in number of plates in freshwater include predator-prey dynamics, swimming agility and buoyancy, changes in osmoregulation, limited nutrient availability, and energy allocation to growth and development rather than to dermal plates (Wiig *et al.* 2016).

The development of lateral plates is controlled by numerous genes, the most dominant of which is the ectodysplasin A (*Eda*) gene on chromosome IV (Wiig *et al.* 2016). This gene

encodes a signaling protein which is also central to growth and development of the skeleton, skin, and teeth (O'Brown *et al.* 2015). *Eda* is a recessive gene which has been associated with a reduction in total plate counts in homozygous (aa) freshwater populations (Wiig *et al.* 2016). Homozygous (AA) sticklebacks are commonly found saltwater with full plating, whereas heterozygous fish (Aa) found in brackish water have only partial plating. Research by O'Brown *et al.* (2015) found that low-plated freshwater stickleback have a specific T to G base pair change in the Eda enhancer *Wnt*. The *Wnt* gene signals early proliferation and specification of tissues but also affects *Eda* expression (O'Brown *et al.* 2015). Results from this study found that the T to G base pair change decreases *Wnt* responsiveness, decreasing *Eda* expression, ultimately reducing the number of lateral plates. When *Eda* was mutated in its coding region, fish had a complete loss of plates and partial loss of fins and teeth (Iida *et al.* 2014). However, the T to G change has been shown to lower plate count in stickleback without removing plates, fins, or teeth. This suggests that a nucleotide mutation could be one of the only ways genetically to reduce lateral plate number while still preserving the other important functions of the *Eda* gene (O'Brown *et al.* 2015). There is also evidence from other species that *Eda* is involved in the development of ectodermal structures such as hair, feathers, teeth, and sweat glands (Zhang *et al.,* 2018). Disruptions to this gene can lead to hair loss, abnormal feathers or teeth, and even the removal of sweat glands (Zhang *et al.,* 2018). Harris *et al.,* (2008) found that the *Eda* signaling pathway has an ancestral role in growth of the fish skeleton, and that changes in the functions of these genes will also lead to changes in morphology (Harris *et al.,* 2008)

Predator – prey dynamics play a large role in driving the evolutionary changes associated with the loss of lateral plates in freshwater stickleback populations (Reimchen 1994). While spine length can help stickleback avoid predation entirely, the robustness of the dermal plates often allow it to survive the encounter. Research by Marchinko (2009) found that aquatic insect predation on freshwater stickleback resulted in a reduction of armored plates. One reason is that a higher number of lateral plates can reduce fish speed and velocity, thereby making them easier for a predator to catch (Bergstrom 2002). A heavier body will require a higher energy expenditure to move, and predators will usually have more success capturing a fish encumbered by heavy plating. Additionally, it is possible that a predator can indirectly select for lateral plate number

when taking advantage of other another trait, such as the length of spines or slower growth rates (Miller *et al.,* 2017). Longer spines in stickleback could be a disadvantage if it allows predatory insects the ability to grab onto the spines. If longer spines are correlated with higher numbers of lateral plates, then predators with grabbing ability could indirectly lower the number of plates (LeRouzic *et al.,* 2011). Total growth of stickleback can be lower if more energy is allocated to developing lateral plates (Marchinko 2009). Slower growth could extend the juvenile phase or stunt maximum growth, increasing the likelihood of an early death from predation. Thus, the degree to which armored plating can benefit stickleback fitness will depend on the heritability of the traits and the selective pressures of the environment (Bergstrom 2002).

1.3.2 Pelvic Girdle and Spine Adaptations

Marine threespine stickleback have a sturdy pelvic girdle made of dermal bone which is connected to two adjacent pelvic spines. The pelvic girdle is used to strengthen the body and to increase size to avoid predation by gape-limited predators (Ostlund-Nilsson *et al.* 2006). The pelvic spines are set on a hinge which can be raised or lowered depending on the impeding threat level. Through parallel evolution, many freshwater stickleback populations have either reduced their pelvic girdle or completely lost it (Bell *et al.,* 1993). A leading theory suggests that when predation by fish and birds is strong, the pelvic girdle will become more robust and the pelvic spines will lengthen (Marchinko 2009). When stickleback populations are threatened by high predation by insects, the whole apparatus could be reduced or lost (Miller *et al.* 2017). Pelvic spines can pierce the soft tissue on the mouths of birds and fish, and an enlarged body can aid in preventing oral ingestion. Insect predators avoid swallowing whole fish by grabbing onto the spines and then ingest the fish piece by piece (Chan *et al.,* 2010). Because fish predation is a strong selective factor in the ocean, genes are continuously passed on that support a strong pelvic apparatus in marine stickleback. Predation by insects is not a factor in the oceans as much as in inland lakes and rivers, which is evidence for why pelvic girdle reduction is only found in freshwater stickleback populations (Marchinko 2009). In the “calcium limitation hypothesis” by Klepaker *et al.* (2013), it is suggested that freshwater stickleback juveniles have a survival benefit when calcium concentrations in the water are low because it enables them to grow and develop faster without the need to produce extra dermal bone. The reduction of pelvic defense elements

have been associated with reductions in lateral plate number in some stickleback populations, suggesting that these processes evolved under similar selection pressures (Klepaker *et al.* 2013)

Genetically, reduction of the pelvic region is controlled by expression of the Pituitary homeobox 1 locus (*Pitx1*) at the telomeric end of linkage group 7, and has the accompanying *Pel* enhancer (Chan *et al.* 2010). This can occur with a single deletion which removes the enhancer and cripples pelvic growth (Chan *et al.* 2010). Alleles for pelvic reduction arose independently in many populations of stickleback and all have deletions within the same 484 base pair genomic region where the *Pel* enhancer is located (Klepaker *et al.* 2013). Many stickleback populations with a modified pelvic region show directional asymmetry with the right side more reduced than the left (Ostlund-Nilsson *et al.* 2006). This can also be seen in mice with a null mutation on *Pitx1*, in which their hind legs are reduced on the right side more than the left (Chan *et al.* 2010). It has been suggested that this effect occurs due to compensation by *Pitx2,* which has some control over pelvic function, but not to the degree of *Pitx1* (Chan *et al.* (2010). Research by Chan *et al.* (2010) found *Pitx1* to be one of the most flexible regions of the stickleback genome due to its susceptibility to double-stranded DNA breaks and repair through nonhomologous end joining. Evidence for this extreme flexibility is the high prevalence of deletion mutations in the same genomic region across most stickleback with pelvic reduction (Shapiro *et al.,* 2004). *Pitx1* and *Pel* enhancer mutations arose from natural selection to better adapt stickleback to survive local predation, as has been shown in many freshwater populations (Shapiro *et al.,* 2004).

1.4 Threespine Stickleback Biogeography

Comparing stickleback populations from northern Germany to northern Norway offers an interesting model system to study rapid adaptation due to their recent presence in the region. Here, populations along this latitudinal gradient can be dated to roughly 12,000 years ago, coinciding with the last glacial retreat and glacial buildup around the coasts. Although they have only recently expanded into the region studied here, stickleback have a long evolutionary history beginning in the Pacific Ocean and then spreading into the Artic and Atlantic Oceans (Fang et al., 2018). A study of the biogeographical distribution of threespine stickleback found that most ancestral populations resided in the eastern Pacific Ocean from at least 137.7 thousand years ago

(Fang *et al.* 2018). For the marine clades of the Pacific, there are two main subclades: an eastern Pacific lineage on the west coast of North American, and a western Pacific lineage near Japan and the east coast of Russia. The ancestral stickleback populations in the eastern Pacific Ocean began colonizing the western Pacific Ocean between 79.7 to 37.3 thousand years ago (Fang *et al.* 2018). In Japanese waters, these two sub-lineages have become reproductively incompatible, representing the Japan Sea and Pacific Ocean clades (Ravinet *et al*. 2014). Research by Ravinet *et al.* (2014) also found that freshwater stickleback around Japan were direct descendants of the Trans-Pacific Clade and not of the Japan Sea clade. This may indicate higher adaptive potential of the Trans-Pacific Clade, which enabled it to colonize the Arctic and Atlantic Ocean areas (Ravinet *et al.* 2014). Earth's last glacial period during the Pleistocene epoch was defined by frigid temperatures and glaciation throughout most landmasses above 60^{o} N, and included the formation of a Bering Sea Land Bridge (Stroeven *et al.* 2016). Stickleback of the Pacific were only able to colonize the Atlantic after the Bering Sea opened between 110 and 11 thousand years ago (Elias *et al.,* 1996). However, there is also evidence for much earlier stickleback colonization of the Atlantic around 2 million years ago based on mtDNA linages (Orti *et al.* 1994). This ancient population did not gain a foothold in the region, probably due to population bottlenecks or extinction at the end of the late Pleistocene (Orti *et al.* 1994)

Through analyses of nuclear and mitochondrial genomes, the two major clades of threespine stickleback are the Euro-North American (ENA) and the Trans-North-Pacific clade (TNP) (Lescak *et al.* 2014). The TNP clade is found only in the Pacific Ocean whereas the ENA clade occurs both in the Atlantic and eastern Pacific Ocean. Pacific populations expanded from 150-100 Kya to 15-14 Kya, and likely had numerous migrations into refugia during glaciation events over their evolutionary history. Research by Lescak *et al.* (2014) in the Pacific Ocean found that the two clades follow the isolation-by-distance theory: TNP stickleback had fewer mtDNA haplotypes the further they occurred from the coast of Japan. These linages diverged 1.3-0.9 Mya, and all known subclades of saltwater or freshwater threespine stickleback can trace their genetic lineage back to one of these two clades. Their work also found an environmental barrier to dispersal in the Bussol Strait within the Kuril Island chain, in which the ENA haplotype was absent south of the strait. In the Aleutian Islands, Amchitka Pass was another impasse for

stickleback in which different subclades formed on opposing sides of the deep-water channel. Lescak *et al.* (2014) suggest that a lack of Pleistocene glaciation in the western Pacific allowed the TNP clade to spread more rapidly than the ENA clade, which could only colonize the area after the North American glaciers retreated. Nevertheless, there is some overlap of haplotypes where the two clades meet, resulting in admixture (Lescak *et al.,* 2014).

Euro-North American threespine stickleback were found to have two main mtDNA sub-lineages, Greenlandic and Northern European populations. Research by Liu *et al.* (2016) suggests that similar demographic history between the two stickleback sub-lineages denotes a similar evolutionary history near the rise and decline of Pleistocene glaciers. However, this does not confirm that the two populations originated from the same refugia, only that their environmental conditions were analogous. One difference between regions is that currently Greenland contains both sub-lineages, whereas in northern Europe only the Northern European lineage is present (Liu *et al.* 2016). The expansion of the Euro-North American clade began 25-20 Kya and coincided with glacial retreat. Recolonization routes into northern Europe are slightly ambiguous because the Greenlandic clade was close, but a lack of the Greenlandic clade in northern Europe suggests that this was not the path taken, perhaps because of a barrier to dispersal in the northeast Atlantic (Liu *et al.* 2016). Instead, northern expansion from southern or central European refugia remains the leading theory, in part because this would have occurred in parallel to other historical migrations of fish such as the brown trout, bullhead, grayling, and perch at the end of the last glacial maximum (Teacher *et al.* 2011). Overall, ENA stickleback show a more recent and faster expansion whereas the TNP clade is much older but expanded at a slower rate (Liu *et al.* 2016).

1.5 The North Sea and Norwegian Sea: Past, Present, and Future

Lasting from 2.588 million years ago to 11,700 years ago, the present-day Arctic Ocean, North Sea, and coasts of Norway were covered by the Eurasian Fennoscandian Ice Sheet (Soulet *et al.* 2013). This event, known as the Weichselian Glaciation, reached its peak coverage during the last glacial maximum about 24,000 years ago (Stroeven *et al* 2016). In addition to ice cover, glaciation also caused a global drop in sea levels because of the thermal contraction of seawater,

storage of water in glaciers, and "glacial isostatic adjustment"; the gravitational potential and modification of the ocean's surface in response to a fluctuating surface load (Lambert *et al.* 2013). Most research on the last glacial maximum has concluded that the present-day northern North Sea was covered by the fusion of the British and Fennoscandian Ice Sheets (Carr *et al.* 2006). Part of the present-day southern North Sea became tundra, whereas the area north of it became "Doggerland", an ancient land bridge near a glacier which eventually flooded. After the Younger Dryas period of renewed glaciation ended in 12,000 BP, the global climate warmed and the Fennoscandian Ice Sheet dissolved into a fraction of its maximum size (Borzenkova et al., 2015). The southwestern coast of Greenland was ice-free after 10-9.5 Kya and the Jutland Peninsula was clear by 14 Kya (Liu *et al.* 2016). In the North Sea, the northern glacial bridge was broken, the British and Fennoscandian Ice Sheets separated, the tundra was flooded, and the modern North Sea was formed. In Denmark, this glaciation period left many fjords such as the Marianger Fjord and the large Limfjord, which spans the entire northern Denmark region. In Norway, where glaciation was more intense, today, the majority of the coastal landscape is fjord lands (Farmer and Freeland 1983).

Today, the North Sea has a total surface area of 575,300 km^2 and a total volume of 42,294 km^3 (Ices 1983). In the North Sea, the coldest waters are typically found in the southern North Sea, and the warmest waters in the north at the entrance of the Gulf Stream (Perry *et al.,* 2005). The Gulf Stream enters the North Sea from the north as it rounds the coast of the United Kingdom and moves eastward towards northern Germany. A smaller current of Atlantic water enters the southern North Sea via the English Channel. This current is deflected north to Skagerrak, a large water way between northern Denmark and southern Norway (Hordoir *et al.,* 2013). The Norwegian Atlantic Current moves north from the North Sea bringing warm and salty water throughout the Norwegian Sea (Christensen *et al.,* 2018). The Norwegian Coastal Current lies between the Norwegian mainland and the Norwegian Atlantic Current and carries cold, freshwater from the Baltic Sea up along western coast of Norway to the Barents Sea and the Arctic Ocean. These two currents eventually come together which forms the Norwegian Sea, with a total area of 1.1 million km^2 and a volume of over 2 million km^3 (Ices 2007). The Baltic Sea has been identified as the main supplier of freshwater to the Norwegian Coastal Current (Hordoir *et*

al., 2013), and the summer months are typically when the waters along the Norwegian coasts are the least saline. Reasons for this include wind-based Ekman transport that moves more surface freshwater of the Baltic Sea into the Norwegian current in the summer, as well as the seasonal snow and glacier melt from the Norwegian mainland (Núñez-Riboni and Akimova 2017). Importantly, there is evidence that the average temperature of the Norwegian current has increased by 1^{o}C since 1961 (Christensen *et al.,* 2018).

The Gulf Stream is responsible for the massive transport of heat to western Europe, with winter temperatures up to 10^{o}C warmer than similar latitudes in Russia and Canada (Palter 2015). The Gulf Steam plays a vital role in the hydrology of the North Sea and Norwegian Sea by bringing warm surface water from the equator up into the northern temperate region (Palter 2015). In addition to temperature transport, the Gulf Stream also brings saltier water north which mixes with the fresher northern waters that are fed by glacial and ice melt of the Arctic ocean (Rhines *et al.,* 2008). One of the most pressing outcomes of climate change is the weakening of the Gulf Stream and possible changes to the thermohalinity composition in this region. Stenevik and Sundby (2007) suggests with a medium confidence of 33-67%, that the global balance of temperature and salinity will weaken because of a warming climate. A weaker Gulf Stream current will bring a reduced amount of warm water to the North and Norwegian Seas, which will lower temperatures and could decrease the salinity of the oceans. Artic sea ice melting and glaciers melting in Norway and Greenland will likely add a large volume of freshwater into the Arctic ocean, which would be prevented from mixing if the reduction of thermohaline cycling creates a less turbulent ocean (Polyakov *et al.,* 2010). Additionally, there are effects of "albedo" creating a positive feedback loop which could speed up warming in this region. Albedo is the reflection of solar energy back to the atmosphere when coming into contact with reflective ice (Perovich *et al.,* 2007). If enough surface ice were to melt, then more solar radiation will be absorbed by the Earth and increase climate warming (Palter 2015). The extent of these effects on the temperature of the North Sea and Norwegian Sea are currently not known and difficult to determine because at least some of the temperature changes will offset each other. For example, there will be a cooling effect from a weakened Gulf Stream but a warming effect from anthropogenic causes and reduced albedo effects (Perovich *et al.,* 2007).

Increasing water temperatures will lead to decreases in the amount of dissolved oxygen in the water, leading to expansive hypotonic regions in the oceans. This is, in part, could drive the northward movement of aquatic species in which organisms seek more habitable and oxygenated conditions towards the poles (Shaffer *et al.,* 2009). In theory, the most northern populations are at the highest risk of extinction under climate change scenarios because there is less new space to migrate to in the north. Populations in the southern range are also at risk of extirpation due to living on the periphery of their optimal conditions and extremes warm temperatures (Shaffer *et al.,* 2009). However, southern populations and species will usually have a wide area north in which to shift their range, increasing their likelihood of survival in the long-term. In warmer waters, fish will suffer from oxygen-limited stress as dissolved oxygen decreases. These restrictions limit functions that require aerobic activity such as overall growth, swimming ability, and reproduction (Portner and Knust 2007). For example, Pacific salmon can be blocked from migrating upriver when the water temperature is too high due to higher aerobic costs imposed on them (Farrell *et al.,* 2008). If these higher temperatures are combined with greater difficulty in reaching spawning grounds, reproduction may be impossible, as was the case in 2004 for the Weaver Creek Sockeye population (Farrell *et al.,* 2008).

1.6 Epigenetic Mechanisms of Stickleback Divergence

Ecological epigenetics is an expanding research field due to the potential for epigenetic modifications to lead to faster phenotypic variation that genetic change (Giuliani *et al.,* 2015). With genetic change, an organism's genotype and phenotypes are modified slowly over time due to changes in the underlying DNA sequence being shaped by natural and sexual selection. While DNA sequence change occurs more slowly, it maintains a high degree of stability and is more resistant to change, whereas epigenetic modifications happen faster but are more unstable and liable to change (Richards *et al.,* 2010). Epigenetic modifications can regulate gene expression without modifying the underlying DNA sequence (Metzger and Schulte 2017). Epigenetic responses initiate chemical or structural modifications in chromatin, histone protein complexes, and sites of DNA spooling (Deichmann 2016). With genetic change, the specific order of cytosine, guanine, adenine, and thymine nucleotides are affected, and this can only occur across successive generations. Epigenetic change, however, can work much faster though effects such as

methylation of cytosines, which does not affect the underlying nucleotide structure and can occur solely based on environment stimuli (Giuliani *et al.,* 2015). Potentially thousands of CpG methylation events can occur in just 30 generations, which is typically much faster than genetic evolution (Johannes and Schmitz 2018). This rate of methylation is not only affected by the rate of new methylation events, but also resistance to demethylation (Graaf *et al.,* 2015). If environmental conditions remain stable for a long enough time, it is possible that epigenetic changes could lead to genetic evolution over time (Graaf *et al.,* 2015).

The most commonly studied epigenetic mechanism in wild population is DNA methylation. DNA methylation is the addition of a methyl group onto a cytosine nucleotide causing regulatory changes to gene expression, typically resulting in the repression of a gene (Metzger and Schulte 2018). This involves a covalent modification of cytosine that is copied during cell division at 5'-cytosine-phosphate-guanine-3' sites (CpG) by the enzyme DNA methyltransferase I (Feinberg and Fallin 2015). The vertebrate genome contains many CpG sites and heritable methylation can only occur at these dinucleotide sequences (Schübeler 2015). While contiguous regions of methylated CpG can affect gene expression, it is also possible that a single methylation can influence the regulation of a gene (Smith *et al.* 2015). This methylation is functionally involved in the repression of genetic traits, X chromosome inactivation, and the silencing of repetitive DNA (Jones 2012). DNA methylation also plays a role in differentiation of pluripotent cells, such as diverging somatic cells from stem cells (Feinberg and Fallin 2015), and methylation in the centromere is important in maintaining chromosomal stability (Jones 2012). Bisulfite (HSO_3^-) treatments are used on DNA to replace unmethylated cytosines with uracil while leaving the 5-methylcytosine intact (Schübeler 2015). Afterwards, polymerase chain reactions (PCR) are used to amplify this sequence which enables mapping of the methylated DNA even to a single base resolution (Olova *et al.* 2018). This analysis can be completed with dead cells, a limited amount of DNA, or on low quality DNA unlike more sensitive RNA or protein analyses (Schübeler 2015).

Besides DNA methylation, other epigenetic mechanisms include post-translational modifications of nucleosome proteins, and varying densities of nucleosomes and chromatin within the nucleus (Feinberg and Fallin 2015). The occurrence of an epigenetic modification is

reliant on a combination of environmental influences and existing genetic structure. Indeed, Johannes and Schmitz (2018) postulate that the malleability of the epigenome being resistant to spontaneous methylation is genetically based. Phenotypic plasticity is the ability of an organism's genome to respond to varying environmental signals (Pigliucci *et al.,* 2006). Developmental plasticity is a type of phenotypic plasticity that can occur in early development when exposed to an environmental stimulus such as changing temperature or salinity, and can cause lifelong changes in the organism (Hanson *et al.,* 2011; Bateson *et al.,* 2004). This mechanism can give the organism an early benefit to thrive in its immediate environment, but can be negative if the environmental factors it adjusted to are in flux (Hanson *et al.,* 2011). Another type of plasticity, known as phenotypic flexibility, occurs when epigenetic-induced changes to gene expression result in temporary acclimation that is reversible depending on the organism's current environment (Metzger and Schulte 2018). This type of epigenetic acclimation is more 'loosely' held by the organism and can be continually adjusted throughout the life of the organism. However, the degree of benefit the organism receives is less than with developmental plasticity (Hanson *et al.,* 2011; Metzger and Schulte 2018). Epigenetic modifications have the potential to shape future generations of an organism if the addition of a methyl group can persist through cell division, potentially leading to genetic diversification of a population and possible divergence (Metzger and Schulte 2017). This mechanism occurs because DNA methylation can maintain stability throughout meiotic cell division (gametogenesis) and embryogenesis (Fellous *et al.,* 2018), allowing future cell divisions with the retained epigenetic factor. This effect is plastic because epigenetic-induced DNA methylation can undergo reprogramming and methylation loss in two occurrences, the germline phase and in the initial embryo phase (Fellous *et al.,* 2018). This loss allows for the placement of new occurrences of methylation to be responsive to the environment and allows epigenetic modification to occur once again.

Latitudinal variation of epigenetic diversity within populations is a novel research field because climate change scenarios predict poleward movement of many species, especially marine fishes (Perry 2005). Water temperature typically decreases toward the poles, since the warmer waters of the equator receive the most direct sunlight and the poles the least. Tolerance of water temperatures is driven in large part by genetic differences between populations of a

single species (Pereira *et al.,* 2017). However, there is evidence that average ambient temperatures are also playing a role in thermal tolerance, which could be driven by epigenetic factors (Pereira *et al.,* 2017). As a recently developing field, ecological epigenetic research in wild populations is limited in general, and focused analyses of the potential relationship between epigenetic variation and latitude are even more scarce. Difficulties in studying the correlation between these two factors stems from the need to research a single species that is spread over a large enough area to potentially show epigenetic differences between subpopulations. One species that has been studied in this context is Norwegian Spruce, a boreal confer inhabiting northern Europe. A study by Yakovlev *et al.,* (2010) investigated the 'epigenetic memory' of this spruce in different regions by studying miRNA sequence length. They found that Norwegian Spruce's embryos are affected by ambient temperature at the time of development, which effects the development of its bud (Yakovlev *et al.,* 2010). In follow up research, Yakovlev *et al.* (2014) showed that temperature conditions during zygotic and somatic embryogenesis significantly changed transcriptional profiles in genetically identical Norwegian spruce trees. They proposed that the underlying mechanism may be a type of "multi-positional thermal switch" that can activate or silence certain gene pathways during embryogenesis based on ambient temperature (Yakovlev *et al.,* 2014). While it is currently unknown how an epigenetic "thermal switch" would work, modifications of histone structure, in similar ways to that of DNA methylation, could be a likely candidate (Li *et al.,* 2005; Yakovlev *et al.,* 2014).

Threespine stickleback distribution and abundance has been shaped by its ability to acclimate to a range of temperatures throughout the northern hemisphere (Bell 1994). The retreat of Pleistocene glaciers enabled stickleback to colonize further north and into colder waters, and their ability to respond to selective pressures via phenotypic plasticity has played a large role in shaping short and long-term adaptations (Foster *et al.,* 2003). Fish are ectotherms whose internal body temperatures are regulated by the temperature of their environment. Genomic DNA methylation variation is hypothesized to be the product of temperature affecting the rate of deamination of methylated cytosine, known as the "methylation-temperature-deamination-hypothesis" (Metzger and Schulte 2017). Higher body temperatures are related to reduced guanine-cytosine content because elevated temperatures increase the mutation rate of

cytosine to thymine, thus increasing the rate of deamination (Metzger and Schulte 2017). Amongst different species of fish, previous research has found higher genomic DNA methylation in polar fish compared to equatorial fish (Varriale and Bernardi 2006). For stickleback, research by Metzger and Schulte (2017) found higher occurrences of DNA methylation when stickleback were exposed to increased temperature during early juvenile development and adult acclimation. While the increase in methylation found could result from the methylation-temperature-deamination-hypothesis, it is also a possibility that the raised temperature caused a change in cellular phenotype, such as the proportion of oxidative and glycolytic muscle fibers (Metzger and Schulte 2017). Further research by Metzger and Schulte (2018) found that regulation of muscle growth can vary in response to varying temperature treatments, and this plays an important role in thermal plasticity of fitness-related traits. If these epigenetic changes can be inherited by offspring, this could increase the fitness of stickleback populations in the face of rapid climate change (Metzger and Schulte 2018). For example, Shama et al., (2016) found that expression of genes involved in mitochondrial respiration in F2 generation offspring were differentially regulated depending on the thermal environment that their mother and grandmother experienced, suggesting an underlying epigenetic mechanism of inheritance.

1.7 Temperature and Stickleback

Water temperature is a critical environmental parameter which affects fish growth, reproduction, immune response, oxidative capacity, distribution, rate of metabolism, rate of digestion, and behavior (Dietrich *et al.,* 2018; Long *et al.,* 2013). A fish species´ ability to adapt to temperature can play a major role in its distribution, as this abiotic parameter can create a natural barrier to dispersal. Beitinger *et al.,* (2000) suggest that sudden changes in ambient water temperature are a major cause of large-scale fish kills due to internal surpassing of thermal minimums and maximums. Adaption to temperature requires acclimation to not only a mean optimal temperature but also to fluctuations caused by time of day, weather, ocean currents, and seasonal differences (Huey and Bennett 1990). Diurnal fluctuations in temperature can restrict growth if the mean temperature is above the optimal temperature (e.g. too hot), and when ambient temperature is below optimal, e.g. too cold (Jobling 1997). Stochastically fluctuating environments, however, have been shown to increase growth (Shama 2017), likely

due to nonlinear and exposure time-dependent relationships between temperature and performance in ectotherms (Kingsolver et al., 2015). Marine environments are more thermally stable than freshwater due to a larger volume of water and a higher salinity, resulting in higher heat capacity. In contrast, in freshwater systems, a smaller overall water volume means that summer and winter temperatures can fluctuate faster and with greater intensity than in marine environments, which can induce mortality in organisms not suitable for these habitats, an effect exacerbated at high latitudes (Lee and Bell 1999).

Different populations of the same species can vary in a range of facets depending solely on the environmental factors in each region. For example, in research of the marine copepod, *Tigriopus californicus*, populations at different latitudes had different degrees of thermal adaptation to heat-stress (Pereira *et al.,* 2017). One study by Levine *et al.* (2010) showed that ambient temperature during rearing of the common fruit fly affects the degree of their phenotypic plasticity, with a higher plasticity in tropical populations than in temperate populations. When compared to genotype-based plasticity (genotype x environment interaction), epigenetic-based plasticity could allow organisms to adapt to local environments in fewer generations, and has been shown to be a potentially useful mechanism wielded by invasive species to colonize new territory (Herden *et al.,* 2019). Still, while epigenetic variation can alter the resistance of an organism to some degree, it cannot create massive changes which would enable the organism to survive wholly new environments. For instance, climate change may catastrophically effect species closer to the equator because those populations will already be near their physiological temperature maximum (Pereira *et al.,* 2017). Nevertheless, epigenetic and non-genetic inheritance mechanisms can facilitate fast, adaptive responses to changing environmental conditions. For instance, Zizzari and Ellers (2014) found that the water temperature during maternal rearing of offspring raised the thermal resistance for those offspring. In threespine stickleback, transgenerational plasticity in response to ocean warming resulted in relatively larger offspring if mothers were acclimated to high temperature during reproductive conditioning (Shama et al., 2014; Shama 2015).

Typically, fish development is faster in warmer temperatures and slower in cold water due to an increased metabolic rate (Gibbons *et al.,* 2017). However, average fish body size tends

to be smaller in warmer water temperatures than in cold water due to thermal energy costs involved with increasing metabolism trading off with growth (Gibbons *et al.,* 2017). Maximum growth in colder temperatures can surpass growth in warm waters, which has been theorized to be because of more energy available, lower predation, less competition, or anthropogenic factors (Fernández-Torres *et al.,* 2018). The metabolism-temperature relationship has been well studied in fish, including studies focused on the effects of short term and long term acclimation (Enders and Boisclair 2015). Metabolic rate changes annually with the seasons caused by the tilt of the Earth, and is an effect that can be seen in the analysis of e.g. otolith rings (Scartascini *et al.,* 2015). Fish growth rates typically increase during warm temperature periods (i.e. summer) and decrease when the water temperature is lower (i.e. winter). One reason this occurs is because mitochondria are affected by temperature changes, and ATP production will increase during warming but is hindered when conditions are colder (Pörtner et al., 2005). When near a thermal maximum or minimum, the ability of an organism to respire and process oxygen decreases, which hinders ATP production (Pörtner et al., 2005). In otolith rings, this is reflected by light-colored bands that expand during fast growth, and thinner, darker bands during slower periods of growth (Scartascini *et al.,* 2015). Sea temperatures at polar latitudes are colder than equatorial ocean waters, and marine life has adapted accordingly to each environment. Typically, polar fish have a slower metabolism than equatorial fish due to lower temperatures reducing the demand for oxygen (Enzor *et al.,* 2013).

Different ecotypes of stickleback have varying degrees of surviving and thriving in a range of temperatures. Early studies of stickleback thermal limitations focused on the relationship between salinity, ambient temperature and survival (Jordan and Garside 1972). Jordan and Garside (1972) found that when stickleback faced greater salinity gradient pressures, their thermal maximums suffered. They hypothesized that this was due to a limited amount of stored energy which needed to be allotted for repairing both saline damage and thermal damage. As stated above, freshwater stickleback are more likely to have to endure extreme cold and hot water temperatures, so it can be theorized that freshwater acclimation could be related to thermal resistance in some way (Beitinger *et al.,* 2000). Temperature as a selective agent could be a primary factor in determining whether marine stickleback can colonize freshwater. In

research by Gibbons *et al.,* (2017), marine stickleback suffered a significant growth reduction in extreme cold water which did not occur for freshwater stickleback. Additionally, the ability to osmoregulate could play a role in determining overall growth rates in different ecotypes due to osmoregulation using a significant portion of the fish's energy budget (Boeuf and Payan 2001). Here, epigenetic mechanisms (e.g. DNA methylation) have been shown to play an important role in shaping stickleback adaptive responses to salinity selective pressures, with consequences for their distribution and abundance in freshwater habitats (Li *et al.,* 2017). However, a comprehensive survey of epigenetic mechanisms underlying local adaptation to marine habitats with differing thermal conditions has not yet been conducted.

Many populations of marine and freshwater stickleback have evolved to withstand warmer habitats than optimal, and freshwater stickleback can also withstand colder temperatures (Barrett *et al.,* 2011). As the bridge between marine and freshwater ecotypes, anadromous colonizers of freshwater would likely need to be adapted for overwintering in cold water in order to survive the winter. While temperature alone might not necessarily be a barrier for marine stickleback, Gibbons *et al.,* (2016) suggest that size at first reproduction plays a major role in fecundity, which if diminished because of cold temperatures, could place a limit on the species' distribution. They also found that freshwater stickleback, opposed to marine stickleback, had a better tolerance of cold temperatures even after being acclimatized to similar spring temperatures. Other research found that over 5,700 genes across marine and freshwater stickleback were plastic in facilitating genetic change to factors such as temperature (Morris *et al.,* 2014). The research by Morris *et al.* (2014) found 1600 temperature-affected genes in marine stickleback and over 3300 affected genes in freshwater populations. Additionally, under future climate change conditions, warmer surface waters could make it easier for stickleback to invade new habitats without the selective pressure of low temperature. Particularly, this effect would be greatest towards the Arctic, which sits at the edge of the threespine stickleback's native range (Bell and Foster 1994).

1.8 Epigenetic actors potentially influencing thermal adaptation

Threespine stickleback, like all fish, are ectotherms who do not maintain their own body heat and instead reflect the temperature of their environment. Levels of DNA methylation are higher in fish than in endothermic mammals and birds, and this difference has been theorized, in part, because of differences in internal temperature (Varriale 2014). Higher internal temperature could cause higher deamination rates which might be responsible for the decreased methylation level patterns seen in warm-blooded vertebrates (Varriale and Bernardi 2006). Because fish conform to the temperature of their environment, studying stickleback in a wide range of latitudes is interesting because each population should have a different average temperature profile. If the oceans warm due to climate change, than a fish's ability to epigenetically adapt to thermal stress could determine survival outcomes. DNA methylation, chromatin regulation, and histone modification can work in tandem in response to temperature-related stressor (Kim *et al.* 2015). Due to DNA methylation being heritable throughout reproduction, if cold acclimation can change DNA epigenetically, then through many successive generations, there could be offspring born with already enhanced thermal resistance. Perhaps any thermal factors that influence methylation could eventually cause a population-wide phenotypic change, and ultimately affect the species as a whole (Varriale 2014).

1.8.1 DNMT

DNA methyltransferases (Dnmt) are enzymes typically responsible for the promotion of DNA methylation, and its expression can be an indicator for global DNA methylation in the organism's genome (Goll and Bestor 2005). These enzymes facilitate the addition of a methyl group to the fifth carbon atom of cytosine, and are thus, responsible for DNA methylation (Giannetto *et al.,* 2013). Levels of DNMT expression in different organs can be associated with differential gene expression or behaviors (McGhee and Bell *et al.,* 2014). Dnmt1 is a maintenance gene for DNA methylation which controls the DNA methylation pattern during replication, and can maintain preexisting methylation after DNA repair has occurred (Feng *et al.,* 2010; Zachariah and Rastegar 2012). Dnmt3a and Dnmt3b are enzymes responsible for *de novo* DNA methylation, with Dnmt3b possibly having a role in early neurogenesis (Feng *et al.,* 2010; Zachariah and

Rastegar 2012). Research has shown that the lack of Dnmt1 and Dnmt3a in brain neurons could cause synaptic plasticity issues, leading to reduced memory and learning capabilities (Feng *et al.,* 2010). In humans, reduced amounts of Dnmt decrease levels of DNA methylation, typically leading to neurological retardation through Rett Syndrome (Zachariah and Rastegar 2012). Studies have shown that Dnmt2 is not necessary for organism survival and appears to have little or no critical function (Goll and Bestor 2005).

1.8.2 TET

Ten-eleven translocation (TET) proteins in a family of TET1, 2, and 3, are the antithesis of DNMT in that they are involved with the active demethylation of DNA. TET proteins are involved in the regulation of epigenetic gene transcription, and in early-life development in embryos and stem cells (Pastor *et al.,* 2013). Besides TET, DNA can be passively demethylated due to dilution during the replication of cells (Kohli and Zhang 2013). TET, however, works in an active pathway to promote demethylation, and thus, can be more influenced by environmental factors. TET accomplishes this by first converting methylated cytosine to 5-hydroxymethylcytosine, then into 5-formylcytosine, and finally into 5-carboxylcytosine (Tahiliani *et al.,* 2009; Ito *et al.,* 2010, 2011; He *et al.,* 2011 Yang *et al.,* 2013). TET achieves this by first using oxygen to catalyze oxidative decarboxylation to convert methylcytosine into 5-hydroxymethylcytosine (Kohil and Zhang 2013). 5-hydroxymethylcytosin is a key intermediary, because it is typically found to be inversely proportional to 5-methylcytosine, and is thus, another way to predict demethylation patterns (Kohli and Zhang 2013). Once in the 5-carboxylcytosine stage, either passive dilution of the oxidized base or DNA repair enzymes in the base excisions repair pathway can remove the carboxyl group and complete demethylation (He *et al.,* 2011; Kohli and Zhang 2013).

1.8.4 MacroH2A

Histones are a family of proteins whose function in the cell is to spool DNA around itself into packaged units called nucleosomes (Zentner and Henikoff 2013). About 147 base pairs of DNA is wrapped 1.7 turns around eight core histone proteins in order to better package the long genome size of a eukaryote (Malik and Henikoff 2003; Weber and Henikoff 2014). The octamer of core histones is made up of two sets of four proteins – H2A, H2B, H3, and H4, and inside that

is a tetramer of two sets of H3 and H4 (Weber and Henikoff 2014). MacroH2A's are in the lineage of H2A, but instead of being a typical canonical histone, it is a histone variant which modifies the structure of the histone and is specific to vertebrates (Malik and Henikoff 2003). The 'macro' of MacroH2A reflects that H2A contains a connected macro segment, a nonhistone domain which is nearly 60-70% similar to H2A but increases its size to three times longer (Buschbeck *et al.,* 2009; Weber and Henikoff 2014). While macroH2As are one of the least understood histone variants, they have the largest role in organism development, morphogenesis, organ formation, general transcriptional regulation, and tumor suppression (Buschbeck *et al.,* 2009; Gaspar-Maia *et al.,* 2013). There is also evidence for macroH2A being involved with X chromosome inactivation and for preventing differentiated stem cells from differentiating again by nullifying the pluripotent genes that cause reactivation (Constanzi *et al.,* 2000; Gaspar-Maia *et al.,* 2013). Research into MacroH2A in zebrafish revealed that it plays a necessary role in embryogenesis because disruptions to it caused fatal deformations in fish structure (Buschbeck *et al.,* 2009). As a histone modifier, MacroH2A could play a role in temperature acclimatization. In the common carp, MacroH2A is more expressed in the winter and results in hypermethylation which can facilitated physiological adaptation to the lower temperatures (Pinto *et al.,* 2005).

1.8.4 Sirtuin

Sirtuins, or 'Silent Information Regulators' are core domains that either promote NAD^+ dependent histone deacetylases or are involved as an ADP-ribosyltransferase (Yamamoto *et al.,* 2007; Verdin *et al.,* 2010). These two primary functions have been heavily conserved in organisms because they play key roles in chromatin, transcriptional, and recombination silencing, cellular survival and DNA repair (Yamamoto *et al.,* 2007; Verdin *et al.,* 2010). Histone modification function controls chromatin structure and regulates gene expression, which has a role in mediating the effects of aging including the shorting of telomers (Carmins *et al.,* 2010). Sirtuins range from sirtuin1 through 7, and each have individual biological functions such as a role in cellular metabolism, insulin secretion, or DNA repair (Yamamoto *et al.,* 2007). Much research has been conducted on sirtuin 1 function in mammals and humans because of its role in cell apoptosis, cell survival, and aging, of which a better understanding could be used to treat diseases or cancer-caused tumors (Verdin *et al.,* 2010; Carmins *et al.,* 2010). This occurs because

Sirtuin 1 deacetylates p53 is responsible for initiated cell death in response to stress or damage (Verdin *et al.,* 2010; Carmins *et al.,* 2010). The relationship between Sirtuin and caloric restriction has been studied, and suggests that caloric restriction has life-extending properties because glucose metabolism and mitochondrial activity increases (Nogueiras *et al* 2012). In zebrafish, the seven Sirtuins are widely distributed across most major organs but expression can differ between tissues (Pereira *et al.,* 2011). Research into Sirtuin in fish is limited due to the much larger focus on humans, however, this will likely increase in the near future in order to gain a better understanding of fish development and survival.

In this thesis project, the main goal was to investigate potential links between thermal habitat conditions and expression of genes involved in epigenetic mechanisms potentially underlying local adaptation of marine stickleback populations across a latitudinal gradient. The project involved extensive sampling of wild stickleback populations from Germany to Norway, and used a targeted gene expression approach to gain insight into the potential for epigenetic mechanisms to promote fast adaptive responses of fish populations in the face of ongoing climate change in the Northern Atlantic and Arctic Oceans.

2. Materials and Methods

2.1 Field sampling in Germany, Denmark and Norway

Field sampling was identified in the planning phase as requiring two routes or "loops" (southern and northern) in order to maximize time and resources. Since the target samples were marine stickleback as opposed to freshwater or brackish ecotypes, the chosen sampling locations needed to have access to the ocean, contain marine flora and fauna within, have marine or near-marine salinity, and stickleback needed to have complete or nearly complete lateral plating (most indicative of a marine ecotype). Salinity and water temperature was recorded at each location using a hand-held multiparameter probe (Knick Portamess® 911 Cond). Sampling locations were reached by car, ferry or a mixture of both. Over the course of 23 days, 6500 kilometers of driving distance was completed for the southern route to reach six marine stickleback sites between

55.0°N and 63.5°N latitude. The “southern route” was from Sylt, Germany to Marianger, Denmark, and then to Norway. In Norway, the sampling locations were Oslofjord, Haugesund, Bergen, Ålesund, and Trondheim (Figure 2.1). After Trondheim, the car was driven south and returned to Sylt, Germany.

The three main pieces of fishing equipment used on the southern route were a beach seine net, dip nets, and minnow traps with bait. The beach seine net measured 15 meters in length, 1.5 meters in height, and had 10-millimeter mesh size. The fish-line attachment was the addition of four loops to the seine net which allowed for two stainless steel rods to attach at both ends. One dip net (D-shaped brailer) had a 60-centimeter width and a 6-millimeter mesh size. A second dip net had a 40-centimeter width and a 6-millimeter mesh size. Minnow traps (Three Gees Feets G-40) measured 41.91 cm in overall length, 19.05 cm diameter, and a 0.64 cm mesh size. For bait, a mix of cat food and canned fish such as tuna and mackerel was put into a plastic bag with puncture holes and placed inside the traps. Traps were tied to a fixed object on shore and set for at least 24 hours.

The southern loop (Table 2.1, Figure 2.1) began from the Alfred Wegener Institute in List auf Sylt, Germany on May 6th, 2019 and Mariangerfjord, Denmark was reached that same day. There, stickleback were caught using minnow traps attached to a dock at a marina near the coast over a two day period. Afterwards, the trip proceeded north by ferry from Hirtshals, Denmark to Larvik, Norway, and then to the town of Drøbak, south of Oslo. There, the trip was aided by the University of Oslo fieldstation at Drøbak who provided housing, food, and the use of their boat, siene net, and students to capture 30 stickleback in the bay of Sandspollen along the west coast of Oslofjord. Moving to the west coast of Norway in the Haugesund area, stickleback were found in the shallow bay of Lindovika, caught first by dip netting and then more efficiently by siene netting. Next in the Bergen area, stickleback were found to be extremely abundant and were successfully captured in the shallow bay of Straumen by seine net. The next location, Ålesund, was unsuccessful with no marine stickleback (completely plated) found, however, brackish morphs of stickleback in freshwater with reduced lateral plating were found. The trip progressed to the Trondheim area and a stickleback population was located at a boat marina near Stjørdal bay, however, only 14 individuals were successfully captured. After this site, the van was driven

back to List auf Sylt, Germany on May 28th, 2019 where a final marine stickleback population was located and captured in a tidal pool just outside the Alfred Wegener Institute in List.

Table 2.1. Site and GPS coordinates of the “southern loop” fieldwork

Site Name, (Site Region), Country	GPS Coordinates
Mariangerfjord, DK	56.656395, 9.979952
Sandspollen (Oslofjord), NO	59.665971, 10.585359
Lindonvika (Haugesund), NO	60.147081, 5.433129
Straumen (Bergen), NO	60.225057, 5.276420
Stjørdal (Trondheim), NO	63.471358, 10.893145
List auf Sylt (Sylt), DK	55.025657, 8.430818

Figure 2.1. Map of the route of the "southern loop" of the stickleback sampling fieldwork. Sylt, Germany was both the origin and the final destination of the trip.

The northern loop was sampled between June 3rd and June 20th, 2019 and culminated in 4000 kilometers of driving distance for 4 stickleback capture locations throughout central and northern Norway (Table 2.2, Figure 2.2). The trip was led by Neal Scheraga and also included support from a team from Nord University in Bodø: Prof. Dr. Joost Raeymaekers, and students Jørgen Hetzler, Camela Haddad, and Thijs Bal. On June 4th, the team drove two vehicles to Ringstad, a small fishing village in Vesterålen. The next day, a population was located in a small stream between two freshwater streams and the ocean. After catching 4 fish by dip net, minnow traps were used to catch the rest of the sample by the next day. The next destination of Tromsø failed to produce stickleback so the trip proceeded north to the city of Alta. On June 12th, a stickleback population was located in a brackish water stream in Alta bay and was deemed marine by the presence of marina fauna and flora. Next, the car drove south to Mo I Rana where stickleback were located in a tidal pool in Drevjaleira. From there, the car returned to Bodø and the final sampling site. A mutual contact had been established with a sheep farmer in the Helligvær Island chain who had confirmed the presence of stickleback in tidal pools on his land. The next day, Neal Scheraga and Joost Raeymaekers arrived on the island of Fjølvågan, retrieved the captured stickleback from the traps, and dissected them on June 18th, 2019. Neal Scheraga then returned back to Germany by plane on June 20th, 2019. The final sampling site in northern Denmark was taken on July 1st 2019 in Doverrode Marina by seine net. This was completed during a two-day trip leaving and returning from Sylt, Germany.

Table 2.2. Site and GPS coordinates of the "northern loop" fieldwork

Site Name, (Site Region), Country	GPS Coordinates
Sandstrand (Vesterålen), NO	68.745997, 15.345146
Latharistranda (Alta), NO	69.984096, 23.453836
Drevjaleira (Mo i Rana), NO	65.936303, 13.131886
Fjølvågan (Bodø), NO	67.402270, 13.862751
Doverodde Harbor (Limfjord), DK	56.717403, 8.472333

Figure 2.2. Map of the route of the "northern loop" of the stickleback sampling fieldwork. Bodø, Norway was both the origin and the final destination of the trip

Figure 2.3. Location of the captured Sylt stickleback population.

Figure 2.4. Location of the captured Bergen stickleback population.

Figure 2.5. Location of the captured Mo i Rana stickleback population

Figure 2.6. Location of the captured Alta stickleback population

2.1.1 Dissection of samples

The dissection of stickleback for tissue samples followed a standardized protocol across all sampling locations. After capture, fish were stored in 5 liter buckets of seawater from their local habitat (with an average density of 6 fish per liter of water). From the complete sample of stickleback caught at any one location, the 30 largest individuals were selected for dissection because of the desire to target adult fish and the ease of dissecting larger fish. After selection, buckets were covered by a lid and stored in a cool, dark area inside the vehicle and transported immediately to the dissection location. Sites to perform the dissections were chosen based on their close distance to the sampling site, their location indoors, and the availability of chairs and tables. At the dissecting sites, 1.5 ml Eppendorf tubes were filled with 150 microliters of Qiagen's RNA*later* – RNA Stabilization Reagent using Biosphere® 100 – 1000 microliter Filter Tips. After the tissue samples were placed in tubes, all tubes were stored in cryoboxes with a maximum capacity of 90 tubes per box. Boxes were labeled, sealed with two rubber bands and stored either in a refrigerator, or in a cool, dark place with icepacks surrounding them. At the end of each sampling loop, cryoboxes were packaged with icepacks and transported back to Sylt, Germany within one day.

All dissections were performed on a plastic tray (50 cm x 25 cm) containing a laminated measurement grid, an icepack, and a paper towel. Semperguard® latex, innercoating, powder-free, disposable gloves were worn by both dissector and assistant. The assistant was responsible for note taking, labeling the Eppendorf tubes and doublechecking that the tissue samples were fully placed into the RNA*later*. In cases where the tissue sample was too large for the volume of RNA*later,* the assistant would add a second 150 microliters to the Eppendorf tube. Using a permanent black marker, the assistant would then write the date, the code for the tissue sample type (O - ovary, T – testis, P – pectoral fin muscle, S – skin/lateral plates, B – brain, G – gills), the identification number of the fish, the designated site number, and the sex of the fish onto each tube. All information was written on top of the tube cap and then repeated on the side of the Eppendorf tube. The dissection procedure was standardized to keep the tissue sample quality

and quantity as consistent as possible across locations. Stickleback were kept alive from capture until dissection. Fish were removed from the bucket, gently dried with a paper towel, and placed on a measuring grid to record standard length (± 1 mm). Each fish was photographed on the measuring grid for future reference.

Figure 2.7. An image of a threespine stickleback immediately before dissection. Each large square measured 1 by 1 centimeter, and each small square measured 1 by 1 millimeter. Lateral plating is clearly visible along the torso.

Fish were euthanized using a precise cut severing the spinal cord between the pectoral fin and gill flap. The head was placed on ice while other tissues were dissected. A ventral cut was made from the front of the torso to the anus, and all intestines were removed. After opening the torso, the fish was sexed and each sexual organ (ovaries or testis) was individually placed into separate Eppendorf tubes. Female stickleback were designated “gravid female” if their ovaries contained fully developed eggs and these eggs were loosely held or freely suspended in the body cavity. Next, both pectoral fin muscles were removed and placed into a tube. A rectangular piece of skin, approximately 1 cm^2 , from the right side of the body was removed by four directional

cuts as seen in Figure 2.8. To remove the brain, the head was cut twice beginning from the roof of the mouth towards the back of the top of skull forming an acute angle as seen in Figure 2.9. Tweezers (90 mm) were then used to pull up on the flap of skull to reveal the brain. Lastly, the gills were removed by cutting their two attachment points from the back of the head and pulling them out with tweezers. All tissue types were stored in separate tubes (n=6 tubes per fish). Once all 6 tubes were filled with tissue samples, the dissecting area and tools were washed with 70% ethanol before proceeding to the next fish.

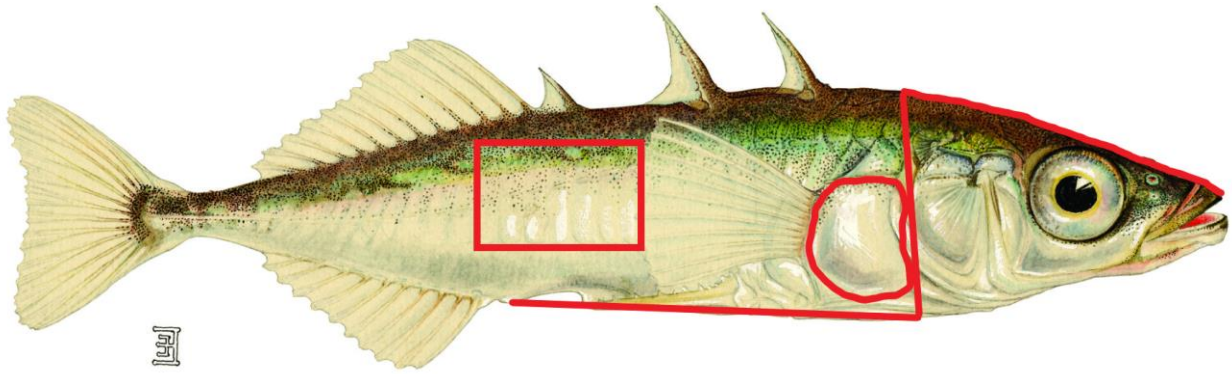

Figure 2.8. The cuts (in red) required for stickleback tissue dissection

Figure 2.9. The V-shaped cuts required for dissecting the brain

2.1.2 RNA Extraction

When tissue samples arrived at the Alfred Wegener Institute, they were immediately stored in a -80^{o}C freezer. Just prior to extraction, samples were thawed at room temperature. Pectoral fin and gonad were chosen as the target tissues for the project. From each of four populations (Sylt, Bergen, Mo I Rana, Alta), n=4 male, female, and gravid female tissue samples were extracted (n=96 extractions in total). Next, tissue samples of 5 mm^2 were placed into individual collection tubes containing 600 ml β-mercaptoethanol for lysis, and a guanidine-isothiocyanate buffer for denaturing (Buffer RLT Plus; Qiagen) and centrifuged for 3 minutes at 14,000 RPM. Together, this lysis and buffer mixture inactivates any DNases or RNases to preserve DNA and RNA. Samples were then crushed with a plastic pestle and centrifuged, and the supernatant was used for DNA/RNA extraction following the Qiagen® AllPrep™ DNA/RNA manufacturers protocol. This procedure purifies DNA and RNA from the same sample consecutively, and although this thesis focuses only on RNA, the extracted DNA was saved for future research. In short, the supernatant passes first through a "DNA Spin column" which has a filter that binds the DNA. The flow-through from this contains the RNA which, after adding ethanol, is passed through a "RNA Spin Column" which binds the RNA. After a multi-step washing process, both the RNA and DNA are eluted using RNase-Free Water and a Tris-buffered saline solution with HCL, respectively. This elution process was done twice for all samples to ensure the RNA and DNA were completely collected. However, in almost every case the first elution contained the majority of the RNA or DNA. RNA sample amounts were deemed satisfactory if they measured greater than or equal to 10 nanograms per microliter using a NanoDrop 1000 Spectrophotometer (Thermo Fisher Scientific). If the samples were below this amount, then the elutant was dried in a vacuum heater, and then re-eluted and re-evaluated. If this step failed to reach 10 ng/ul, then a second pectoral fin or gonad was used for extraction. If that step failed to produced usable RNA, then a new fish was used for both the pectoral muscle and gonad.

2.2 Gene expression assays using Quantitative Real Time PCR

RNA was converted into cDNA to be used in the targeted qPCR. For this, random primers and reverse transcriptase were used to convert RNA into single-stranded cDNA using a Qiagen Omniscript Reverse Transcription Kit. RNA extractions resulted in different amounts of purified

RNA content among samples, and each had to be diluted with RNase-Free water to reach equal concentrations among all samples. All samples were diluted to 10 nanograms per microliter of RNA solution. Following this, samples were further diluted so that exactly 13 microliters of RNA solution was created which had a total mass of 130 nanograms. Next, 7 microliters of a reverse transcriptase solution were added to facilitate the conversion into cDNA: 2 ul of 10x Buffer RT, 2 ul of dNTPs (deoxyribonucleotide triphosphate), 2 ul "random primer", and 1 ul of Omniscript Reverse Transcriptase. dNTPs are the substrate for DNA and the "random primer" hybridizes to the 3' end of the RNA tail and ensures this tail is created. The 20-microliter final solution was placed into a thermocycler (TGradient, Biometra) at 37°C for 60 minutes with a 4°C end pause until the solution was removed. Next, each cDNA solution was diluted with RNase-Free Water to 1 nanogram per microliter and placed into a refrigerator at 4 °C until use.

2.2.1 Housekeeping Gene Validation Tests

Table 2.3. Results of validation tests for 8 candidate housekeeping genes (shown as abbreviations) with average Ct values and standard deviations (SD). Bold font indicates the two housekeeping genes selected for the experiment.

	TBP	SD	EF	SD	ACTB	SD	UBC	SD
Gonad Ct	27.89	1.20	25.35	2.37	13.34	6.41	23.83	2.32
Pectoral Muscle Ct	29.36	3.08	24.06	1.17	14.57	5.00	31.27	4.53
	RPL	SD	ACTB2	SD	**18S**	**SD**	**18SRNA**	**SD**
Gonad Ct	25.86	2.42	26.51	2.65	**18.94**	**1.19**	15.37	5.45
Pectoral Muscle Ct	30.63	2.47	21.61	2.30	24.31	3.16	**10.73**	**1.53**

Eight candidate housekeeping genes were analyzed using a cDNA sample of each sex, each site, and each organ (gonad and pectoral muscle) to determine which would produce the most stable melting curves, have the correct intermediary Ct value, and the smallest standard deviation. A Ct value between 10 and 20 is considered ideal for a housekeeping gene, and a small standard deviation is necessary to limit differences between samples. 18SRNA and "18S" are both

18S ribosomal RNAs with slight differences between them, yet they are still considered housekeeping genes.

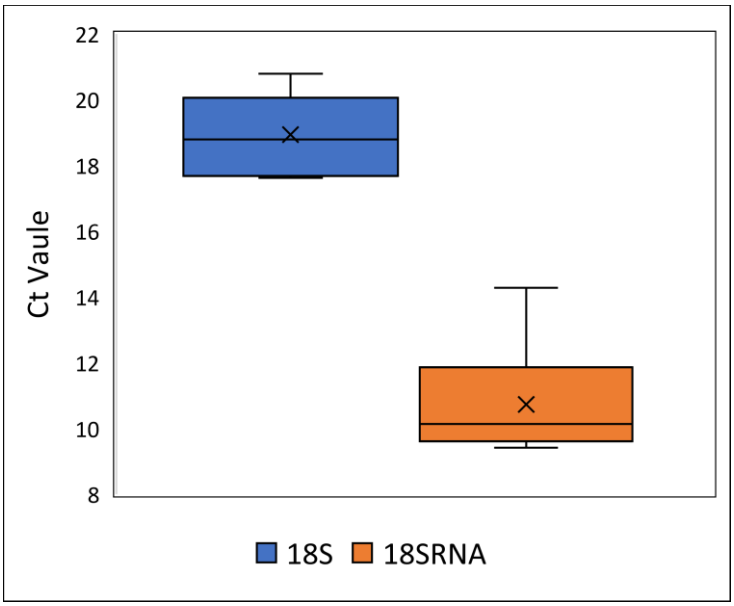

Figure 2.10. Box plot of median (horizontal line) and mean ('X' ± SD) Ct values of 18S and 18SRNA housekeeping gene validation tests prior to the experiment.

The validation of the housekeeping genes 18S and 18SRNA were tested with a mix of gonad and pectoral muscle cDNA from all sites to ensure Ct values did not vary too greatly between samples (i.e. Ct values between 10 and 20). 18S was tested using gonad cDNA (n=12 samples), and had an average Ct of 18.94, and a range of 17.68 to 20.79 cycles. 18SRNA primers were used with pectoral muscles cDNA (n=10 samples), and had an average Ct of 10.73 with a range of 9.42 to 11.93 cycles (Figure 2.10). 18S was not used on pectoral muscle since the average Ct and standard deviation was 24.31 and 3.16, respectively, both of which were too high (Table 2.3). 18SRNA was not used on gonad tissue because despite having an adequate Ct value of 15.37, its standard deviation of 5.45 was too high. The housekeeping genes were only used on their respective organs because only with those specific combinations did they have Ct values between 10 and 20, and standard deviations below 1.6. 18S and 18SRNA both had the lowest Ct values paired with the smallest standard deviations for gonad and pectoral muscle cDNA, respectively. 18S and 18SRNA were the only housekeeping genes tested that fulfilled both of these requirements for their respective tissue types. Housekeeping genes that were not selected for

the experiment were: TATA-binding protein (TBP), elongation factor protein (EF), beta-actin (ACTB) and beta-actin 2 (ACTB2), Ubiquitin C gene (UBC), and L ribosomal proteins (RPL).

2.2.2 Validation of Target Genes

Primer sequences for the target genes are shown in Annex Table 8.6. Target genes used in the experiment were also first validated to ensure that the primers would amplify the gene, and that Ct values were in the correct melting temperature range with low standard deviations. Standard curves were deemed successful when their efficiency percentage was within the range of 90% and 110%, reflecting the percentage by which the concentration increased per cycle.

Table 2.4. Standard curve efficiencies of candidate target genes during the validation tests. Bold indicates the target genes used in the experiment.

Gene	Standard Curve Efficiency %
DMNT1_1	**104.4**
DMNT1_2	131.6
DMNT3ab_1	169.2
DMNT3ab_2	**108.2**
TET1_1	146.9
TET1_2	**98.3**
TET3_1	**91.9**
TET3_2	165.3
MacroH2A_1	**100.2**
MacroH2A_2	0.0
Sirt2_1	**107.6**
Sirt2_2	108.4
Ano1_1	132.1
Ano1_2	145.3

Each gene was tested with two technical replicates of the same cDNA sample and two technical replicates of the associated housekeeping gene (for each cDNA sample). For the housekeeping genes, 18SRNA was used for pectoral fin muscle samples and 18S, a slightly modified 18SRNA, was used for gonad samples because they produced the most stable melting curves for their respective tissue types (Table 2.3). Target gene primers (n=12) were tested as two variants, and were also first validated to be sure they maintained stable melting curves and had similar Ct values across tested samples. To test the target genes, a solution was made which

contained 2 microliters of cDNA from each of the 96 cDNA samples. Next, 10 microliters of this cDNA solution were taken and diluted with 90 microliters of RNase-Free Water. This process was done three more times resulting in a dilution series (n=4) of exponentially decreasing amounts of pooled cDNA solution. For the plate set-up, 3 wells from each dilution were used to test the target genes, and their cycle thresholds (Ct value) were plotted onto a standard curve to determine their slope. Only genes with a slope between -90 and -110 could be used in the experiment. Of the 14 primers tested, 7 primers representing 6 genes passed validation (Table 2.4). Both Sirt2 primers passed, but Sirt2_1 was selected for the experiment because the efficiency value (107.6%) was closer to the ideal (100%) than Sirt2_2. Neither of the two Ano1 primers passed the efficiency test and were excluded from the experiment. MacroH2A had an interesting set of primers due to one being nearly perfect at 100.2%, while MacroH2A_2 did not show any gene amplification.

2.2.3 qPCR of Target Genes

qPCR was done using a 96 well plate (Applied Biosystems MicroAmp™ Optical 96-Well Reaction Plate) with each well containing 2 microliters of cDNA solution and 13 microliters of TaqMan™ Universal PCR Mastermix as a part of QuantiFast SYBR® Green PCR Kit. For each reaction, the master-mix contained 7.5 microliters of QuantiFast SYBR® Green Buffer, 0.23 microliters of 5x forward primer, 0.23 microliters of 5x reverse primer, and 5.04 microliters of RNase-Free Water, for a total reaction volume of 15 ul. Master-mixes were added to the wells first using an electronic multi-step pipette (Eppendorf Repeater), followed by manual addition of the two microliters of sample cDNA.

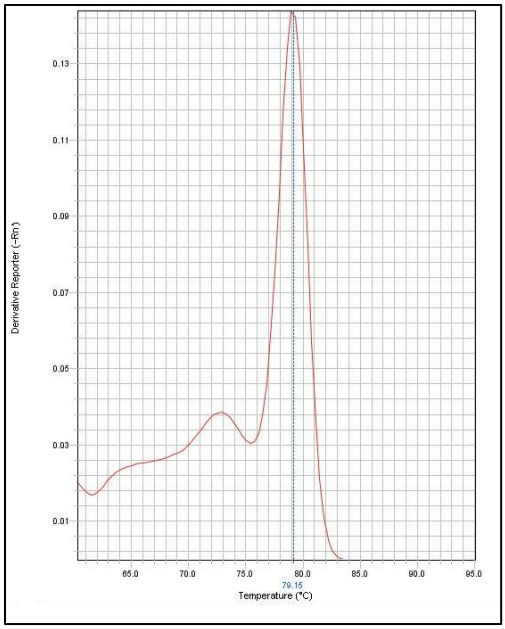

Figure 2.11. An example of a good melting curve showing that DNMT1_1 passed validation.

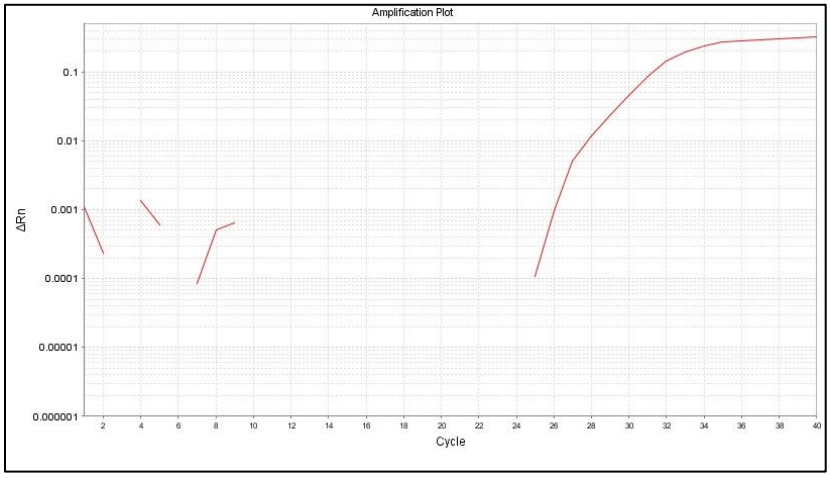

Figure 2.12. An example of a good amplification curve showing that DNMT1_1 passed validation.

The melting curve shown in Figure 2.11 was considered good because of the strong peak at the correct melting temperature and no other peaks elsewhere. The small peak at around 73°C shows the formation of some primer-dimer, the product of primer hybridization which can have a negative effect on the PCR due to less primer material available for cDNA synthesis. The amplification curve was considered good because it is smooth and without a spike, and after reaching a threshold, it continuously doubles after each cycle.

For the experiment, each plate was set-up so that every row contained 1 male, 1 female, and 1 gravid female from each of the Sylt, Bergen, Mo i Rana, and Alta sites (n=12 samples) for each gene. Three target genes and one housekeeping gene were run on each plate, with a technical replicate for each sample – gene combination. For each gene, one sample was left blank (no cDNA) to act as a negative control. After the plates were filled, they were sealed with a clear plastic, adhesive film and centrifuged for 30 seconds at 1000 RPM. Plates were kept cold until they were ready for thermocycling. Samples were run on an Applied Biosystems™ 7500 Real-Time PCR Systems with the associated analysis software. Cycling conditions were: initial heat activation at 95 ^{o}C for 5 minutes, then a two-step cycle of denaturation at 95^{o}C for 10 seconds and an annealing/extension step at 58 ^{o}C for 30 seconds. This two-step cycle was repeated 40 times until completion. For validation of genes, cycles were run on the "Standard" program taking 2 hours for the PCR, and for the experiment itself, I used the "FAST" program taking approximately 1.5 hour per run. In total, 12 plates were run to test three fish from each site for six genes, with organs run on separate plates. Samples that failed to achieve a good C_t value and melting curve were redone. In total, 8 additional plates were run to obtain the highest possible usable PCR data.

2.2.4 Data Analysis

PCR results (raw data) were exported from Applied Biosystems™ 7500 Real-Time PCR Systems into Microsoft Excel. Values used in the statistical analyses of gene expression were the ΔCt values from the qPCR, which was calculated as the difference between the Ct value of the target gene expression minus the Ct value of the housekeeping gene analyzed for that sample. The ΔCt value is thus representative of the amount of change in gene expression of the target gene corrected for baseline expression of the housekeeping gene. Only samples with single peaks at the corresponding melting temperature were used in the analyses (n=83 samples were removed from the analysis). Gene expression in gonads and pectoral fin muscle were analyzed separately because they were calculated using different housekeeping gene expression. All genes were analyzed using ANOVA in the same way, testing for main effects of site (4 sampling locations/latitudes) and sex (male, female, gravid female), plus their interaction. Tukey post-hoc

tests of significant terms were used to identify significant pair-wise contrasts. All analyses were run in the R statistical environment (version 3.6.1).

3. Results

3.1 Field sampling of temperate to Arctic stickleback populations

Approximately two months of fieldwork in Scandinavia culminated in 11 populations of marine stickleback being sampled. The sampling locations were all marine environments with salinities over 13 parts per thousand (PPT), contained marine fauna and flora, and had easy access to the ocean for stickleback migrations. The sampled populations contained complete or nearly complete lateral plate morphs almost exclusively, and individual fish were selected for based on large size. Locating stickleback populations was often difficult and time consuming, however, success increased with experience in the recognition of preferred stickleback environmental features such as shallow, calm areas, freshwater river inputs, and significant amounts of seagrasses and other vegetation.

Figure 3.1. Map of all threespine stickleback locations sampled; red circles indicate the populations used for gene expression analyses.

The full map of stickleback sampling locations illustrates the narrow range of longitude within which a broad range of latitudes were sampled (Figure 3.1). A nearly 15 ° latitudinal gradient was sampled, stretching from temperate to Arctic marine habitats. Populations were sampled from a wide range of major waterbodies including the North Sea, the Kattegat and Skagerrak at the entrance to the Baltic Sea, the Norwegian Sea, and the edge of the Arctic Ocean (Figure 3.1). Eight of the 11 sites sampled were located along the coast of a fjord, and the Sylt, Bodø, and Vesterålen sites were island coastal habitats. The four sites used for gene expression

analyses (Sylt, Bergen, Mo I Rana, and Alta) were chosen because they are roughly equidistant from one another (each approximately 660 kilometers apart), and represent the entire latitudinal range sampled encompassing approximately 1981 kilometers. The goal was to sample 30 fish from each population, however, those targets were not always reached due to time constraints and/or fish abundance (Table 3.1).

Table 3.1. Sampling site locations ordered by capture date with their GPS coordinates, the date of fish capture, the number of fish sampled, salinity, water temperature, and the main method of capture.

Site Name, (Site Region), Country	GPS Coordinates	Capture Date	Number of Fish Sampled	Salinity	Sampled Temp. °C	Main Capture Method
Mariangerfjord, DK	56.656395, 9.979952	7/5/2019	27	15.6	10.9	Traps
Sandspollen (Oslofjord), NO	59.665971, 10.585359	10/5/2019	30	25.7	9.8	Seine Net
Lindonvika (Haugesund), NO	60.147081, 5.433129	13/5/2019	30	25.4	7.8	Seine Net
Straumen (Bergen), NO	60.225057, 5.276420	17/5/2019	24	32.6	11	Seine Net
Stjørdal (Trondheim), NO	63.471358, 10.893145	26/5/2019	14	17	12.8	Seine Net
List auf Sylt (Sylt), DK	55.025657, 8.430818	29/5/2019	30	27.2	19.3	Dip Nets
Sandstrand (Vesterålen), NO	68.745997, 15.345146	6/6/2019	30	30.2	14.5	Traps
Latharistranda (Alta), NO	69.984096, 23.453836	12/6/2019	30	15.1	16.6	Dip Nets
Drevjaleira (Mo i Rana), NO	65.936303, 13.131886	15/6/2019	30	13.2	16.6	Dip Nets
Fjølvågan (Bodø), NO	67.402270, 13.862751	18/6/2019	30	33.1	14.6	Traps
Doverodde Harbor (Limfjord), DK	56.717403, 8.472333	1/7/2019	30	25.8	19	Seine Net

Populations of stickleback were sampled at 11 different sites along the coasts of Germany, Denmark, and Norway. Populations were on average 1.49° degrees of latitude apart, with a total range of 14.95 degrees (Table 3.1). Since one degree of latitude is equivalent to approximately

111 kilometers, the average distance between sites was approximately 166 kilometers of latitudinal difference. In terms of longitude, populations differed by an average of 1.82° with a total range of 18.18 degrees. However, unlike latitude which has a constant position with a fixed distance between degrees, longitude is widest at the equator and narrows towards the poles, thus average distance is not comparable.

Table 3.2. Water temperatures of the yearly average, February and August monthly temperatures of the sampled locations listed with increasing latitude. Data provided by www.weather-atlas.com

Site	Yearly Average Temperature °C	February Average Temperature °C	August Average Temperature °C
Sylt, DE	10.6	4	18
Mariangerfjord, DK	10.3	2.9	18.3
Limfjord, DK	10	4.8	15.7
Oslofjord, NO	9.5	3	17.9
Haugesund, NO	10.1	4.8	16.2
Bergen, NO	10	4.8	15.7
Trondheim, NO	9.5	4.9	14.8
Mo I Rana, NO	8.3	3.8	13.8
Vesterålen, NO	8.1	4.9	12.3
Bodø, NO	7.7	5	12
Alta, NO	6.3	4	10

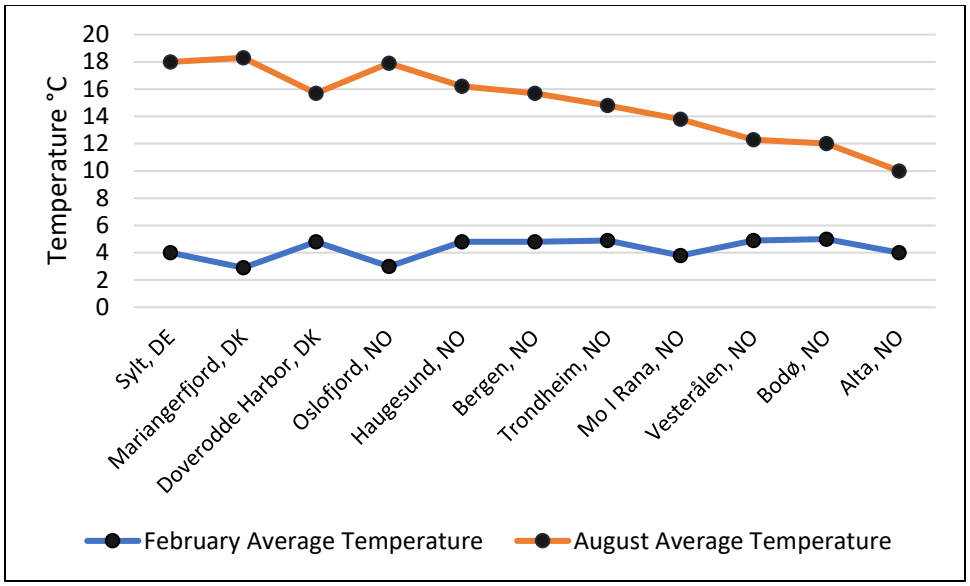

Figure 3.2. The average February and August 2019 ocean temperatures at each sampled location. Location increases with latitude along the x-axis. Data provided by www.weather-atlas.com

3.2 Sea surface temperature and stickleback body size across a latitudinal gradient

Figure 3.2 shows that sea surface temperatures in August predictably decreased as latitude increased, whereas in February, ocean temperatures were stable throughout and showed a 0°C temperature difference per northward site. In contrast, maximum monthly temperatures decreased by -0.8 °C per northward site. February and August average temperatures were selected for each sampling location because they represent approximately the average minimum and maximum yearly ocean temperatures. The overall average monthly temperature range narrowed as latitude increased, with the range decreasing by -1.3°C per site. For instance, the southernmost location (Sylt) had a range of 14°C between the warmest and coldest month, whereas the northernmost location (Alta) had a 6°C change between the warmest and coldest months. Locations were sampled during May and June, and thus, temperatures were closer to the August average temperature rather than February. Because sampled temperature reflects the immediate water temperature, the values obtained were a product of air temperature, direct sunlight, water volume, and salinity, in addition to average sea surface temperatures. These values can change quickly throughout the day and may not necessarily represent the average ambient temperatures stickleback populations would experience.

Table 3.3. Number of stickleback of each sex category caught at each sampling site.

	Male	Female	Gravid Female	Total
Sylt, DE	12	14	4	30
Marianger, DK	12	11	4	27
Limfjord, DK	4	13	13	30
Oslofjord	5	17	8	30
Haugesund	0	12	18	30
Bergen	19	6	7	24
Trondheim	0	10	4	14
Mo i Rana	7	17	6	30
Bodø	7	18	5	30
Vesterålen	13	6	11	30
Alta	9	14	7	30

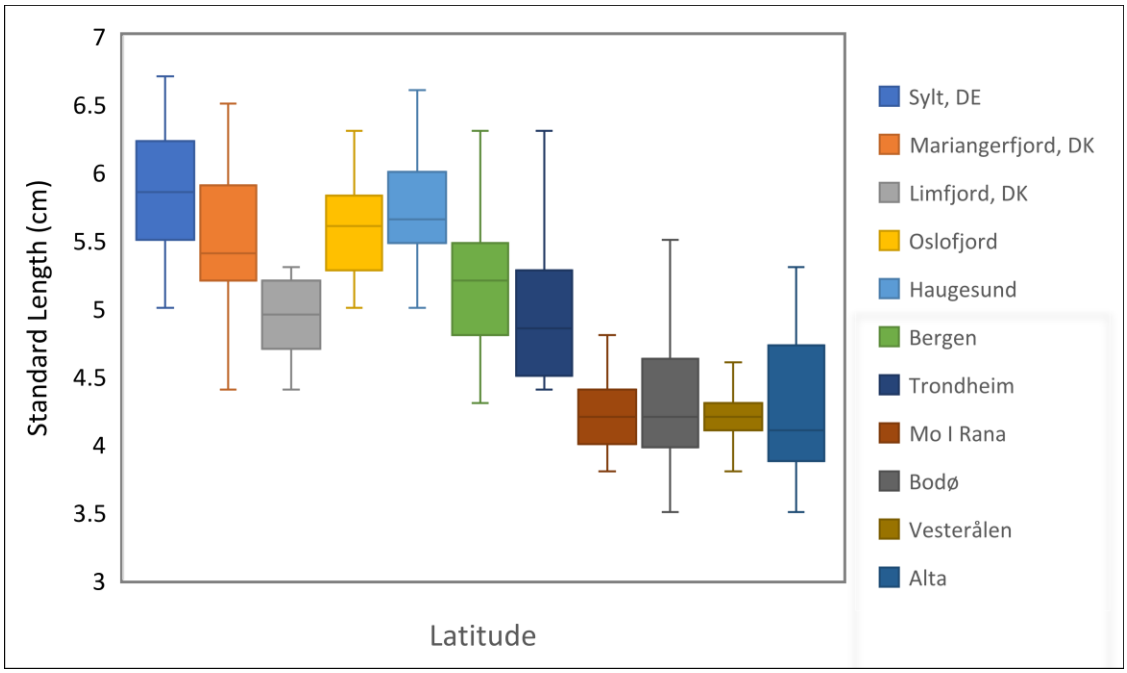

Figure 3.3. Box plot of median standard length (and range) of all stickleback populations sampled in order of ascending latitude.

Stickleback standard length was significantly influenced by site and sex (Table ?). This relationship is illustrated in Figure 3.3, and shows a steady decrease of stickleback standard length as latitude increases. Stickleback from Sylt, Germany were the longest, with a mean length of 5.85 ± 0.46 cm, a median of 5.85, and ranged from 5 to 6.7 cm. Fish from Mariangerfjord had a mean length of 5.52 ± 0.56 cm, median of 5.4 cm, and ranged from 4.4 to 6.5 cm. Fish from

Limfjord were noticeably smaller, a mean length of 4.89 ± 0.30 cm, a median of 4.95 cm, and ranged from 4.4 to 5.3 cm. Fish from Oslofjord had a mean of 5.6 ± 0.35, a median length of 5.6 cm, and ranged from 5 to 6.3 cm. At Haugesund, fish had a mean length of 5.75 ± 0.42 cm, a median length of 5.7 cm and ranged from 5 to 6.6 cm. The Bergen population showed a mean and median length of 5.2 ± 0.58 cm, and a range from 4.3 to 6.3 cm. The Trondheim population had a mean of 4.99 ± 0.55 cm, median of 4.9 cm, and a range of 4.4 to 6.3 cm. The Mo i Rana population had a mean 4.2 ± 0.25, and a range of 3.8 to 4.8 cm. The Bodø population had a mean of 4.38 ± 0.7 cm, median 4.2 cm, and ranged from 3.5 to 5.5 cm. The Vesterålen population had a mean of 4.23 ± 0.26 cm, a median of 4.2 cm, and a range of 3.8 to 4.6 cm. Lastly, the Alta population had mean of 4.32 ± 0.65 cm, a median of 4.1 cm and a range of 3.5 to 5.3 cm.

Table 3.4. ANOVA results for standard length of threespine stickleback populations testing the effects of Site and three sex categories (Sex). Note: due to the lack of male stickleback caught in Haugesund and Trondheim, these populations were excluded from the analysis. Significant terms are highlighted in bold.

	Df	Sum Sq	Mean Sq	F value	Pr(>F)
Site	8	82.61	10.33	48.82	**<0.001**
Sex	2	4.445	2.223	10.51	**<0.001**
Site:Sex	16	4.751	0.2969	1.404	0.140
Residuals	242	51.19	0.2115		

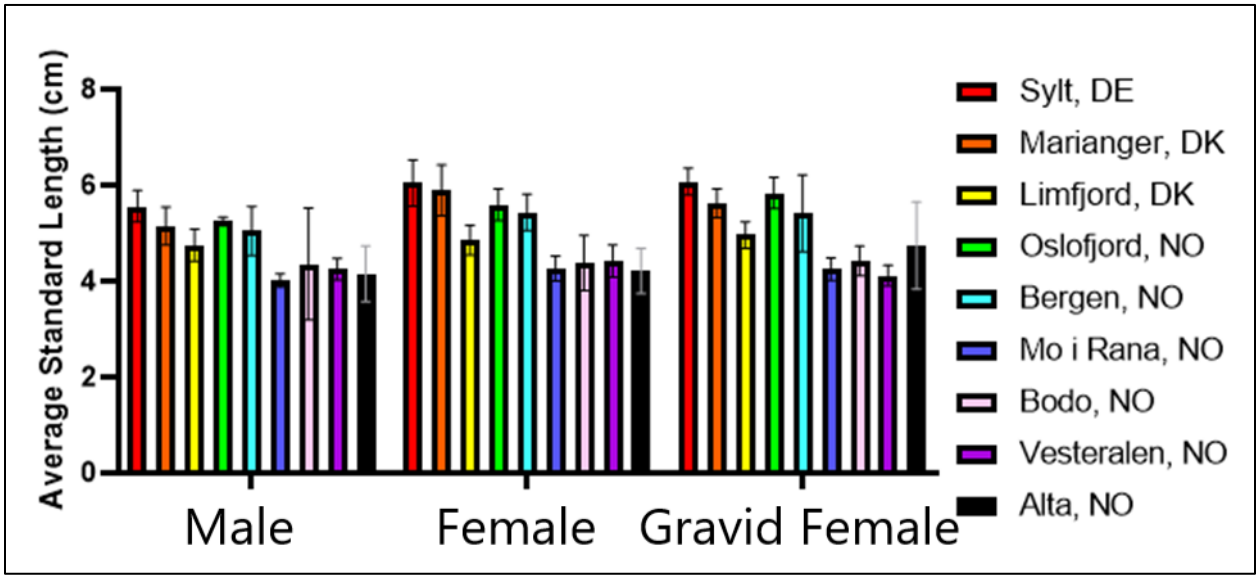

Figure 3.4. Mean standard length (± SD) of stickleback compared between sexes using 9 sampling sites arranged with ascending latitude.

Standard length was significantly influenced by sex (Table 3.4; Figure 3.4), with gravid females (n=87) having the longest standard lengths (5.14 ± 0.78 cm), and an overall range of 3.8 to 6.7 cm. Females (n=138) were the second largest, with an average length of 5.03 (± 0.78) cm, and ranged from 3.7 to 7 cm. Males (n=88) were the smallest, with a mean length of 4.78 (± 0.78) cm, and ranged from 3.5 to 6.9 cm.

3.3 Targeted Gene Expression

Overall, expression of the target genes used in the experiment showed a weak relationship with sampling site (latitude), but differed more strongly between the sexes. Several genes also showed interactive effects between site and sex. Gonad and pectoral muscle gene expression were always analyzed separately due to the different housekeeping genes used which would affect the delta C_t values. ANOVA of housekeeping gene expression for gonad tissue samples (18S) did not show statistically significant effects of sex or site (Annex tables 8.1 and 8.2). However, for 18SRNA used with pectoral fin muscle samples, there was a significant effect of site and sex on expression (Annex tables 8.3 and 8.4), despite this housekeeping gene passing the validation tests before the start of the experiment (see Methods). Posthoc Tukey Test pairwise analysis showed that 18SRNA expression in pectoral muscle of males differed significantly from both females and gravid females, but female types did not differ from each other (Annex table 8.5). This may have introduced a potential bias in ΔC_t values for gene expression of pectoral muscle samples in males. It is possible that with a larger sample size the variance in 18SRNA expression variance would be reduced, removing any difference between the sexes.

For the target gene expression, only figures with significant or noticeable results are presented in the results. For figures of total gene expression across all sites and all sexes, please refer to the Annex. The Y-axis for the target gene figures are the ΔC_t values; the difference between the target gene's expression and the housekeeping gene's expression. To interpret the results, the lower the ΔC_t value, the greater the expression of the target gene and vice versa.

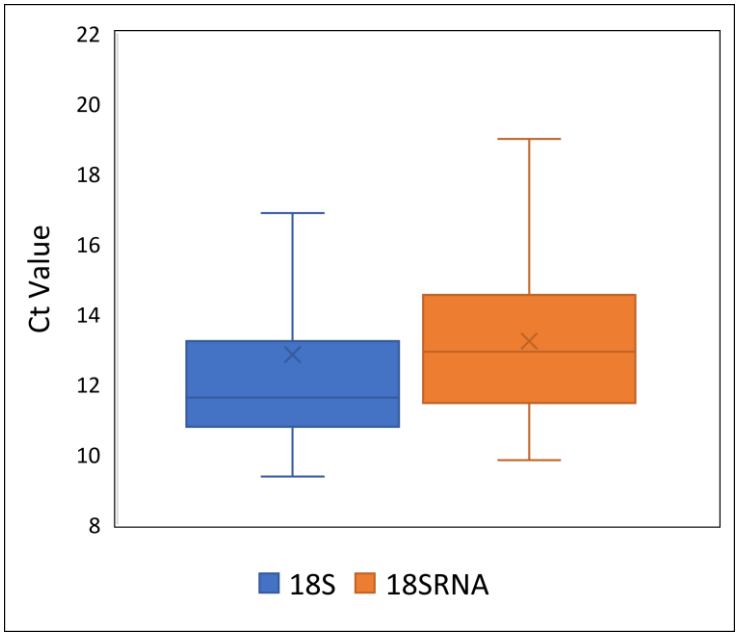

Figure 3.5. Average Ct values (± SD) of 18S and 18SRNA housekeeping genes obtained during the experiment.

Ct values of the two housekeeping genes expressed in samples used in the experiment were compared, and showed acceptable but different Ct values than those obtained during the validation tests (Figure 2.10). The main reason for this change was likely the decision to reduce the amount of primer used from a 10x to 5x concentration to eliminate primer-dimer formation. This change resulted in more useable values, but lowered the average Ct value for 18S considerably and slightly increased Ct values of 18SRNA. During the experiment, 18S used with gonad cDNA (n=191 samples) had on average 11.97 cycles, and ranged between 9.37 and 17.22 cycles. 18SRNA used with pectoral muscle cDNA (n=181) had on average 13.15 cycles, and ranged between 9.83 and 18.99 cycles (Figure 3.5).

3.3.1 DNMT1

The results of the two, two-way ANOVAS shown in Table 3.5 show that DNMT1 expression in both gonad and pectoral muscle tissue was not statistically influenced by site or sex. Tukey tests for pairwise comparisons additionally found no significant effects on DNMT1 expression in gonads or pectoral muscle for both site and sex. Nevertheless, as seen in Figure 3.6, DNMT1 expression was higher in Mo i Rana female gonad tissue (one-way anova $F_{3,7} = 4.969$, P=0.037). While Sylt (n=3), Bergen (n=3), and Alta (n=3) had similar DNMT1 expressions (mean ΔC_t,= 18.71,

18.61, and 19.13, respectively), Mo i Rana (n=3) expression was much higher with an average ΔC_t of 14.91. DNMT1 expression in male pectoral muscle was not significantly influenced by site or sex (anova $F_{3,5}$= 1.555, P=0.310) and suffered from a low sample size, however visual inspection of the data showed higher expression in the Alta site compared to the other sites (Figure 3.7). DNMT1 expression in pectoral muscle did not differ between the sexes (Figure 3.8), however there was a trend of similar expression by females (n=8) and gravid females (n=12) with mean ΔC_t values of 19.58 and 19.64 respectively, whereas expression in males (n=9) had a higher average ΔC_t of 18.70.

Table 3.5. ANOVA results for expression of DNMT1 in gonad and pectoral muscle tissue across four threespine stickleback populations (Site) and three sex categories (Sex). Significant terms are highlighted in bold.

	Gonad					Pectoral Muscle				
	Df	Sum Sq	Mean Sq	F value	Pr(>F)	Df	Sum Sq	Mean Sq	F value	Pr(>F)
Site	3	45.629	15.210	2.138	0.136	3	9.668	3.223	1.680	0.209
Sex	2	2.125	1.063	0.149	0.862	2	5.182	2.591	1.351	0.285
Site:Sex	5	35.097	7.019	0.987	0.456	6	7.924	1.321	0.689	0.662
Residuals	16	113.814	7.113			17	32.601	1.918		

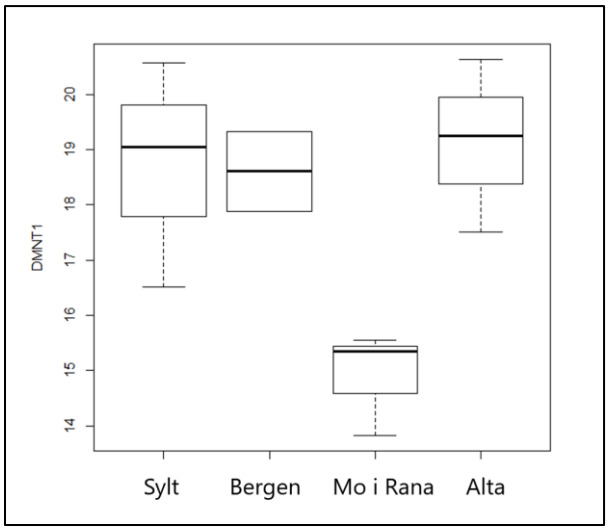

Figure 3.6. Box plot of median (and range) DNMT1 expression in both female and gravid female gonads for each of the four sampled populations. Populations are ordered on the x-axis with increasing latitude.

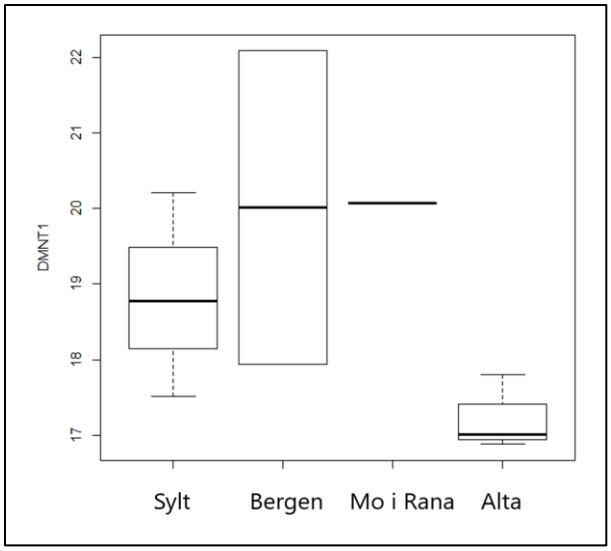

Figure 3.7. Box plot of median (and range) DNMT1 expression of male pectoral muscle averaged for each of the four sampled populations. Populations are ordered on the x-axis with increasing latitude.

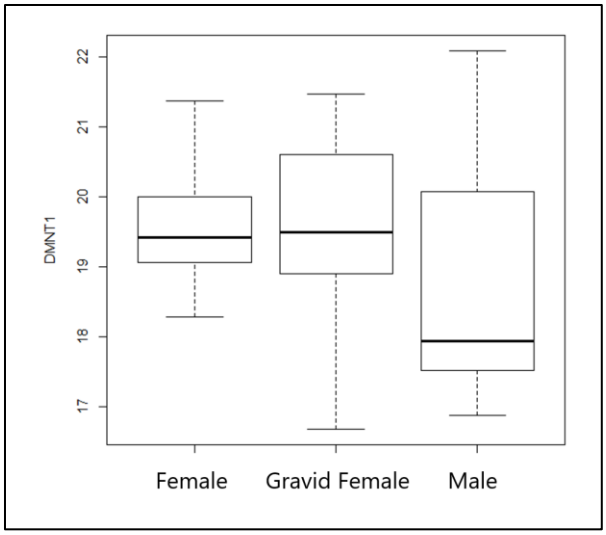

Figure 3.8. Box plot of median (and range) DNMT1 expression of pectoral muscle tissue averaged from all sampled populations for each of the three sexes.

3.3.2 DNMT3ab

Results of the two-way ANOVAs shown in Table 3.6 conclude that DNMT3ab expression in gonads differed significantly by site, sex and their interaction, and by site in pectoral fin muscle. Expression in female gonads (Figure 3.9) had a wide range, but gravid females (n=2) had a much higher expression (mean ΔC_t = 10.33) than males (n=6) with a mean ΔC_t of 17.55. Posthoc Tukey Tests found significance differences in DNMT3ab expression in gonads between males and gravid

females (t value = 3.086, p = 0.041), with males showing higher expression than gravid females (Figure 3.9). Pectoral muscle DNMT3ab expression was also significantly influenced by site. Significant differences in DNMT3ab expression in pectoral muscle were found between Bergen and Mo i Rana (Tukeys t value = 2.990, p = 0.040), and Bergen and Alta (Tukeys t value = 2.988, p = 0.040; Figure 3.11). As shown in Figure 3.10, DNMT3ab expression in pectoral muscle did not differ significantly among the sexes. However, males tended to express less DNMT3ab than females and gravid females, which were more similar to each other. DNMT3ab expression in male pectoral muscle (Figure 3.11) differed significantly with site ($F_{3,15}$= 4.510, P=0.019). Sylt (n=5) and Bergen (n=7) had higher levels of DNMT3ab expression (ΔC_t = 20.37 and ΔC_t = 19.02, respectively) than Mo i Rana (n=3) and Alta (n=4), where ΔC_t = 21.46 and ΔC_t = 21.23, respectively.

However, despite many statistically significant effects for DNMT3ab expression, this gene had the lowest overall sample size due to a high amount of samples failing to achieve a good C_t value, melting curve, or amplification curve. The low sample size likely had at least some effect on these results. The samples may have failed because of issues with lab procedures or because DNMT3ab expression was not present at detectable levels. More samples would need to be tested to validate which possibility is the most likely.

Table 3.6. ANOVA results for expression of DNMT3ab in gonad and pectoral muscle tissue across four threespine stickleback populations (Site) and three sex categories (Sex). Significant terms are highlighted in bold.

	Gonad					Pectoral Muscle				
	Df	Sum Sq	Mean Sq	F value	Pr(>F)	Df	Sum Sq	Mean Sq	F value	Pr(>F)
Site	2	24.984	12.492	43.477	**0.002**	3	18.833	6.278	4.055	**0.040**
Sex	2	85.902	42.951	149.483	**< 0.001**	2	1.288	0.644	0.416	0.671
Site:Sex	1	31.269	31.269	108.826	**< 0.001**	3	4.113	1.371	0.886	0.481
Residuals	4	1.149	0.287			10	15.480	1.548		

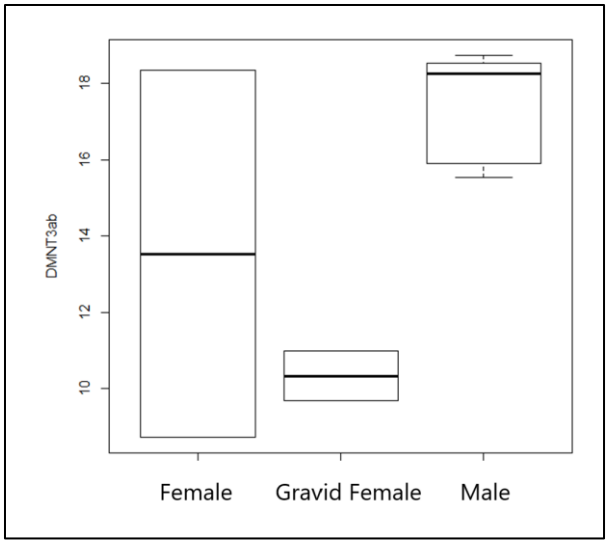

Figure 3.9. Box plot of median (and range) DNMT3ab expression of gonad tissue averaged from the three sexes averaged for each the four sampled populations.

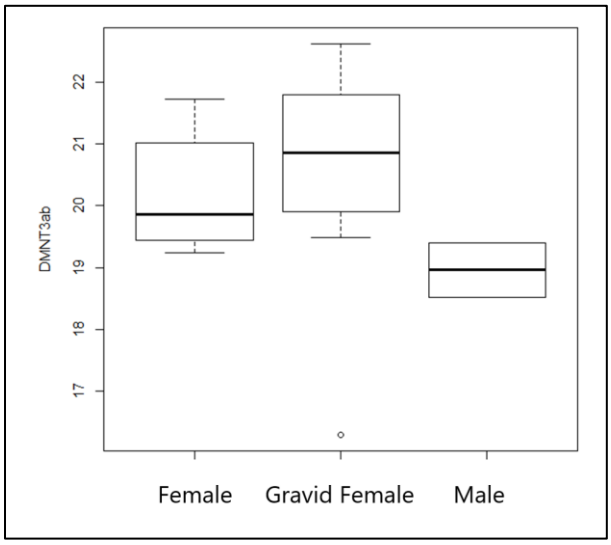

Figure 3.10. Box plot of median (and range) DNMT3ab expression of pectoral muscle tissue averaged from each of the three sexes and for each the four sampled populations.

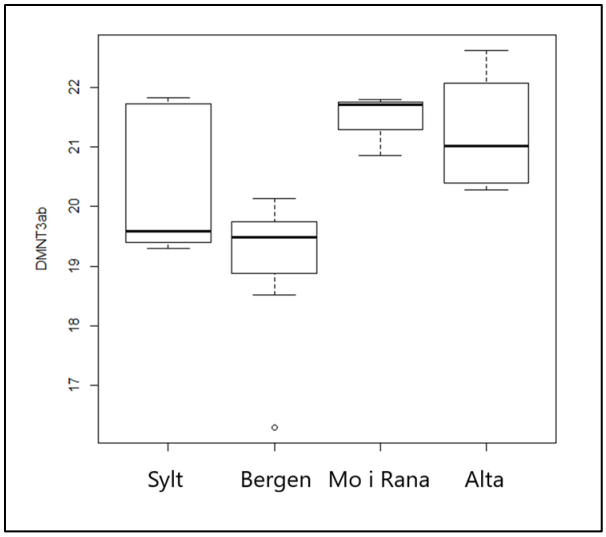

Figure 3.11. Box plot of median (and range) DNMT3ab expression of male pectoral muscle for each of the four sampled populations. Populations are ordered on the x-axis with increasing latitude.

3.3.3 TET1

TET1 expression in pectoral muscle was significantly influenced by both site and sex, whereas expression in gonads was not influenced by site or sex (Table 3.7). Overall, expression of TET1 in female gonads (n=12) was higher than in gravid female gonads (n=11), with mean ΔC_t of 17.41 and 19.73, respectively (Figure 3.12). TET1 expression in gravid females did not differ significantly by site (anova $F_{3,7} = 1.093$, P= 0.413), however there was a trend of lower expression in Bergen (Figure 3.13). TET1 expression in pectoral muscle shown in Figure 3.14 showed statistically significant differences among the sexes. Females (n=12) and gravid females (n=12) had very similar levels of expression (mean ΔC_t of 18.66 and 18.69, respectively), whereas male (n=12) expression was higher with a mean ΔC_t of 17.40. Female pectoral muscle expression of TET1 differed significantly by site (anova $F_{3,8} = 9.016$, P= 0.006), and showed a decreasing trend with latitude (Figure 3.15). Sylt (n=3) had the highest mean ΔC_t of 19.95, then Bergen (n=3) ΔC_t= 19.40, Mo i Rana (n=3) ΔC_t= 17.08, and Alta (n=3) ΔC_t= 18.22. Lastly, TET1 expression in male pectoral muscle was not significantly influenced by site (anova $F_{3,8} = 2.585$, P= 0.126), however the two southernmost sites, Sylt (n=3) and Bergen (n=3) had lower expression (mean delta C_t of 20.65 and 16.80, respectively) than the two northern sites Mo i Rana (n=3) and Alta (n=3) which had mean C_ts of 18.43 and 17.7, respectively (Figure 3.16).

Table 3.7. ANOVA results for expression of TET1 gonad and pectoral muscle tissue across four threespine stickleback populations (Site) and three sex categories (Sex). Significant terms are highlighted in bold.

	Gonad					Pectoral Muscle				
	Df	Sum Sq	Mean Sq	F value	Pr(>F)	Df	Sum Sq	Mean Sq	F value	Pr(>F)
Site	3	11.523	3.841	0.470	0.706	3	21.259	7.086	3.949	**0.020**
Sex	2	29.023	14.512	1.776	0.192	2	13.154	6.577	3.666	**0.040**
Site:Sex	6	52.495	8.749	1.071	0.408	6	7.595	1.266	0.706	0.648
Residuals	23	187.939	8.171			24	43.064	1.794		

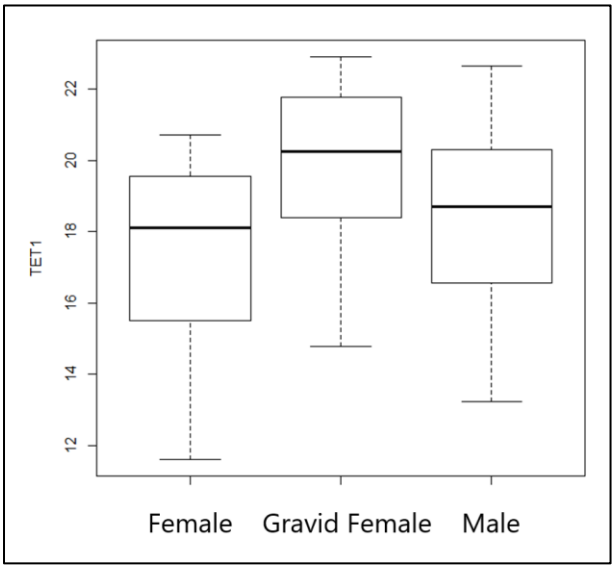

Figure 3.12. Box plot of median (and range) TET1 expression of gonad tissue averaged from each of the three sexes for each the four sampled populations.

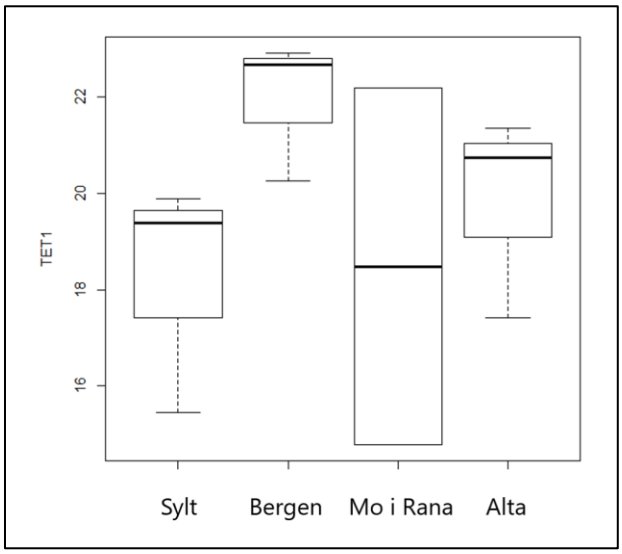

Figure 3.13. Box plot of median (and range) TET1 expression of gravid female gonads averaged for each of the four sampled populations. Populations are ordered on the x-axis with increasing latitude.

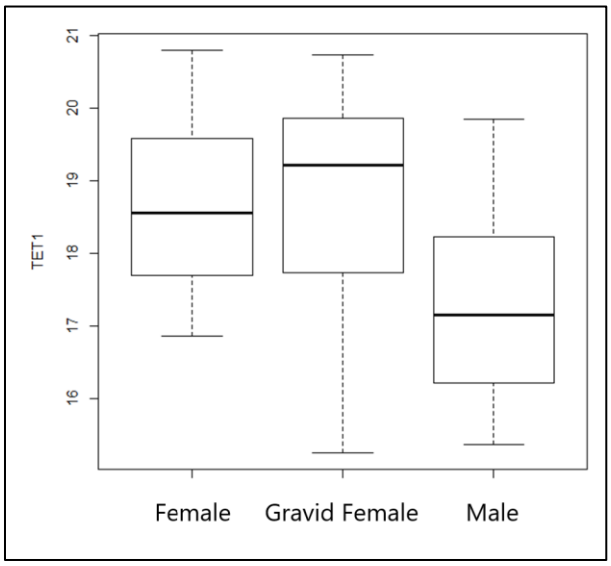

Figure 3.14. Box plot of median (and range) TET1 expression of pectoral muscle tissue averaged from the three sexes and for each the four sampled populations.

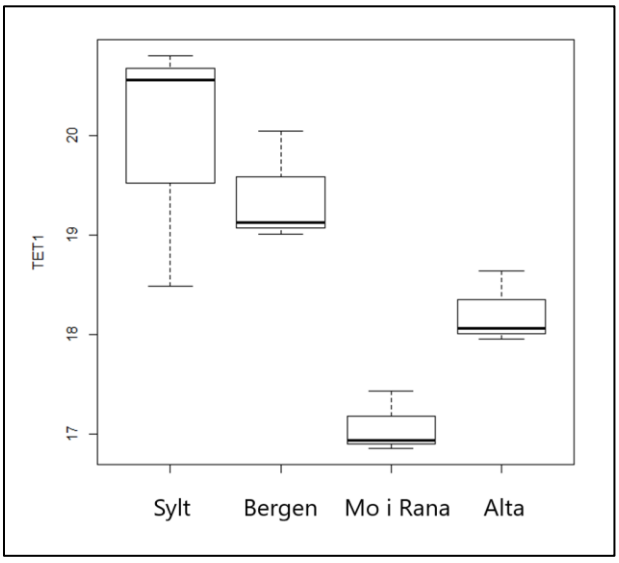

Figure 3.15. Box plot of median (and range) TET1 expression of female pectoral muscle tissue averaged for each of the four sampled populations. Populations are ordered on the x-axis with increasing latitude.

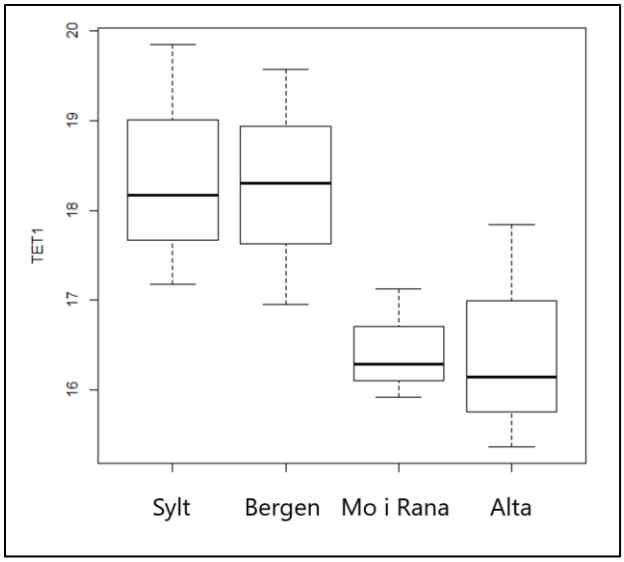

Figure 3.16. Box plot of median (and range) TET1 expression of male pectoral muscle tissue averaged for each of the four sampled populations. Populations are ordered on the x-axis with increasing latitude.

3.3.4 TET3

Results of the two-way anovas shown in Table 3.8 show that TET3 expression was not significantly influenced by site or sex in gonads, but was significantly influenced by site and sex in pectoral muscle. Despite the lack of significant effects in gonad expression by site, box plots and ANOVAs of female ($F_{3,8}$ = 0.263, P= 0.850) and gravid female ($F_{3,8}$ = 1.109, P= 0.401) expression of TET3 in Figures 3.17 and 3.18 showed remarkable similarities; a wide range for Sylt, and lower expressions in Bergen and Alta than in Mo i Rana. Both figures show a wide range of ΔC_t values for Sylt, with a range of 12.40 and 14.27 for females (n=3) and gravid females (n=3), respectively. Mean ΔC_t in females for Bergen (n=3) was 20.06, Mo i Rana (n=3) was 18.18, and Alta (n=3) was 19.66. Mean ΔC_t in gravid females for Bergen (n=3) was 21.61, Mo i Rana (n=3) was 17.08, and Alta (n=3) was 22.13.

Pectoral muscle TET3 expression (shown in Figure 3.19) was significantly influenced by site, with an average expression in Sylt of 18.59 (n=7), 16.96 in Bergen (n=9), 19.80 in Mo i Rana (n=9), and 18.16 in Alta (n=9). A Tukey Test for pairwise interactions found statistically significant contrasts of pectoral muscle TET3 expression between Mo i Rana and Bergen (t value = 4.846, p <0.001), and Mo i Rana and Alta (t = -2.793, p =0.042). Pectoral muscle TET3 expression by sex

(Figure 3.20) also differed significantly with males (n=11) showing higher expression (average ΔC_t of 17.52) than females (n=12) and gravid females (n=11), with average ΔC_t of 18.92 and 18.61, respectively. Female pectoral muscle TET3 expression differed by site (Figure 3.21; anova $F_{3,8} = 4.196$, P=0.047) with higher expression in Bergen (n=3) with an average ΔC_t of 17.28 than in Mo i Rana (n=3) and Alta (n=3) with average ΔC_t's 19.74 and 19.69, respectively.

Table 3.8. ANOVA results for expression of TET3 gonad and pectoral muscle tissue across four threespine stickleback populations (Site) and three sex categories (Sex). Significant terms are highlighted in bold.

	Gonad					Pectoral Muscle				
	Df	Sum Sq	Mean Sq	F value	Pr(>F)	Df	Sum Sq	Mean Sq	F value	Pr(>F)
Site	3	79.36	26.454	1.661	0.202	3	36.906	12.302	9.943	**<0.001**
Sex	2	7.17	3.587	0.225	0.800	2	11.991	5.996	4.846	**0.018**
Site:Sex	6	66.50	11.083	0.696	0.653	6	7.017	1.169	0.945	0.484
Residuals	24	382.23	15.926			22	27.221	1.237		

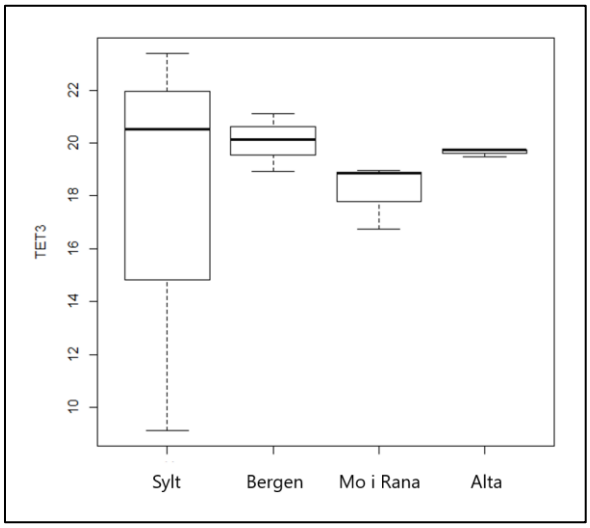

Figure 3.17. Box plot of median (and range) TET3 expression of female gonads averaged for each of the four sampled populations. Populations are ordered on the x-axis with increasing latitude.

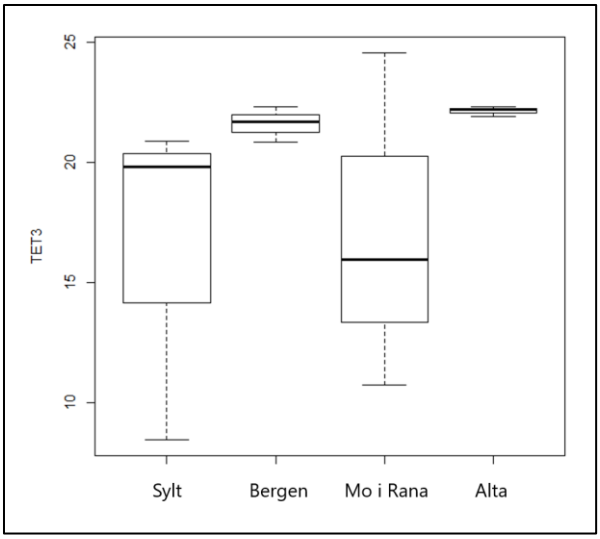

Figure 3.18. Box plot of median (and range) TET3 expression of gravid female gonads averaged for each of the four sampled populations. Populations are ordered on the x-axis with increasing latitude.

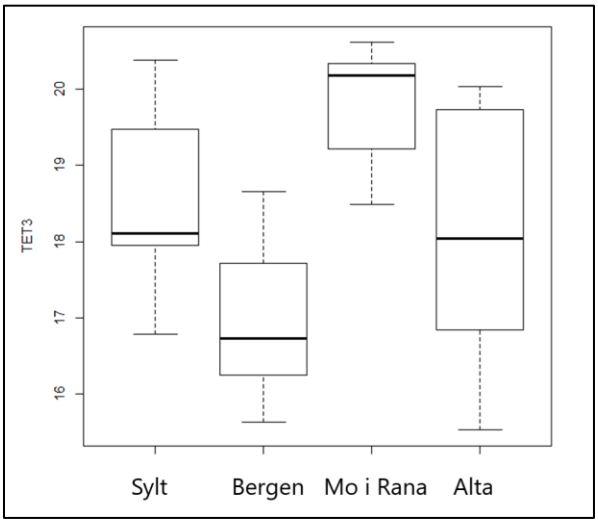

Figure 3.19. Box plot of median (and range) TET3 expression of pectoral muscle tissue averaged for all sexes for each of the four sampled populations. Populations are ordered on the x-axis with increasing latitude.

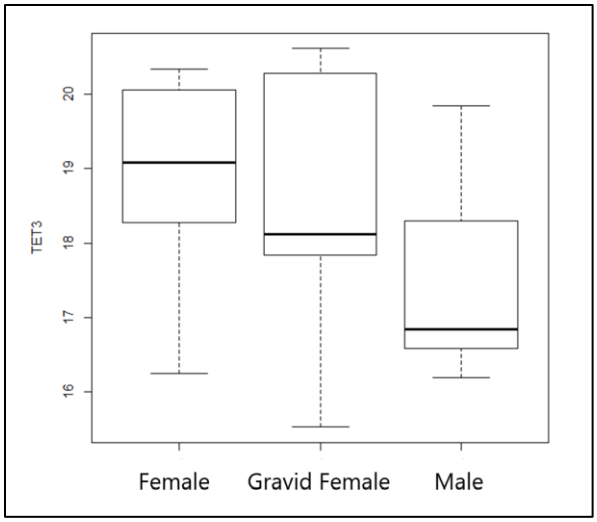

Figure 3.20. Box plot of median (and range) TET3 expression of pectoral muscle tissue averaged from each of the three sexes for each the four sampled populations.

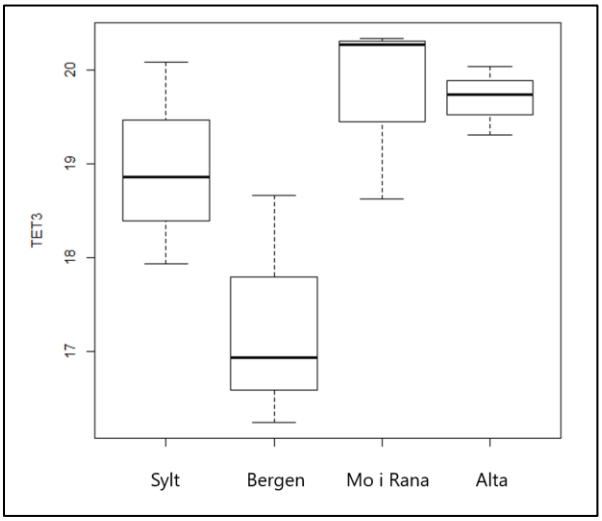

Figure 3.21. Box plot of median (and range) TET3 expression of female pectoral muscle averaged for each of the four sampled populations. Populations are ordered on the x-axis with increasing latitude.

3.3.5 MacroH2A

Results of the two-way anova shown in Table 3.9 shows that MacroH2A expression in gonads was not significantly influenced by site or sex in gonads, but was significantly influenced by sex in pectoral muscle. A Tukey Test for pairwise interactions found nearly statistically significant contrasts of MacroH2A expression between males and gravid females in gonads (t value = -2.445, p = 0.053). In Figure 3.22, a one-way anova found that MacroH2A expression was

significantly influenced by sex, and was most expressed in gravid females and least expressed in males. Average ΔC_t in gonads for females (n=11) was 21.15, in gravid females (n=9) C_t=23.02, and in males (n=11) C_t=18.49. In Figure 3.23, anova of MacroH2A expression in pectoral muscle found significant differences among the sexes, and similar to the expression pattern in gonads, males showed the lowest expression. Average ΔC_t of MacroH2A expression in pectoral muscle in females (n=11) was 23.75, in gravid females (n=10) C_t=23.50, and in males (n=9) C_t=21.52.

Table 3.9. ANOVA results for expression of MacroH2A gonad and pectoral muscle tissue across four threespine stickleback populations (Site) and three sex categories (Sex). Significant terms are highlighted in bold.

	Gonad					Pectoral Muscle				
	Df	Sum Sq	Mean Sq	F value	Pr(>F)	Df	Sum Sq	Mean Sq	F value	Pr(>F)
Site	3	65.33	21.777	1.030	0.402	3	2.910	0.970	0.282	0.838
Sex	2	91.21	45.605	2.157	0.143	2	27.208	13.604	3.959	**0.038**
Site:Sex	6	20.81	3.469	0.164	0.983	6	4.155	0.693	0.202	0.972
Residuals	19	401.71	21.143			18	61.855	3.436		

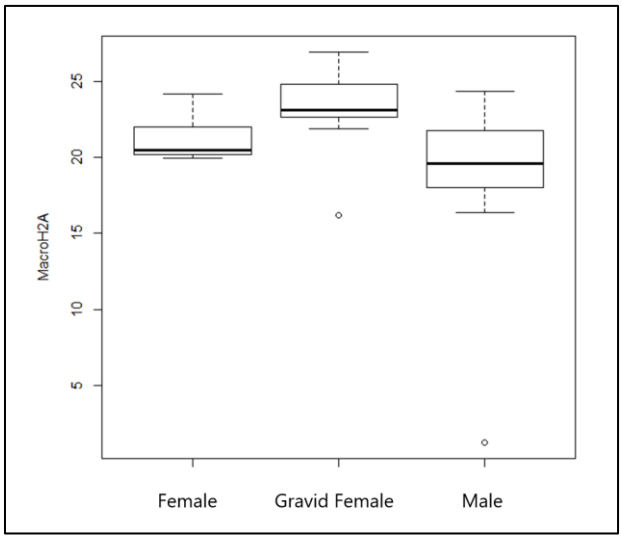

Figure 3.22. Box plot of median (and range) MacroH2A expression of gonads averaged from the four sampled populations for each of the three sexes.

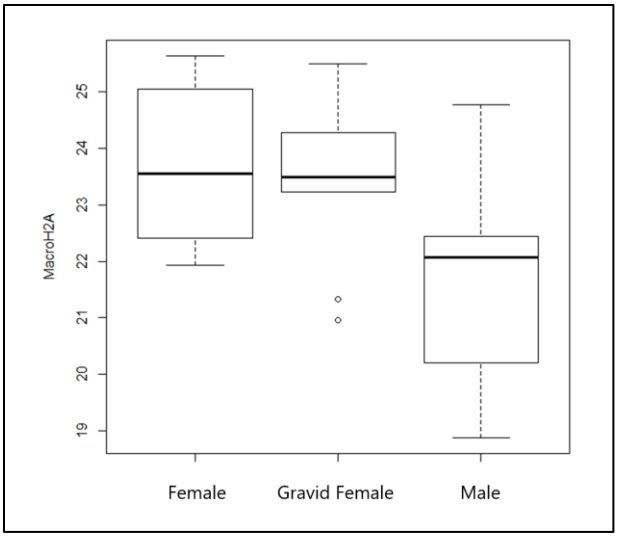

Figure 3.23. Box plot of median (and range) MacroH2A expression of pectoral muscle tissue averaged from the four sampled populations for each of the three sexes.

3.3.6 Sirt2

Results of the two-way anova shown in Table 3.10 shows that Sirt2 expression in gonads was not significantly influenced by sex or site, but expression in pectoral muscle was significantly influenced by both site and sex. In Figure 3.24, a one-way anova was run comparing Sirt2 expression in gonads by sex, which showed a weak relationship between the sexes (highest expression in gravid females and lowest expression in males). Average ΔCt of gonads from females (n=12) was C_t =14.06, in gravid females (n=11) C_t =15.46, and in males (n=10) C_t =13.31 (Figure 3.26). Female gonad Sirt2 expression did not differ significantly by site (anova $F_{3,8}$ = 2.002, P=0.192), but there was a trend of lower expression in the southern sites, Sylt and Bergen, than in the northern sites, Mo i Rana and Alta (Figure 3.25).

Sirt2 expression in pectoral muscle differed among the sexes, a nearly statistically significant relationship was found, with female and gravid female expression nearly identical to each other and both lower than expression in males (Figure 3.26). Mean ΔCt in females (n=12) was C_t =13.75, in gravid females (n=12) C_t =13.71, and in males (n=12) C_t =11.89. Sirt2 expression in pectoral muscle showed a weak relationship with site, in which average Sirt2 expression in Sylt was lower than the other three sites (Figure 3.27). Mean ΔCt for Sylt (n=9) was C_t =14.70, Bergen (n=9) C_t =12.49, Mo i rana (n=9) C_t =12.95, and Alta (n=9) C_t =12.34.

Table 3.10. ANOVA results for expression of Sirt2 gonad and pectoral muscle tissue across four threespine stickleback populations (Site) and three sex categories (Sex). Significant terms are highlighted in bold.

	Gonad					Pectoral Muscle				
	Df	Sum Sq	Mean Sq	F value	Pr(>F)	Df	Sum Sq	Mean Sq	F value	Pr(>F)
Site	3	15.964	5.321	1.127	0.361	3	31.725	10.575	3.101	**0.046**
Sex	2	22.410	11.205	2.372	0.118	2	27.031	13.516	3.964	**0.033**
Site:Sex	6	16.280	2.713	0.574	0.746	6	28.388	4.731	1.388	0.260
Residuals	21	99.193	4.724			24	81.839	3.410		

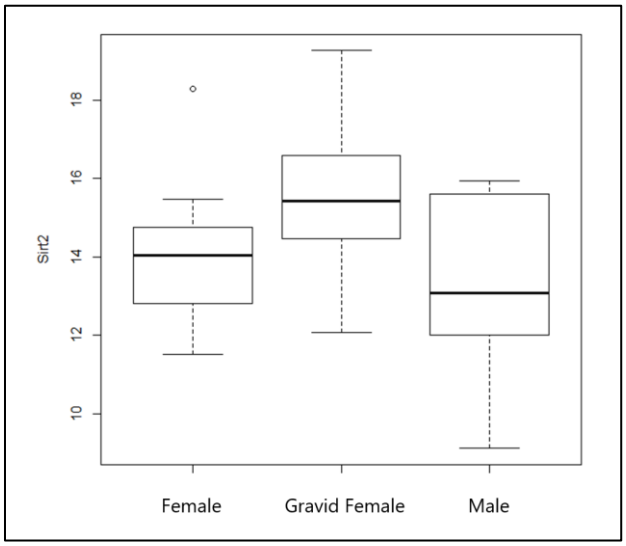

Figure 3.24. Box plot of median (and range) Sirt2 expression of gonads from all sites for each of the three sexes.

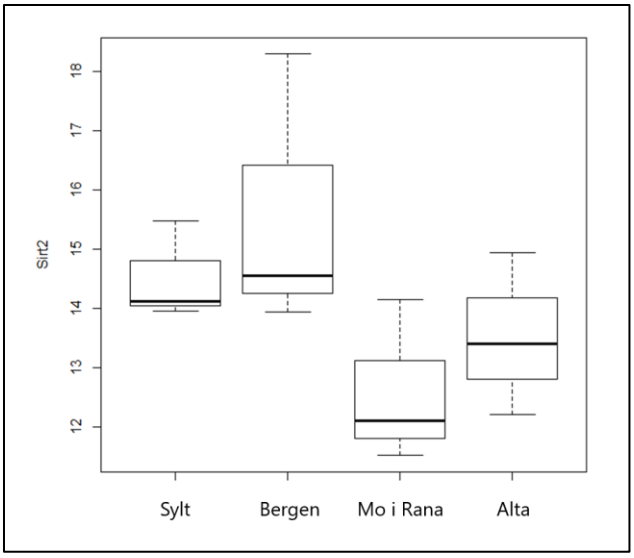

Figure 3.25. Box plot of median (and range) Sirt2 expression of female gonads averaged for each the four sampled populations. Populations are ordered on the x-axis with increasing latitude. Populations are ordered on the x-axis with increasing latitude.

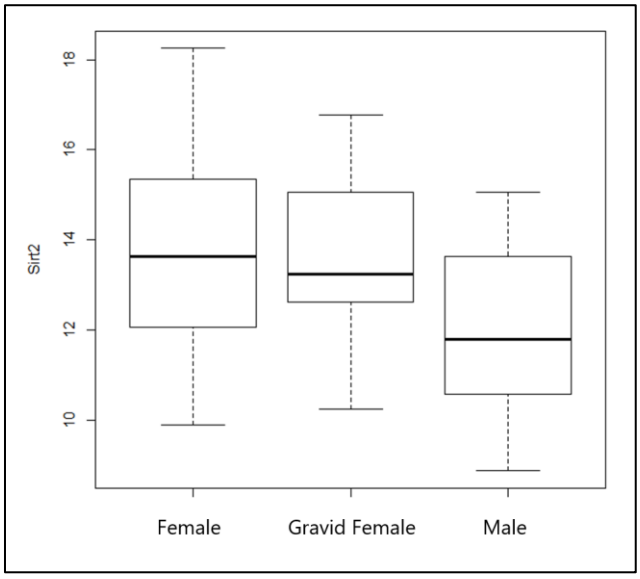

Figure 3.26. Box plot of median (and range) Sirt2 expression of pectoral muscle tissue averaged from all four sampled populations for each of the three sexes.

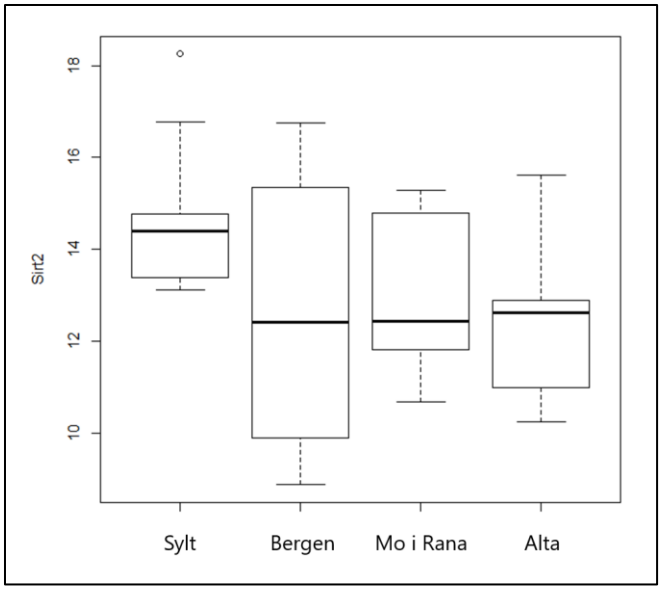

Figure 3.27. Box plot of median (and range) Sirt2 expression of pectoral muscle tissue averaged from all sexes for each of the four sampled populations.

4. Discussion

This investigation into threespine stickleback populations found differences amongst individuals in relation to size and gene expression of epigenetic actors. Stickleback average standard length decreased across all sexes as latitude increased. This could be due to differences in maximum water temperature, light availability, ecosystem richness, or predation. Epigenetic mechanisms have the potential to change methylation states and gene expression in this species based on their immediate environment. Here, different populations of stickleback expressed genes at different levels. Additionally, gene expression across males, females, and gravid females showed varying levels of target gene expression. Low sample size may have affected some of the data, however it could be shown that populations in northern latitudes could exhibit stronger epigenetic responses to cold acclimation than southern populations.

4.1 Stickleback Populations Across a Latitudinal Gradient

Threespine were stickleback found and captured in almost every region investigated. They were present throughout the coasts of northern Germany, Denmark, and Norway. The only locations where no marine stickleback were found was around the area of Ålesund in west central Norway and in Tromsø in northwestern Norway. In Ålesund, freshwater and brackish stickleback were found, but not marine morphotypes (e.g. complete lateral plates). Field observations of stickleback presence appeared to suggest a higher abundance in the southern latitude locations than in the northern latitude sites. The optimal capture method varied greatly based on physical limitations of the immediate environment. For instance, beach seining was always the preferred method of capture in terms of sampling efficiency but required a large, shallow area devoid of large rocks. This method was used in all four southernmost sites in Norway but was not used anywhere else. When the seine net was deployed, the target of 30 stickleback was always reached with the first pull of the net. The precise angle of the net pull had to be prepared in advance to prevent disturbance of the target area, which could potentially scare stickleback away. Trapping was used in sampling sites that were too deep or too difficult to dip net to catch stickleback. Minnow traps were baited with a mix of assorted cat food and tuna fish due to previous research establishing that baited traps are more successful due to stickleback using olfactory cues to hunt (Merilä 2015). In the southern loop, minnow traps with a black vinyl coating were used, whereas in the northern loop silver minnow traps were used. Research by Merilä *et al.* (2013) found silver traps to be the superior color, and this was reflected by my catch success as only one population was successfully caught with black traps as opposed to two sites in the northern loop where silver traps were used. Dip nets were successful in shallow water streams where traps or seine nets were not appropriate. Having all three fishing methods available throughout the field sampling campaign was key in being able to catch stickleback in various habitat types and new (unpublished) locations.

Standard length of stickleback differed between the sexes, with females being slightly larger than males, and gravid females being longer than non-mature females. Slight sexual dimorphism between the sexes were noticeable as males were consistently smaller across all populations, however large males which were similar in size to the largest females were also found. Mature females were consistently larger than non-mature females likely because they

need to reach a minimum size and developmental state to be able to reproduce. Stickleback usually reach maturity after one full year of life and only after ingesting enough food to convert biomass into developing eggs (Bell and Foster 1994). Stickleback spawn and develop most during the warm summer months, which coincides with the time of highest primary productivity, and thus, the most available food (Bell and Foster 1994). Males were consistently the smallest sex, and in Bergen and Trondheim, no males were sampled. This could be due to either a low abundance in that environment, or to sampling bias since for large fish.

When comparing standard length across sampling locations, stickleback showed a clear pattern of decreasing length with increasing latitude. The largest (mean and median) stickleback were found in Sylt, Germany, whereas the smallest fish were located in the two most northerly sites of Vesterålen and Alta. Bergmann's Rule postulated by the German biologist Carl Bergmann in 1847 describes how animals increase in mass towards higher latitudes (Bergmann 1847). Bergmann's theory states that larger, endothermic animals have a smaller surface area to volume ratio to better protect against heat loss, and thus energy expenditure. Fish are ectothermic and do not fit into this model, and instead are theorized to increase in size towards northern latitudes due to higher fecundity and more selective mate selection due to longer gestation times (Wilson 2009). However, fish vary from Bergmann's Rule much more than endothermic mammals due to many other factors such as competition and foraging success, bottom water temperatures, and ecosystem richness (Fisher *et al.,* 2010). My results for stickleback standard length show the opposite pattern to Bergmann's rule (see also Geist 1987; Fisher *et al.,* 2010). The most common argument against this theory is that body size is primarily a function of how long the organism has unrestricted access to quality food (Geist 1987). Northern populations could have less competition from other species occupying a similar niche (e.g. lower overall biodiversity), which could aid certain species in foraging success. While it is impossible to identify the root cause of declining stickleback size with increasing latitude, field observations suggest there was a decline in the environmental richness (e.g. structural habitat complexity) and biodiversity as latitude increased. Additionally, northern latitudes experience higher variability in daily sunlight than in the south where it is more moderate. Sunlight intensity promotes primary production in plankton

and plants which fuels ecosystem productivity. It is likely that a combination of these factors were working in concert to reduce stickleback standard length with increasing latitude.

4.2 Sex-specific and Site-specific Expression of Epigenetic Genes

DNMT1 expression in gonads did not differ between the sexes, but DNMT3ab showed higher expression in males than in females and gravid females. Neither TET1 nor TET3 expression in gonads differed between males and females, however, TET1 expression appeared to be higher in gravid females than in males or females. As a promoter of DNA methylation, DNMT1 and DNMT3ab levels are typically elevated wherever higher amounts of methylation occur (Metzger and Schulte 2016). In half smooth tongue sole, warmer temperatures during development skew sex-ratios in favor of males due to the promotion of Doublesex and mab-3 related transcription factor 1 (Dmrt1) (Chen *et al.,* 2014). When Dmrt1 expression is present in male gonads, it is related to higher levels of DNA methylation, whereas higher expression of Dmrt1 in female gonads is related to increased methylation (Wen *et al.,* 2014). In mammalian embryos, it has been observed that a global loss of methylation occurs around the ninth day of development due to active demethylation by TET3 (Gu *et al.,* 2011). If TET3 were found to be elevated in gravid females (potentially detectable with a larger sample size), than this could reflect the methylation patterns in the developing embryos. DNA methylation in European sea bass gonads are promoted, in part, by Gonadal Aromatase (cyp19a), and its expression during early development can influence sex ratios (Navarro-Martin *et al.,* 2011). Cyp19a is less methylated in male gonads than females, and some genetic females with very high levels of DNA Methylation developed into males (Navarro-Martin *et al*. 2011). In this study, expression of the DNA methylation promoter DNMT3ab was higher in males, and TET1, a demethylation promoter, was also higher in males compared to females. This suggests that overall gonad methylation was higher in males than females, a result that was also shown by Navarro-Martin *et al*. (2011) in their study of sex ratio variation caused by DNMTs.

Expression of the DNA methylation target genes in gonad tissue showed inconsistent patterns across the sampled populations. For instance, gravid females had higher expression of TET1 and TET3 in Bergen, and higher expression of TET3 in Alta. DNMT1 expression was much

higher in Mo i Rana than any other population, which is interesting because the Mo i Rana population also showed higher expression of TET1 and TET3, particularly in gravid females. This could mean that methylation in gonads is more stable in the Mo i Rana population due to a lack of expression of genes which have the potential to cause methylation change. DNMT1 enzymes can act as a maintenance methyltransferase, and facilitate preservation of methylation (Kim *et al.,* 2015). DMNT3ab is responsible for *de* novo methylation and its absence (or expression suppression) can cause global genome methylation patterns to be removed entirely (Goll and Bestor 2005). In addition to Mo i Rana and Alta populations being the northernmost sites, they also had the lowest salinities, which could influence gonad methylation. DNA methylation of the internal organs of fish can be affected by ambient salinity conditions, as Li *et al.,* (2017) found in liver tissue of the half smooth tongue sole. They found that epigenetic mechanisms were more expressed during antagonistic conditions, such as abnormal salinity stress (Li *et al.,* 2017). This suggests that fish that are not well adapted or acclimated to a particular salinity gradient could undergo more salinity damage, and thus have a different methylation pattern altogether. In this study, stickleback populations might have shown elevated expression for DNA methylation and demethylation genes in response to a less varied salinity gradient. For example, the Mo i Rana area, which had lower expression of methylation genes could reflect a more variable salinity environment.

Expression levels of DNMT1 and DNMT3ab in pectoral fin muscle did not significantly differ between the sexes, however, these two genes appeared to show slightly higher expression in males than in females and gravid females. DNMT3ab expression overall appeared to be absent from many of the stickleback, with less than half of all replicates expressing the gene. TET1 and TET3 both followed a similar trend to DNMT1 and DNMT3ab with similar expression levels between females and gravid females and slightly higher expression in males. However, sex-specific differences in gene expression in pectoral fin muscle samples may be due, in part, to the housekeeping gene showing differences in expression based on sex (Annex table 8.4). DNMTs and TETs expression in pectoral muscle could be related to metabolic epigenetic modifications (Lu and Thompson 2012). DNMTs methylate S-adensoyl methionine, which together with S-adensoyl homocysteine metabolizes carbon, and thus can be affected by levels of expression (Lu

and Thompson 2012). Moreover, additional DNA methyltransferases were shown to turn off skeletal muscle genes during periods of low energy in the green striped burrowing frog (Hudson *et al.,* 2008). Regulation of DNMTs can lower organism metabolism to ensure that the organism survives harsh conditions that would otherwise drain energy through a constant metabolism. In northern latitudes, a lack of primary production in the winter could cause food shortages and increase the need for DNMTs expression in pectoral muscle.

DNA methylation and demethylation target gene expression in pectoral muscle showed no clear pattern across populations. The demethylation gene TET1 was less expressed in the northern populations of Mo i Rana and Alta than in the southern populations of Sylt and Bergen. However, TET3 had higher expression in Mo i Rana and higher expression in females from Alta than from Sylt and Bergen, with Bergen showing particularly less TET3 expression. DNMT3ab was less expressed in Mo i Rana and Bergen males, although these results are likely affected by a low amplification of DNMT3ab throughout the populations, in pectoral muscle as well as in the gonads. In these cases, the housekeeping gene used for pectoral muscle was significantly affected by sex and site, which could introduce a potential bias to the results. Nevertheless, the lack of successful DNMT3ab amplifications could also be due to a lack of expression throughout the populations which only a presence/absence survey could pick up. Expression of target genes for methylation in pectoral muscle reflect that in males, expression of DNMT1 was similar for the three southernmost populations, but had the lowest expression at the northernmost population, Alta. While these results could be affected by the housekeeping gene expression, there is also previous research suggesting that warmer water, such as those in lower latitudes, have lower levels of myogenin, a gene involved with the formation of skeletal muscle (Burgerhout *et al.,* 2017). Myogenin acts as a DNA methylation promoter in muscle tissue and its expression can elevate DNA methyltransferases such as DNMT1 and DNMT3ab (Campos *et al.,* 2013). Myogenin in teleost fish can vary with temperature, and during development is significantly higher expressed in warmer ambient temperatures than in colder waters (Fernandes *et al.,* 2006). Burgerhout *et al.* (2017) demonstrated how the relationship between thermal phenotypic plasticity and epigenetic variation can affect muscle growth and development in fish. Due to the wide range of yearly temperature maximums (Figure 3.2) in this study's southern populations,

stickleback development occurring at these temperatures could result in variation in the expression of DNA methyltransferases in the pectoral muscle.

MacroH2A expression in gonads did not differ between the sexes, but appeared to show lower expression in gravid females that in females or males. In pectoral muscle, there was sex-specific expression of MacroH2A, with higher expression in males than in either females or gravid females. MacroH2A modifies the protein histone (into histone variants) and has been shown (from gonad tissue) to reduce deformations of embryogenesis in zebrafish (Buschbeck *et al.,* 2009). MacroH2A is also involved with X chromosome inactivation, particularly in female zebrafish, with the purpose of regulating 'silent chromatin' regions of the chromosome that are not actively being transcribed (Buschbeck *et al.,* 2010). In female mammals that have two X chromosomes, one chromosome is always silenced, and MacroH2A1 has been found to be preferentially expressed in the silenced chromosome (Costanzi and Pehrson 1998). MacroH2A also plays a role in cold acclimatization, and research by Pinto *et al.* (2005) suggests that it is used in reorganizing chromatin and controlling other gene's expression during that time. Through this function, it could be expected to see higher expression of MacroH2A in northern populations than southern ones. Results from this study did not find significant differences in MacroH2A expression based on latitude, but more populations may be needed to detect these effects.

Sirtuin expression in gonad tissue was not significant between the sexes, however visual observation of the data suggests that expression was higher in gravid female than in non-gravid females. Research by Pereira *et al.* (2011) studying Sirtuin2 expression in adult zebrafish found male gonads to have higher expression than female gonads. Sirtuin2 expression in female gonads was lower in the southern populations of Sylt and Bergen than in the northern populations of Mo i Rana and Alta. Sirtuin2 expression in pectoral muscle also differed by site and sex. Overall, the Sylt population had lower expression of Sirtuin2 than Alta, whereas Bergen and Mo i Rana had an intermediate level. Male stickleback appeared to have slightly higher expression of Sirtuin2 (in pectoral muscle). Pereira *et al.* (2011) found Sirtuin2 expression in skeletal muscle to be quite low comparative to other zebrafish internal organs, having lower expression than gonads, brain, heart, and liver. Sirtuin2 is a homologous gene found throughout many species of fish, insects, and mammals that is involved with the regulation of metabolism and can affect aging (Kelly

2010). Sirtuin is found commonly in connective tissue and cytoplasm, and can show increased expression during periods of fasting (Kelly 2010). Additionally, Sitruin2 is related to cold acclimation in stickleback, and transcript levels increase in response to cold temperatures (Teigen *et al.,* 2015). Sirtuin achieves this is by protecting against oxidative stress, regulating metabolism, and potentially inducing heat shock proteins to refold damaged proteins (Wang *et al.,* 2007; Orczewska *et al.,* 2010). In pectoral muscle, Sirtuin2 expression decreases or stays constant in response to cold water, whereas other tissues vary with different intensities (Teigen *et al.,* 2015). It is likely that stickleback would express Sirtuin2 more in northern populations where cold acclimatization is necessary, than in in southern populations.

5. Conclusion

Threespine stickleback have been known to be present throughout the northern temperate region of the Atlantic Ocean, and indeed, populations were found in almost every coastal region studied across northern Germany, Denmark, and Norway. Stickleback appeared to show large intraspecies variation in size across the latitudinal gradient studied. Male stickleback were consistently smaller than females, and gravid females which were ready to reproduce were larger than non-gravid females. Between populations, average standard length could be seen as a product of growth rate and development, and stickleback were found to be significantly larger in lower latitudes and shorter in higher latitudes. While the low average temperatures remain relatively constant in these oceans, the maximum summer temperature drops as latitude increases, decreasing the total range of ambient water temperatures marine stickleback experience. Thermal regimes, amount of yearly sunlight, nutrient availability, and ecosystem complexity could all potentially factor into the reasons for the pattern of smaller body size in northern latitudes that were found.

Plasticity underlain by epigenetic mechanisms in stickleback have played an important role in their ability to colonize a wide range of temperatures and salinities around the world. In

particular, the ability to acclimate to cold water temperatures has enabled further northward expansion. DNA methyltransferases can promote new methylation and maintain previous patterns of methylation that can be passed on to future generations. Some trends were found, such as gonads from Mo i Rana having the lowest expression of methylation promoters and demethylators, possibly raising methylation stability in that population. Male gonads had higher expressions of DNMTs and TETs which could then increase methylation plasticity since the genes that turn the methylation of cytosine on and off is so highly expressed. Additionally, DNMT3ab appeared to be the least expressed gene studied with less than half of all samples expressing it. Sirtuin2 was found to be most expressed in the two northern populations of Mo i Rana and Alta than the southern populations. This is a reasonable result because Sirtuin2 is a gene involved with cold acclimation and can be theorized to be more useful for fish in colder ambient temperatures than in warmer waters. While MacroH2A did not show differences in expression based on site, its role in cold acclimation as well could be theorized to be present in northern populations wherever other genes for cold acclimatization are found.

This research is the first to study epigenetic expression in a fish population over a latitudinal gradient. Future research into epigenetic patterns across latitude could benefit from an increased sample size for target genes to be tested on. Additionally, other environmental variables such as light intensity and nutrient availability could be specifically tested for to determine potential environmental parameters underlying epigenetic variations between populations. Stickleback is a good model species due to its widespread occurrence throughout the Northern coasts, and epigenetic research would benefit from more target gene expression studies in this species. As temperatures rise because of future climate change, stickleback will likely adapt via epigenetic mechanisms, and its continued survival could be based on its ability to do so.

6. Acknowledgements

I would like to thank the my supervisors, Dr. Lisa Shama and Dr. Rita Castilho for the generous support and assistant throughout my Master's thesis. Thank you to the Alfred Wegener Institute for their help and support including use of their vehicle, laboratories, and office space for the completion of this thesis. I am grateful to the University of Oslo and Dr. Hans Erik Carlson for the use of their boat, field station, and housing in Drøbak, Norway. Additionally, I want to thank Nord University and Dr. Joost Raeymakers for their support in northern Norway, including use of their vehicle, nets, and traps. Finally, many thanks to the dedicated students who personally accompanied me on the fieldwork in Norway and participated in catching stickleback and aiding in dissection; Alexandre Fellous, Carl Bukowski, Jørgen Hetzler, Thijs Bal, and Camela Haddad.

7. References

Aure, J., Dahl, E., Danielssen, D. S., & Søiland, H. (2000). CHATTONELLA–en ny skadelig alge i norske kystfarvann. *Fisken og Havet, Særnummer*, 2-2000.

Barrett, R. D., Paccard, A., Healy, T. M., Bergek, S., Schulte, P. M., Schluter, D., & Rogers, S. M. (2010). Rapid evolution of cold tolerance in stickleback. *Proceedings of the Royal Society B: Biological Sciences*, *278*(1703), 233-238.

Bateson, P., Barker, D., Clutton-Brock, T., Deb, D., D'Udine, B., Foley, R. A., ... & McNamara, J. (2004). Developmental plasticity and human health. *Nature*, *430*(6998), 419.

Beitinger, T. L., Bennett, W. A., & McCauley, R. W. (2000). Temperature tolerances of North American freshwater fishes exposed to dynamic changes in temperature. *Environmental biology of fishes*, *58*(3), 237-275.

Bell, M. A., & Foster, S. A. (1994). Introduction to the evolutionary biology of the threespine stickleback. *The evolutionary biology of the threespine stickleback*, *1*, 27.

Bell, M. A., Orti, G., Walker, J. A., & Koenings, J. P. (1993). Evolution of pelvic reduction in threespine stickleback fish: a test of competing hypotheses. *Evolution*, *47*(3), 906-914.

Bergmann C (1847) Über die verhältnisse der wärmeökonomie der thiere zu ihrer grösse. *Göttinger Studien, 1*, 595–708.

Bergstrom, C. A. (2002). Fast-start swimming performance and reduction in lateral plate number in threespine stickleback. *Canadian Journal of Zoology*, *80*(2), 207-213.

Boeuf, G., & Payan, P. (2001). How should salinity influence fish growth?. *Comparative Biochemistry and Physiology Part C: Toxicology & Pharmacology*, *130*(4), 411-423.

Borzenkova, I., Zorita, E., Borisova, O., Kalniņa, L., Kisielienė, D., Koff, T., ... & Subetto, D. (2015). Climate change during the Holocene (past 12,000 years). In *Second assessment of climate change for the Baltic Sea basin* (pp. 25-49). Springer, Cham.

Britschgi, A., Bill, A., Brinkhaus, H., Rothwell, C., Clay, I., Duss, S., … Bentires-Alj, M. (2013). Calcium-activated chloride channel ANO1 promotes breast cancer progression by activating EGFR and CAMK signaling. *Proceedings of the National Academy of Sciences, 110*(11), E1026–E1034.

Burgerhout E, Mommens M, Johnsen H, Aunsmo A, Santi N, Andersen Ø (2017) Genetic background and embryonic temperature affect DNA methylation and expression of myogenin and muscle development in Atlantic salmon (Salmo salar). *PLoS ONE 12*(6): e0179918.

Buschbeck, M., & Di Croce, L. (2010). Approaching the molecular and physiological function of macroH2A variants. *Epigenetics, 5*(2), 118–123.

Buschbeck, M., Uribesalgo, I., Wibowo, I., Rué, P., Martin, D., Gutierrez, A., … Di Croce, L. (2009). The histone variant macroH2A is an epigenetic regulator of key developmental genes. *Nature Structural & Molecular Biology, 16*(10), 1074–1079.

Caldera, E. J., & Bolnick, D. I. (2008). Effects of colonization history and landscape structure on genetic variation within and among threespine stickleback (Gasterosteus aculeatus) populations in a single watershed. Evolutionary Ecology Research, 10(4), 575-598.

Campos, C., Valente, L., Conceição, L., Engrola, S., & Fernandes, J. (2013). Temperature affects methylation of the myogenin putative promoter, its expression and muscle cellularity in Senegalese sole larvae. *Epigenetics*, *8*(4), 389-397.

Carr, S. J., Holmes, R., van der Meer, J. J. M., & Rose, J. (2006). The Last Glacial Maximum in the North Sea Basin: micromorphological evidence of extensive glaciation. Journal of Quaternary Science, 21(2), 131–153

Chan, Y. F., Marks, M. E., Jones, F. C., Villarreal, G., Shapiro, M. D., Brady, S. D., ... & Myers, R. M. (2010). Adaptive evolution of pelvic reduction in sticklebacks by recurrent deletion of a Pitx1 enhancer. *science*, *327*(5963), 302-305.

Chen, B., Feder, M. E., & Kang, L. (2018). Evolution of heat-shock protein expression underlying adaptive responses to environmental stress. *Molecular Ecology, 27*(15), 3040–3054.

Chen, S., Zhang, G., Shao, C., Huang, Q., Liu, G., Zhang, P., ... & Hong, Y. (2014). Whole-genome sequence of a flatfish provides insights into ZW sex chromosome evolution and adaptation to a benthic lifestyle. *Nature genetics*, *46*(3), 253.

Christensen, K. H., Sperrevik, A. K., & Broström, G. (2018). On the Variability in the Onset of the Norwegian Coastal Current. *Journal of Physical Oceanography, 48*(3), 723–738.

Costanzi, C., Stein, P., Worrad, D., Schultz, R. & Pehrson, J. Histone macroH2A1 is concentrated in the inactive X chromosome of female preimplantation mouse embryos. *Development 127*, 2283–2289 (2000)

Dayal, A., Ng, S. F. J., & Grabner, M. (2019). Ca 2+-activated Cl− channel TMEM16A/ANO1 identified in zebrafish skeletal muscle is crucial for action potential acceleration. *Nature communications*, *10*(1), 115.

DeFaveri, J., Shikano, T., Shimada, Y., Goto, A., & Merilä, J. (2011). Global analysis of genes involved in freshwater adaptation in threespine sticklebacks (gasterosteus aculeatus). *Evolution, 65*(6), 1800–1807.

DeWitt, T. J., & Scheiner, S. M. (Eds.). (2004). *Phenotypic plasticity: functional and conceptual approaches*. Oxford University Press, 247.

Dietrich, M. A., Hliwa, P., Adamek, M., Steinhagen, D., Karol, H., & Ciereszko, A. (2018). Acclimation to cold and warm temperatures is associated with differential expression of male carp blood proteins involved in acute phase and stress responses, and lipid metabolism. *Fish & shellfish immunology*, *76*, 305-315.

Donaldson, M. R., Cooke, S. J., Patterson, D. A., & Macdonald, J. S. (2008). Cold shock and fish. *Journal of Fish Biology, 73*(7), 1491–1530.

Elias, S. A., Short, S. K., Nelson, C. H., & Birks, H. H. (1996). Life and times of the Bering land bridge. *Nature, 382*(6586), 60.

Enzor, L. A., Zippay, M. L., & Place, S. P. (2013). High latitude fish in a high CO2 world: synergistic effects of elevated temperature and carbon dioxide on the metabolic rates of Antarctic notothenioids. *Comparative Biochemistry and Physiology Part A: Molecular & Integrative Physiology, 164*(1), 154-161.

Fang, B., Merilä, J., Ribeiro, F., Alexandre, C. M., & Momigliano, P. (2018). Worldwide phylogeny of three-spined sticklebacks. *Molecular phylogenetics and evolution*, *127*, 613-625.

Farmer, D. M., & Freeland, H. J. (1983). The physical oceanography of Fjords. *Progress in Oceanography, 12*(2), 147–219.

Farmer, D. M., & Freeland, H. J. (1983). The physical oceanography of fjords. *Progress in oceanography*, *12*(2), 147-219.

Farrell, A. P., Hinch, S. G., Cooke, S. J., Patterson, D. A., Crossin, G. T., Lapointe, M., & Mathes, M. T. (2008). Pacific Salmon in Hot Water: Applying Aerobic Scope Models and Biotelemetry to Predict the Success of Spawning Migrations. *Physiological and Biochemical Zoology, 81*(6), 697–709.

Fellous, A., Labed-Veydert, T., Locrel, M., Voisin, A. S., Earley, R. L., & Silvestre, F. (2018). DNA methylation in adults and during development of the self-fertilizing mangrove rivulus, Kryptolebias marmoratus. *Ecology and evolution*, *8*(12), 6016-6033.

Feng, S., Cokus, S. J., Zhang, X., Chen, P. Y., Bostick, M., Goll, M. G., ... & Ukomadu, C. (2010). Conservation and divergence of methylation patterning in plants and animals. *Proceedings of the National Academy of Sciences*, *107*(19), 8689-8694.

Fernandes, J. M., MacKenzie, M. G., Wright, P. A., Steele, S. L., Suzuki, Y., Kinghorn, J. R., & Johnston, I. A. (2006). Myogenin in model pufferfish species: Comparative genomic analysis and thermal plasticity of expression during early development. *Comparative biochemistry and physiology Part D: Genomics and Proteomics*, *1*(1), 35-45.

Fernández-Torres, F., Martínez, P. A., & Olalla-Tárraga, M. Á. (2018). Shallow water ray-finned marine fishes follow Bergmann's rule. Basic and applied ecology, 33, 99-110.

Fisher, J. A., Frank, K. T., & Leggett, W. C. (2010). Breaking Bergmann's rule: truncation of Northwest Atlantic marine fish body sizes. *Ecology, 91*(9), 2499-2505.

Foster, S. A., Baker, J. A., & Bell, M. A. (2003). The case for conserving threespine stickleback populations: protecting an adaptive radiation. *Fisheries*, *28*(5), 10-18.

Frischknecht, M. (1993). The breeding colouration of male three-spined sticklebacks (Gasterosteus aculeatus) as an indicator of energy investment in vigour. *Evolutionary Ecology, 7*(5), 439-450.

Frost, M., Baxter, J. M., Buckley, P. J., Cox, M., Dye, S. R., & Withers Harvey, N. (2012). Impacts of climate change on fish, fisheries and aquaculture. *Aquatic Conservation: Marine and Freshwater Ecosystems, 22*(3), 331–336.

Fuller, P., K. Dettloff, and R. Sturtevant, 2019, *Gasterosteus aculeatus* Linnaeus, 1758: U.S. Geological Survey, Nonindigenous Aquatic Species Database

Gaspar-Maia, A., Qadeer, Z. A., Hasson, D., Ratnakumar, K., Adrian Leu, N., Leroy, G., … Bernstein, E. (2013). MacroH2A histone variants act as a barrier upon reprogramming towards pluripotency. *Nature Communications, 4*(1).

Geist, V. (1987). Bergmann's rule is invalid. *Canadian Journal of Zoology, 65*(4), 1035–1038. doi:10.1139/z87-164

Giannetto, A., Nagasawa, K., Fasulo, S., & Fernandes, J. M. O. (2013). Influence of photoperiod on expression of DNA (cytosine-5) methyltransferases in Atlantic cod. *Gene, 519*(2), 222–230.

Gibbons, T. C., Rudman, S. M., & Schulte, P. M. (2017). Low temperature and low salinity drive putatively adaptive growth differences in populations of threespine stickleback. *Scientific reports, 7(*1), 16766.

Giuliani, C., Bacalini, M. G., Sazzini, M., Pirazzini, C., Franceschi, C., Garagnani, P., & Luiselli, D. (2015). The epigenetic side of human adaptation: hypotheses, evidences and theories. *Annals of human biology*, *42*(1), 1-9.

Goll, M. G., & Bestor, T. H. (2005). Eukaryotic cytosine methyltransferases. *Annu. Rev. Biochem.*, *74*, 481-514.

Gomez-Pinilla, P. J., Gibbons, S. J., Bardsley, M. R., Lorincz, A., Pozo, M. J., Pasricha, P. J., … Farrugia, G. (2009). Ano1 is a selective marker of interstitial cells of Cajal in the human and mouse gastrointestinal tract. *American Journal of Physiology-Gastrointestinal and Liver Physiology, 296(*6), G1370–G1381.

Grosell, M. (2006). Intestinal anion exchange in marine fish osmoregulation. *Journal of Experimental Biology, 209*(15), 2813–2827.

Gu, T. P., Guo, F., Yang, H., Wu, H. P., Xu, G. F., Liu, W., ... & Iqbal, K. (2011). The role of Tet3 DNA dioxygenase in epigenetic reprogramming by oocytes. *Nature*, *477*(7366), 606.

Hanson, M., Godfrey, K. M., Lillycrop, K. A., Burdge, G. C., & Gluckman, P. D. (2011). Developmental plasticity and developmental origins of non-communicable disease: theoretical considerations and epigenetic mechanisms. *Progress in biophysics and molecular biology*, *106*(1), 272-280.

Hansson, T. H., Fischer, B., Mazzarella, A. B., Voje, K. L., & Vøllestad, L. A. (2016). Lateral plate number in low-plated threespine stickleback: a study of plasticity and heritability. Ecology and evolution, 6(10), 3154-3160.

Harris, M. P., Rohner, N., Schwarz, H., Perathoner, S., Konstantinidis, P., & Nüsslein-Volhard, C. (2008). Zebrafish eda and edar mutants reveal conserved and ancestral roles of ectodysplasin signaling in vertebrates. *PLoS genetics*, *4*(10), e1000206.

He, Y. F., Li, B. Z., Li, Z., Liu, P., Wang, Y., Tang, Q., ... & Sun, Y. (2011). Tet-mediated formation of 5-carboxylcytosine and its excision by TDG in mammalian DNA. *Science*, *333*(6047), 1303-1307.

Herden, J., Eckert, S., Stift, M., Joshi, J., & van Kleunen, M. (2019). No evidence for local adaptation and an epigenetic underpinning in native and non-native ruderal plant species in Germany. *Ecology and evolution*.

Hordoir, R., Dieterich, C., Basu, C., Dietze, H., & Meier, H. E. M. (2013). Freshwater outflow of the Baltic Sea and transport in the Norwegian current: A statistical correlation analysis based on a numerical experiment. *Continental Shelf Research*, *64*, 1-9.

Hudson, N. J., Lonhienne, T. G. A., Franklin, C. E., Harper, G. S., & Lehnert, S. A. (2008). Epigenetic silencers are enriched in dormant desert frog muscle. *Journal of Comparative Physiology B*, *178*(6), 729-734.

Huey, R. B., & Bennett, A. F. (1990). Physiological adjustments to fluctuating thermal environments: an ecological and evolutionary perspective. *Stress proteins in biology and medicine*, *19*, 37-59.

Huntingford, F. A., Lazarus, J., Barrie, B. D., & Webb, S. (1994). A dynamic analysis of cooperative predator inspection in sticklebacks. *Animal Behaviour, 47*(2), 413–423.

Ices (1983). Flushing times of the North Sea*. Coop, Research Report, 123*. pp.159

Iida, Y., Hibiya, K., Inohaya, K., & Kudo, A. (2014). Eda/Edar signaling guides fin ray formation with preceding osteoblast differentiation, as revealed by analyses of the medaka all-fin less mutant afl. *Developmental Dynamics*, *243*(6), 765-777.

International Council for the Exploration of the Sea (2007). The Barents Sea and the Norwegian Sea (PDF). ICES Advice 2007

IPCC in Climate Change. (2013): The Physical Science Basis. Contribution of Working Group I to the Fifth Assessment Report of the Intergovernmental Panel on Climate Change. *Cambridge Univ. Press, 1535.*

IPCC. (2018) Summary for Policymakers. In: Global Warming of 1.5°C. An IPCC Special Report on the impacts of global warming of 1.5°C above pre-industrial levels and related global greenhouse gas emission pathways, in the context of strengthening the global response to the threat of climate change, sustainable development, and efforts to eradicate poverty. *In Press*.

Iwama, G. K., Thomas, P. T., Forsyth, R. B., & Vijayan, M. M. (1998). Heat shock protein expression in fish. *Reviews in Fish Biology and Fisheries*, *8*(1), 35-56.

Jin, X., Shah, S., Liu, Y., Zhang, H., Lees, M., Fu, Z., ... & Zhang, H. (2013). Activation of the Cl− channel ANO1 by localized calcium signals in nociceptive sensory neurons requires coupling with the IP3 receptor. *Sci. Signal., 6*(290), ra73-ra73.

Jobling, M. A. L. C. O. L. M. (1997, January). Temperature and growth: modulation of growth rate via temperature change. In *Seminar series-society for experimental biology* (Vol. 61, pp. 225-254). Cambridge University Press.

Johannes, F., & Schmitz, R. J. (2019). Spontaneous epimutations in plants. *New Phytologist*, *221*(3), 1253-1259.

Jones, F. C., Grabherr, M. G., Chan, Y. F., Russell, P., Mauceli, E., Johnson, J., ... & Birney, E. (2012). The genomic basis of adaptive evolution in threespine sticklebacks. *Nature, 484*(7392), 55.

Kelly, G. (2010). A review of the sirtuin system, its clinical implications, and the potential role of dietary activators like resveratrol: part 1. *Alternative medicine review, 15*(3).

Kim, B.-M., Mirbahai, L., Mally, A., Kevin Chipman, J., Rhee, J.-S., & Lee, J.-S. (2015). Correlation between the DNA methyltransferase (Dnmt) gene family and genome-wide 5-methylcytosine (5mC) in rotifer, copepod, and fish. *Genes & Genomics, 38*(1), 13–23.

Kim, J. M., Sasaki, T., Ueda, M., Sako, K., & Seki, M. (2015). Chromatin changes in response to drought, salinity, heat, and cold stresses in plants. Frontiers in Plant Science, 6, 114.

Kingsolver, J. G., Higgins, J. K., & Augustine, K. E. (2015). Fluctuating temperatures and ectotherm growth: distinguishing non-linear and time-dependent effects. *Journal of Experimental Biology*, *218*(14), 2218-2225.

Klepaker, T., Østbye, K., & Bell, M. A. (2013). Regressive evolution of the pelvic complex in stickleback fishes: a study of convergent evolution.

Kohli, R. M., & Zhang, Y. (2013). TET enzymes, TDG and the dynamics of DNA demethylation. *Nature, 502*(7472), 472–479.

Kristjánsson, B. K. (2005). Rapid morphological changes in threespine stickleback, Gasterosteus aculeatus, in freshwater. *Environmental Biology of Fishes, 74*(3-4), 357-363.

Lambert, A., Huang, J., van der Kamp, G., Henton, J., Mazzotti, S., James, T. S., ... & Barr, A. G. (2013). Measuring water accumulation rates using GRACE data in areas experiencing glacial isostatic adjustment: The Nelson River basin. *Geophysical Research Letters*, *40*(23), 6118-6122.

Le Rouzic, A., Østbye, K., Klepaker, T. O., Hansen, T. F., Bernatchez, L., Schluter, D., & VØLLESTAD, L. A. (2011). Strong and consistent natural selection associated with armour reduction in sticklebacks. *Molecular ecology*, *20*(12), 2483-2493.

Lee, C. E., & Bell, M. A. (1999). Causes and consequences of recent freshwater invasions by saltwater animals. *Trends in Ecology & Evolution, 14*(7), 284–288.

Lescak, E. A., Marcotte, R. W., Kenney, L. A., von Hippel, F. A., Cresko, W. A., Sherbick, M. L., … Andrés López, J. (2014). Admixture of ancient mitochondrial lineages in three-spined stickleback populations from the North Pacific. Journal of Biogeography, 42(3), 532–539.

Levine, M. T., Eckert, M. L., & Begun, D. J. (2010). Whole-genome expression plasticity across tropical and temperate Drosophila melanogaster populations from Eastern Australia. *Molecular biology and evolution*, *28*(1), 249-256.

Li, S., He, F., Wen, H., Li, J., Si, Y., Liu, M., ... & Meng, L. (2017). Low salinity affects cellularity, DNA methylation, and mRNA expression of igf1 in the liver of half smooth tongue sole (Cynoglossus semilaevis). *Fish physiology and biochemistry, 43*(6), 1587-1602.

Li, S., He, F., Wen, H., Li, J., Si, Y., Liu, M., ... & Meng, L. (2017). Low salinity affects cellularity, DNA methylation, and mRNA expression of igf1 in the liver of half smooth tongue sole (Cynoglossus semilaevis). *Fish physiology and biochemistry*, *43*(6), 1587-1602.

Li, T., Vu, T. H., Ulaner, G. A., Littman, E., Ling, J. Q., Chen, H. L., ... & Hoffman, A. R. (2005). IVF results in de novo DNA methylation and histone methylation at an Igf2-H19 imprinting epigenetic switch. *Molecular human reproduction*, *11*(9), 631-640.

Lindquist, S. (1986). The heat-shock response. *Annual review of biochemistry*, *55*(1), 1151-1191.

Liu, S., Hansen, M. M., & Jacobsen, M. W. (2016). Region-wide and ecotype-specific differences in demographic histories of threespine stickleback populations, estimated from whole genome sequences. Molecular Ecology, 25(20), 5187–5202

Loehr, J., Leinonen, T., Herczeg, G., O'Hara, R. B., & Merilä, J. (2012). Heritability of asymmetry and lateral plate number in the threespine stickleback. *PLoS One*, *7*(7), e39843.

Long, Y., Song, G., Yan, J., He, X., Li, Q., & Cui, Z. (2013). Transcriptomic characterization of cold acclimation in larval zebrafish. *BMC genomics, 14*(1), 612.

Lu, C., & Thompson, C. B. (2012). Metabolic regulation of epigenetics. *Cell metabolism*, *16*(1), 9-17.

Mäkinen, H. S., Cano, J. M., & Merilä, J. (2006). Genetic relationships among marine and freshwater populations of the European three-spined stickleback (Gasterosteus aculeatus) revealed by microsatellites. *Molecular Ecology, 15*(6), 1519–1534

Malik, H. S., & Henikoff, S. (2003). Phylogenomics of the nucleosome. *Nature Structural & Molecular Biology, 10(*11), 882–891.

Marchinko, K. B. (2009). Predation's role in repeated phenotypic and genetic divergence of armor in threespine stickleback. *Evolution: International Journal of Organic Evolution*, *63*(1), 127-138.

Martin, P. A., Green, R. E., & Balmford, A. (2019). The biodiversity intactness index may underestimate losses. *Nature ecology & evolution*, *3*(6), 862.

McGhee, K. E., & Bell, A. M. (2014). Paternal care in a fish: epigenetics and fitness enhancing effects on offspring anxiety. *Proceedings of the Royal Society B: Biological Sciences, 281(1794), 20141146–20141146.*

Merilä, J. (2015). Baiting improves CPUE in nine-spined stickleback (Pungitius pungitius) minnow trap fishery. *Ecology and Evolution, 5*(17), 3737–3742.

Merilä, J., Lakka, H.-K., & Eloranta, A. (2013). Large differences in catch per unit of effort between two minnow trap models. *BMC Research Notes, 6*(1), 151.

Milinski, M., & Bakker, T. C. (1992). Costs influences sequential mate choice in sticklebacks, gasterosteus aculeatus. *Proceedings of the Royal Society of London. Series B: Biological Sciences*, *250*(1329), 229-233.

Milinski, M., K¨lling, D., & Kettler, R. (1990). Tit for Tat: sticklebacks (Gasterosteus aculeatus) "trusting" a cooperating partner. *Behavioral Ecology, 1*(1), 7–11.

Miller, S. E., Barrueto, M., & Schluter, D. (2017). A comparative analysis of experimental selection on the stickleback pelvis. Journal of Evolutionary Biology, 30(6), 1165–1176

Morris, M. R., Richard, R., Leder, E. H., Barrett, R. D., Aubin-Horth, N., & Rogers, S. M. (2014). Gene expression plasticity evolves in response to colonization of freshwater lakes in threespine stickleback. *Molecular ecology*, *23*(13), 3226-3240.

Munk, W. (2003). Ocean freshening, sea level rising. *Science*, *300*(5628), 2041-2043.

Navarro-Martín, L., Viñas, J., Ribas, L., Díaz, N., Gutiérrez, A., Di Croce, L., & Piferrer, F. (2011). DNA methylation of the gonadal aromatase (cyp19a) promoter is involved in temperature-dependent sex ratio shifts in the European sea bass. *PLoS genetics*, *7*(12), e1002447.

Nelson, T. C., Crandall, J. G., Ituarte, C. M., Catchen, J. M., & Cresko, W. A. (2019). Selection, linkage, and population structure interact to shape genetic variation among threespine stickleback genomes. *Genetics*, genetics-302261.

Nogueiras, R., Habegger, K. M., Chaudhary, N., Finan, B., Banks, A. S., Dietrich, M. O., … Tschöp, M. H. (2012). Sirtuin 1 and Sirtuin 3: Physiological Modulators of Metabolism. *Physiological Reviews, 92*(3), 1479–1514.

Núñez-Riboni, I., & Akimova, A. (2017). Quantifying the impact of the major driving mechanisms of inter-annual variability of salinity in the North Sea. *Progress in oceanography, 154*, 25-37.

O'Brown, N. M., Summers, B. R., Jones, F. C., Brady, S. D., & Kingsley, D. M. (2015). A recurrent regulatory change underlying altered expression and Wnt response of the stickleback armor plates gene EDA. Elife, 4, e05290.

Orczewska, J. I., Hartleben, G., & O'Brien, K. M. (2010). The molecular basis of aerobic metabolic remodeling differs between oxidative muscle and liver of threespine sticklebacks in response to cold acclimation. *American Journal of Physiology-Regulatory, Integrative and Comparative Physiology*, *299*(1), R352-R364.

Orti, G., Bell, M. A., Reimchen, T. E., & Meyer, A. (1994). Global Survey of Mitochondrial DNA Sequences in the Threespine Stickleback: Evidence for Recent Migrations. Evolution, 48(3), 608.

Ostlund-Nilsson, S., Mayer, I., & Huntingford, F. A. (2006). *Biology of the three-spined stickleback*. CRC press.

Palter, J. B. (2015). The Role of the Gulf Stream in European Climate. *Annual Review of Marine Science, 7*(1), 113–137.

Parmesan, C., & Yohe, G. (2003). A globally coherent fingerprint of climate change impacts across natural systems. *Nature, 421*(6918), 37–42.

Pereira, R. J., Sasaki, M. C., & Burton, R. S. (2017). Adaptation to a latitudinal thermal gradient within a widespread copepod species: the contributions of genetic divergence and phenotypic plasticity. *Proceedings of the Royal Society B: Biological Sciences*, *284*(1853), 20170236.

Pereira, T. C. B., Rico, E. P., Rosemberg, D. B., Schirmer, H., Dias, R. D., Souto, A. A., … Bogo , M. R. (2011). *Zebrafish as a Model Organism to Evaluate Drugs Potentially Able to Modulate Sirtuin Expression. Zebrafish, 8(1), 9–16.*

Perry, A. L., Low, P. J., Ellis, J. R., & Reynolds, J. D. (2005). Climate change and distribution shifts in marine fishes*. Science, 308*(5730), 1912-1915.

Pigliucci, M., Murren, C. J., & Schlichting, C. D. (2006). Phenotypic plasticity and evolution by genetic assimilation. *Journal of Experimental Biology*, *209*(12), 2362-2367.

Pinto, R., Ivaldi, C., Reyes, M., Doyen, C., Mietton, F., Mongelard, F., ... & Vera, M. I. (2005). Seasonal environmental changes regulate the expression of the histone variant macroH2A in an eurythermal fish. *FEBS letters, 579*(25), 5553-5558.

Pinto, R., Ivaldi, C., Reyes, M., Doyen, C., Mietton, F., Mongelard, F., ... & Vera, M. I. (2005). Seasonal environmental changes regulate the expression of the histone variant macroH2A in an eurythermal fish. *FEBS letters*, *579*(25), 5553-5558.

Polyakov, I. V., Timokhov, L. A., Alexeev, V. A., Bacon, S., Dmitrenko, I. A., Fortier, L., ... & Laxon, S. (2010). Arctic Ocean warming contributes to reduced polar ice cap. *Journal of Physical Oceanography*, *40*(12), 2743-2756.

Portner, H. O., & Knust, R. (2007). Climate Change Affects Marine Fishes Through the Oxygen Limitation of Thermal Tolerance. *Science, 315*(5808), 95–97.

Pörtner, H. O., Lucassen, M., & Storch, D. (2005). Metabolic biochemistry: its role in thermal tolerance and in the capacities of physiological and ecological function. *Fish physiology*, *22*, 79-154.

Raeymaekers, J. A. M., Maes, G. E., Audenaert, E., & Volckaert, F. A. M. (2005). Detecting Holocene divergence in the anadromous-freshwater three-spined stickleback (Gasterosteus aculeatus) system. Molecular Ecology, 14(4), 1001–1014.

Ravinet, M., Takeuchi, N., Kume, M., Mori, S., & Kitano, J. (2014). Comparative analysis of Japanese three-spined stickleback clades reveals the Pacific Ocean lineage has adapted to freshwater environments while the Japan Sea has not. *PLoS One*, *9*(12), e112404

Reimchen, T. E. (1994). Predators and morphological evolution in threespine stickleback. *The evolutionary biology of the threespine stickleback*, 240-276.

Reusch, T. B. H., Wegner, K. M., & Kalbe, M. (2001). Rapid genetic divergence in postglacial populations of threespine stickleback (Gasterosteus aculeatus): the role of habitat type, drainage and geographical proximity. *Molecular ecology*, *10*(10), 2435-2445.

Rhines, P., Häkkinen, S., & Josey, S. A. (2008). Is oceanic heat transport significant in the climate system?. In *Arctic–subarctic ocean fluxes* (pp. 87-109). Springer, Dordrecht.

Richards, C. L., Bossdorf, O., & Pigliucci, M. (2010). What role does heritable epigenetic variation play in phenotypic evolution?. BioScience, 60(3), 232-237.

Ruiz, C., Martins, J. R., Rudin, F., Schneider, S., Dietsche, T., Fischer, C. A., ... & Kunzelmann, K. (2012). Enhanced expression of ANO1 in head and neck squamous cell carcinoma causes cell migration and correlates with poor prognosis. *PloS one, 7*(8), e43265.

Rundle, H. D., Nagel, L., Boughman, J. W., & Schluter, D. (2000). Natural selection and parallel speciation in sympatric sticklebacks. *Science, 287*(5451), 306-308.

Samuk, K., Owens, G. L., Delmore, K. E., Miller, S. E., Rennison, D. J., & Schluter, D. (2017). Gene flow and selection interact to promote adaptive divergence in regions of low recombination. Molecular Ecology, 26(17), 4378–4390

Scartascini, F. L., Sáez, M., & Volpedo, A. V. (2015). Otoliths as a proxy for seasonality: The case of Micropogonias furnieri from the northern coast of San Matías Gulf, Río Negro, Patagonia, Argentina. *Quaternary international*, *373*, 136-142.

Schluter, D. (2010). Resource Competition and Coevolution in Sticklebacks. *Evolution: Education and Outreach, 3(*1), 54–61.

Schuur, E. A. G., McGuire, A. D., Schädel, C., Grosse, G., Harden, J. W., Hayes, D. J., … Vonk, J. E. (2015). Climate change and the permafrost carbon feedback. *Nature, 520*(7546), 171–179.

Shaffer, G., Olsen, S. M., & Pedersen, J. O. P. (2009). Long-term ocean oxygen depletion in response to carbon dioxide emissions from fossil fuels. *Nature Geoscience*, *2*(2), 105.

Shama, L. N. (2017). The mean and variance of climate change in the oceans: hidden evolutionary potential under stochastic environmental variability in marine sticklebacks. *Scientific reports*, *7*(1), 8889.

Shama, L. N., Mark, F. C., Strobel, A., Lokmer, A., John, U., & Mathias Wegner, K. (2016). Transgenerational effects persist down the maternal line in marine sticklebacks: gene expression matches physiology in a warming ocean. *Evolutionary Applications*, *9*(9), 1096-1111.

Shapiro, M. D., Marks, M. E., Peichel, C. L., Blackman, B. K., Nereng, K. S., Jónsson, B., ... & Kingsley, D. M. (2004). Genetic and developmental basis of evolutionary pelvic reduction in threespine sticklebacks. *Nature, 428*(6984), 717.

Song, J., Reichert, S., Kallai, I., Gazit, D., Wund, M., Boyce, M. C., & Ortiz, C. (2010). Quantitative microstructural studies of the armor of the marine threespine stickleback (Gasterosteus aculeatus). *Journal of structural biology, 171*(3), 318-331.

Soulet, G., Ménot, G., Bayon, G., Rostek, F., Ponzevera, E., Toucanne, S., ... & Bard, E. (2013). Abrupt drainage cycles of the Fennoscandian Ice Sheet. Proceedings of the National Academy of Sciences, 201214676.

Stanich, J. E., Gibbons, S. J., Eisenman, S. T., Bardsley, M. R., Rock, J. R., Harfe, B. D., … Farrugia, G. (2011). Ano1 as a regulator of proliferation. *American Journal of Physiology-Gastrointestinal and Liver Physiology, 301*(6), G1044–G1051.

Stenevik, E. K., & Sundby, S. (2007). Impacts of climate change on commercial fish stocks in Norwegian waters. *Marine Policy, 31*(1), 19–31.

Stroeven, A. P., Hättestrand, C., Kleman, J., Heyman, J., Fabel, D., Fredin, O., Jansson, K. N. (2016). Deglaciation of Fennoscandia. Quaternary Science Reviews, 147, 91–121.

Teacher, A. G., Shikano, T., Karjalainen, M. E., & Merilä, J. (2011). Phylogeography and genetic structuring of European nine-spined sticklebacks (Pungitius pungitius)—mitochondrial DNA evidence. PLoS One, 6(5), e19476.

Teigen, L. E., Orczewska, J. I., McLaughlin, J., & O'Brien, K. M. (2015). Cold acclimation increases levels of some heat shock protein and sirtuin isoforms in threespine stickleback. *Comparative Biochemistry and Physiology Part A: Molecular & Integrative Physiology*, *188*, 139-147.

Terekhanova, N. V., Logacheva, M. D., Penin, A. A., Neretina, T. V., Barmintseva, A. E., Bazykin, G. A., ... & Mugue, N. S. (2014). Fast evolution from precast bricks: genomics of young freshwater populations of threespine stickleback Gasterosteus aculeatus. *PLoS genetics*, *10*(10), e1004696.

Van Der Graaf, A., Wardenaar, R., Neumann, D. A., Taudt, A., Shaw, R. G., Jansen, R. C., ... & Johannes, F. (2015). Rate, spectrum, and evolutionary dynamics of spontaneous epimutations. *Proceedings of the National Academy of Sciences*, *112*(21), 6676-6681.

Varriale, A. (2014). DNA methylation, epigenetics, and evolution in vertebrates: facts and challenges. *International journal of evolutionary biology*, *2014*.

Varriale, A., & Bernardi, G. (2006). DNA methylation and body temperature in fishes. Gene, 385, 111-121.

Verdin, E., Hirschey, M. D., Finley, L. W. S., & Haigis, M. C. (2010). Sirtuin regulation of mitochondria: energy production, apoptosis, and signaling. *Trends in Biochemical Sciences, 35*(12), 669–675.

Walker, J. A. (1996). Principal components of body shape variation within an endemic radiation of threespine stickleback. In Advances in morphometrics (pp. 321-334). Springer, Boston, MA.

Wallace, E. W., Kear-Scott, J. L., Pilipenko, E. V., Schwartz, M. H., Laskowski, P. R., Rojek, A. E., ... & Airoldi, E. M. (2015). Reversible, specific, active aggregates of endogenous proteins assemble upon heat stress. *Cell*, *162*(6), 1286-1298.

Wang, F., Nguyen, M., Qin, F.X., Tong, Q., 2007. SIRT2 deacetylates FOXO3a in response to oxidative stress and caloric restriction. *Aging Cell 6*, 505–514.

Warren, R., VanDerWal, J., Price, J., Welbergen, J. A., Atkinson, I., Ramirez-Villegas, J., … Lowe, J. (2013). Quantifying the benefit of early climate change mitigation in avoiding biodiversity loss. *Nature Climate Change, 3*(7), 678–682.

Watanabe, K., Mori, S., & Nishida, M. (2003). Genetic relationships and origin of two geographic groups of the freshwater threespine stickleback,'Hariyo'. Zoological science, 20(2), 265-275.

Weber, C. M., & Henikoff, S. (2014). Histone variants: dynamic punctuation in transcription. *Genes & development, 28*(7), 672-682.

Wen, A. Y., You, F., Sun, P., Li, J., Xu, D. D., Wu, Z. H., ... & Zhang, P. J. (2014). CpG methylation of dmrt1 and cyp19a promoters in relation to their sexual dimorphic expression in the Japanese flounder Paralichthys olivaceus. *Journal of Fish Biology*, *84*(1), 193-205.

Wiig, E., Reseland, J. E., Østbye, K., Haugen, H. J., & Vøllestad, L. A. (2016). Variation in lateral plate quality in Threespine Stickleback from fresh, brackish and marine water: A micro-computed tomography study. PloS one, 11(10), e0164578.

Willacker, J. J., Von Hippel, F. A., Wilton, P. R., & Walton, K. M. (2010). Classification of threespine stickleback along the benthic–limnetic axis. *Biological Journal of the Linnean Society, 101*(3), 595-608.

WILSON, A. B. (2009). Fecundity selection predicts Bergmann's rule in syngnathid fishes. *Molecular Ecology, 18*(6), 1263–1272.

Yakovlev, I. A., Fossdal, C. G., & Johnsen, Ø. (2010). MicroRNAs, the epigenetic memory and climatic adaptation in Norway spruce. *New Phytologist*, *187*(4), 1154-1169.

Yakovlev, I. A., Lee, Y., Rotter, B., Olsen, J. E., Skrøppa, T., Johnsen, Ø., & Fossdal, C. G. (2014). Temperature-dependent differential transcriptomes during formation of an epigenetic memory in Norway spruce embryogenesis. *Tree genetics & genomes*, *10*(2), 355-366.

Yang, H., Liu, Y., Bai, F., Zhang, J. Y., Ma, S. H., Liu, J., ... & Guan, K. L. (2013). Tumor development is associated with decrease of TET gene expression and 5-methylcytosine hydroxylation. *Oncogene, 32*(5), 663.

Zachariah, R. M., & Rastegar, M. (2012). Linking epigenetics to human disease and Rett syndrome: the emerging novel and challenging concepts in MeCP2 research. *Neural plasticity*, *2012*.

Zentner, G. E., & Henikoff, S. (2013). Regulation of nucleosome dynamics by histone modifications. *Nature structural & molecular biology*, *20*(3), 259.

Zhang, C., Tong, C., Ludwig, A., Tang, Y., Liu, S., Zhang, R., & Zhao, K. (2018). Adaptive Evolution of the Eda Gene and Scales Loss in Schizothoracine Fishes in Response to Uplift of the Tibetan Plateau. *International journal of molecular sciences, 19*(10), 2953.

Zizzari, Z. V., & Ellers, J. (2014). Rapid shift in thermal resistance between generations through maternal heat exposure. *Oikos*, *123*(11), 1365-1370.

8. Annex

8.1 Housekeeping Gene Expression

Anova results of the 18S housekeeping gene expression in gonad: effects of site and sex were not statistically significant (Tables 8.1 and 8.2). The lack of statistical significance means that the housekeeping expression was not influenced in any way by the populations or sex of the samples, and thus, their ΔCt values can easily be compared.

Table 8.1. ANOVA results for expression of the housekeeping gene 18S in gonad tissue across four threespine stickleback populations (Site). Significant terms are highlighted in bold.

	Gonad				
	Df	Sum Sq	Mean Sq	F value	Pr(>F)
Site	3	29.01	9.671	0.737	0.531
Residuals	202	2649.49	13.116		

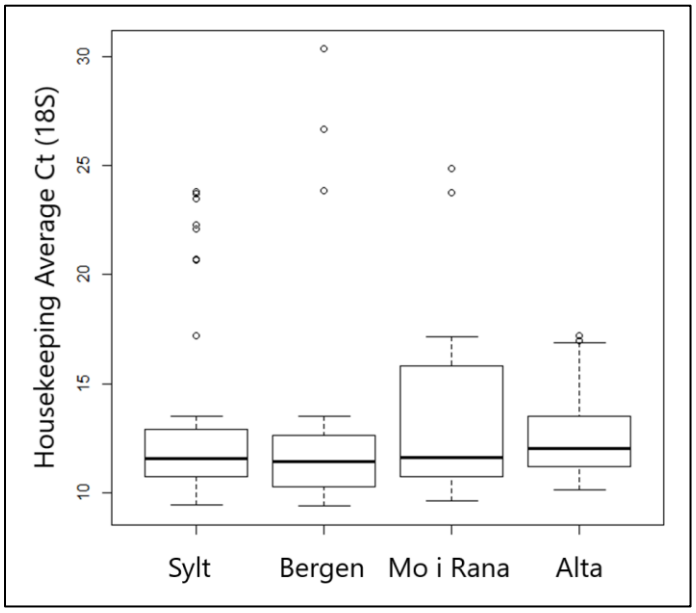

Figure 8.1. Box plot of median (and range) 18S expression averaged over gonads for all sexes across the four sampled populations. Populations are ordered on the x-axis with increasing latitude.

Table 8.2. ANOVA results for expression of the housekeeping gene 18S in gonad tissue across three threespine stickleback sexes (Sex). Significant terms are highlighted in bold.

	Gonad				
	Df	Sum Sq	Mean Sq	F value	Pr(>F)
Sex	2	66.23	33.114	2.573	0.079
Residuals	203	2612.27	12.868		

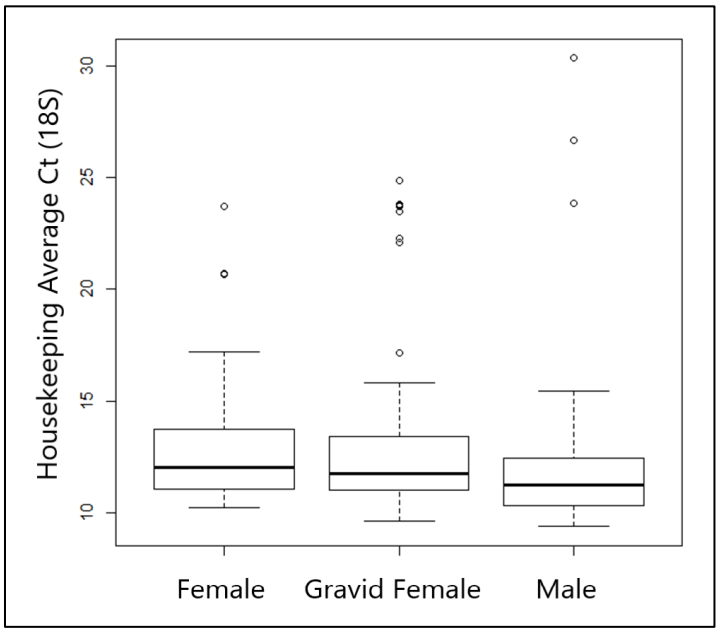

Figure 8.2. Box plot of median (and range) 18S expression in gonads for all sampled populations between the three sexes.

Anova results of all pectoral muscle housekeeping gene expression (18SRNA): site and sex significantly influenced expression (Tables 8.3 and 8.4). This is relevant because ΔCt values are calculated based on the difference between housekeeping expression and target gene expression. Because the housekeeping gene is affected by experiment factors, the ΔCt calculated for each gene could be skewed because of this. It is possible that a larger sample size would negate this affect. In Table 8.5, the mean expression of 18SRNA in the three sexes was compared by Tukey test. Results show that males and females, and males and gravid females were statistically differentially expressed. Females and gravid females were not statistically different from each other.

Table 8.3. ANOVA results for expression of the housekeeping gene 18SRNA in pectoral muscle tissue across four threespine stickleback populations (Site). Significant terms are highlighted in bold.

	Pectoral Muscle				
	Df	Sum Sq	Mean Sq	F value	Pr(>F)
Site	3	152.12	50.705	13.36	**<0.001**
Residuals	179	679.34	3.795		

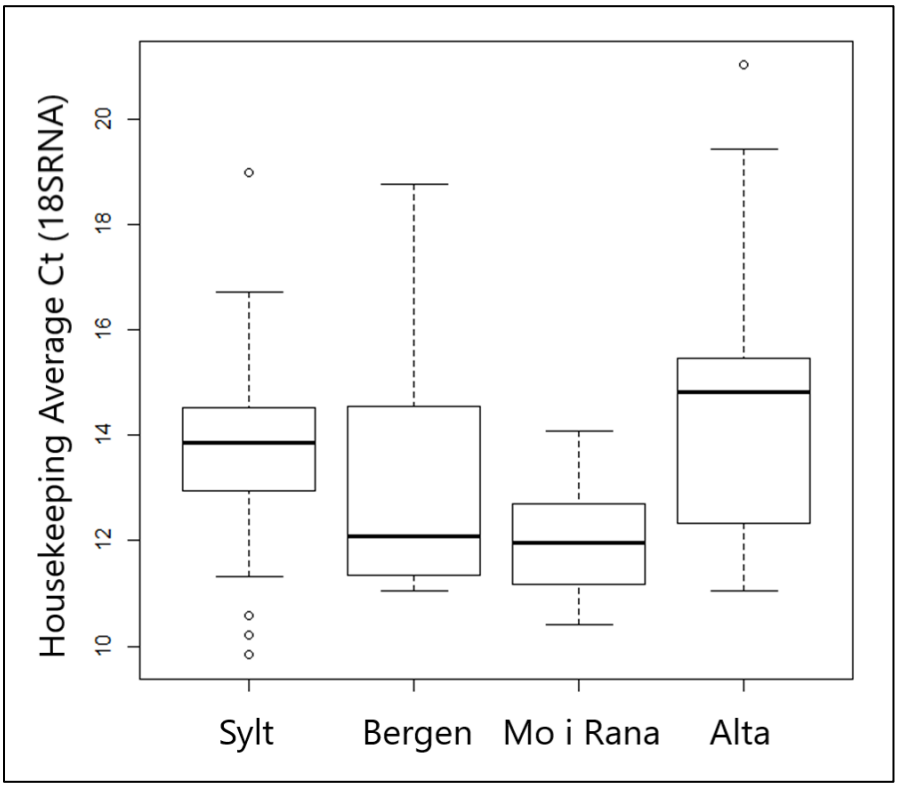

Figure 8.3. Box plot of median (and range) 18SRNA expression averaged over pectoral muscle for all sexes across the four sampled populations. Populations are ordered on the x-axis with increasing latitude.

Table 8.4. ANOVA results for expression of the housekeeping gene 18SRNA in pectoral muscle tissue across three threespine stickleback sexes (Sex). Significant terms are highlighted in bold.

	Pectoral Muscle				
	Df	Sum Sq	Mean Sq	F value	Pr(>F)
Sex	2	113.51	56.755	14.229	**<0.001**
Residuals	180	717.94	3.989		

Table 8.5. Tukey test contrasts, multiple comparisons of means for expression of the housekeeping gene 18SRNA in pectoral muscle tissue across threespine stickleback sexes (Sex). Significant terms are highlighted in bold.

	Pectoral Muscle			
	Estimate	Std. Error	t value	Pr(>F)
Male - Female	1.963	0.370	5.300	**<0.001**
Male – Gravid Female	-1.245	0.367	-3.397	**0.002**
Female – Gravid Female	0.718	0.352	2.041	0.105

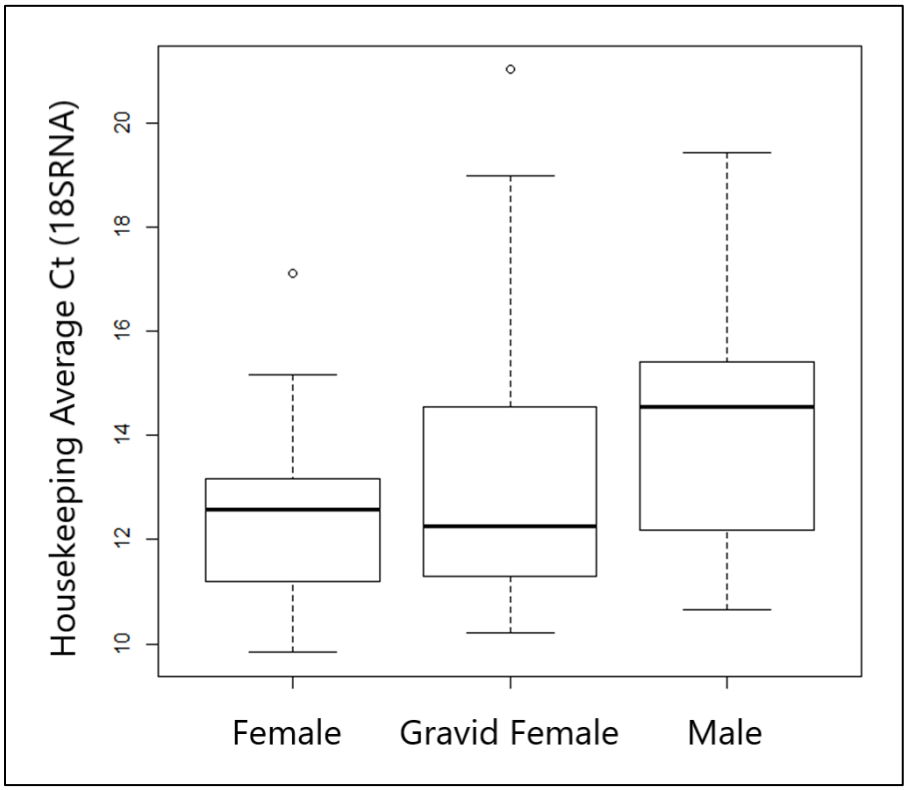

Figure 8.4. Box plot of median (and range) 18SRNA expression in pectoral muscle tissue for all sampled populations between the three sexes.

8.2 Target Gene Site by Sex Plots

Figures 8.5 through 8.15 are box plots showing the median and range for all target gene expression in gonads and pectoral muscle compared for all sites and sexes. Lack of data in the figures means no samples showed successful expression, and these were excluded from the analyses. Sections of some of the graphs below were used in the results section to highlight relationships of note. They are presented in their full form below.

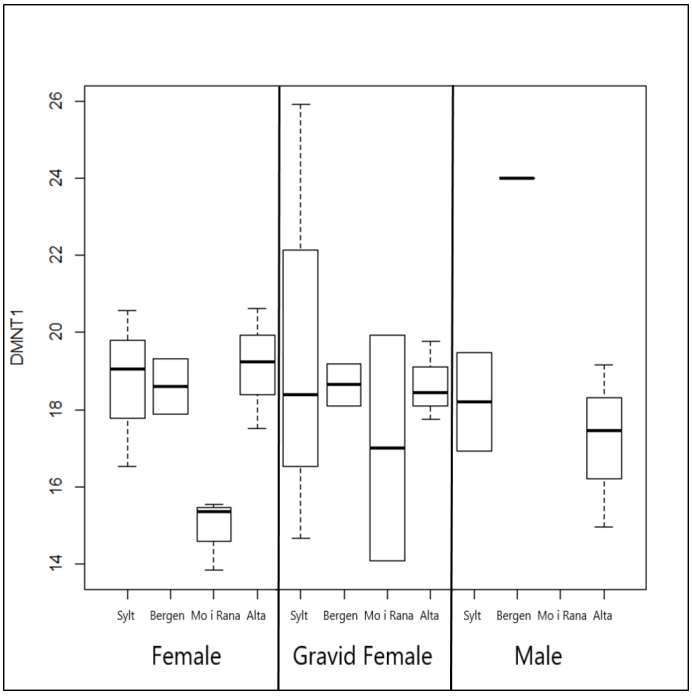

Figure 8.5. Box plot of median (and range) DNMT1 expression averaged over gonads for all sexes for each of the four sampled populations.

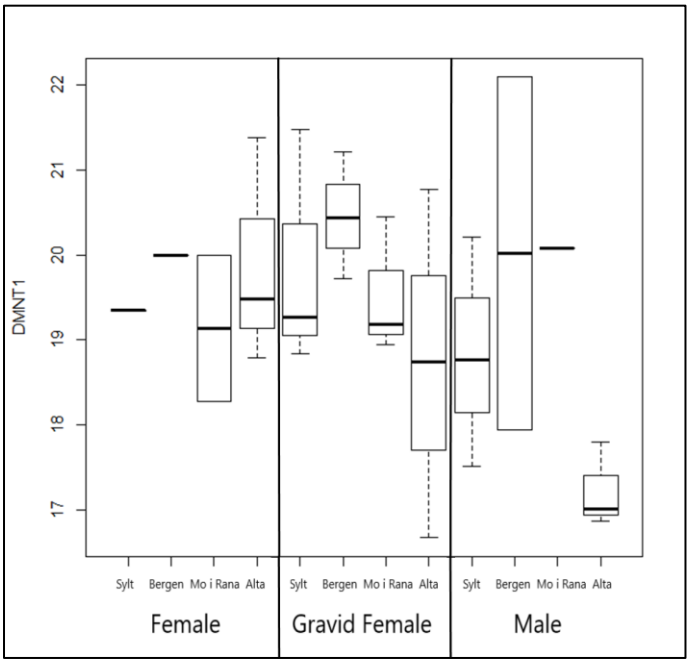

Figure 8.6. Box plot of median (and range) DNMT1 expression averaged over pectoral muscle for all sexes for each of the four sampled populations.

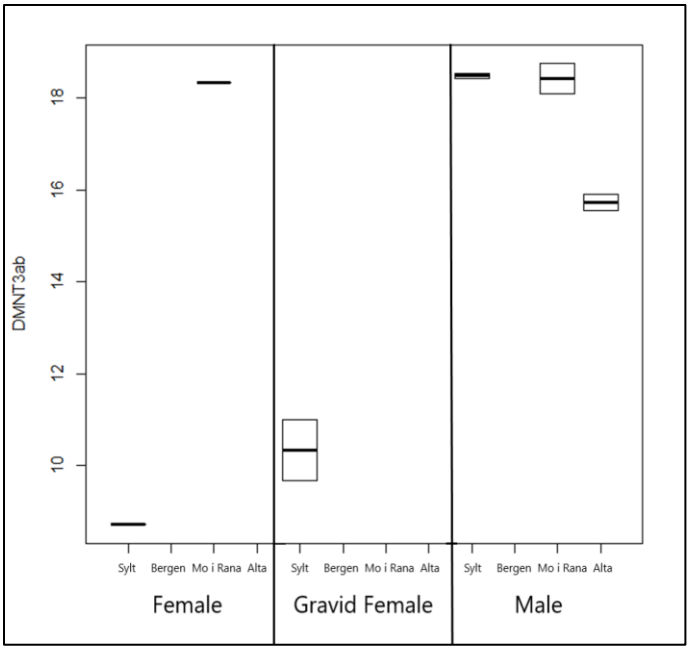

Figure 8.7. Box plot of median (and range) DNMT3ab expression averaged over gonads for all sexes for each of the four sampled populations.

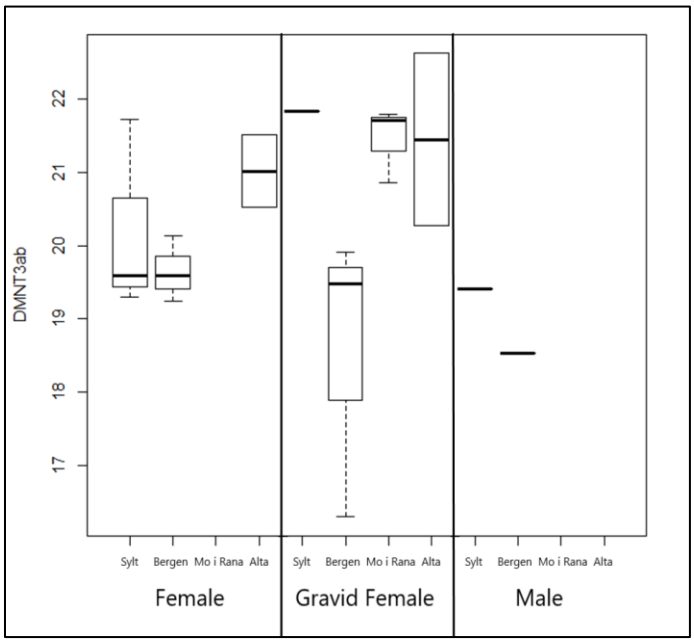

Figure 8.8. Box plot of median (and range) DNMT3ab expression averaged over pectoral muscle for all sexes for each of the four sampled populations.

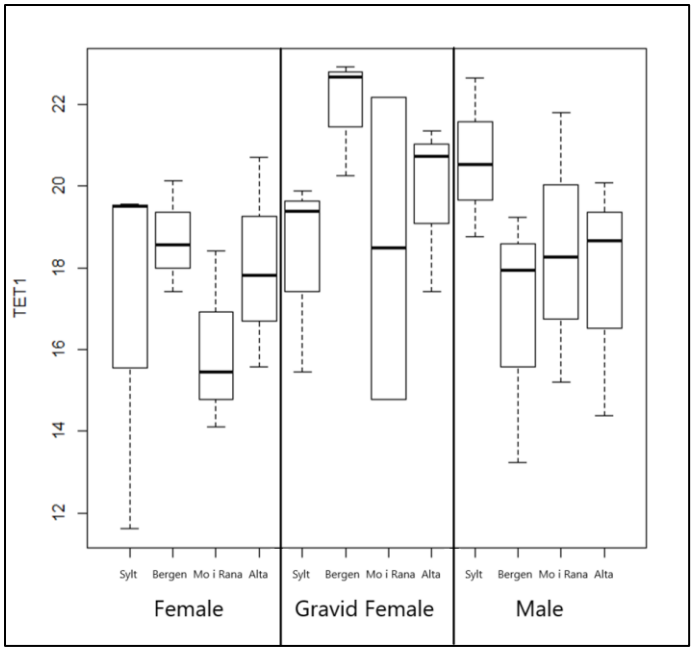

Figure 8.9. Box plot of median (and range) TET1 expression averaged over gonads for all sexes for each of the four sampled populations.

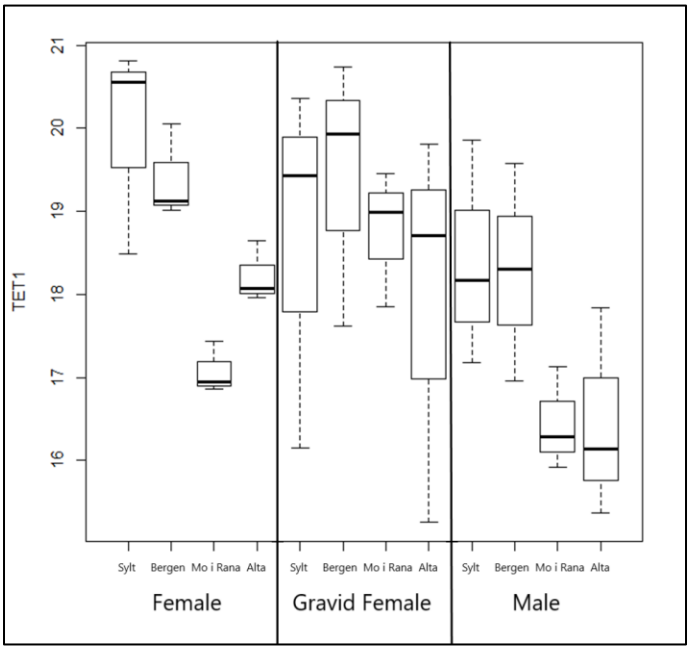

Figure 8.10. Box plot of median (and range) TET1 expression averaged over pectoral muscle for all sexes for each of the four sampled populations.

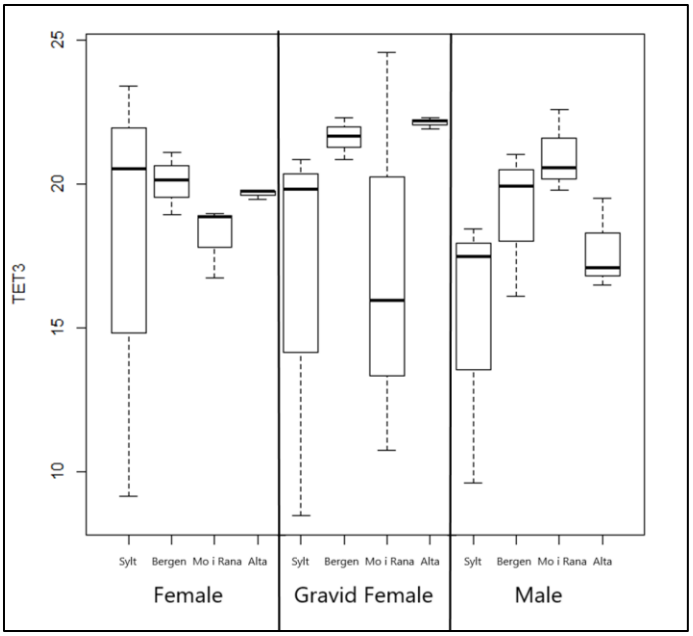

Figure 8.11. Box plot of median (and range) TET3 expression averaged over gonads for all sexes for each of the four sampled populations.

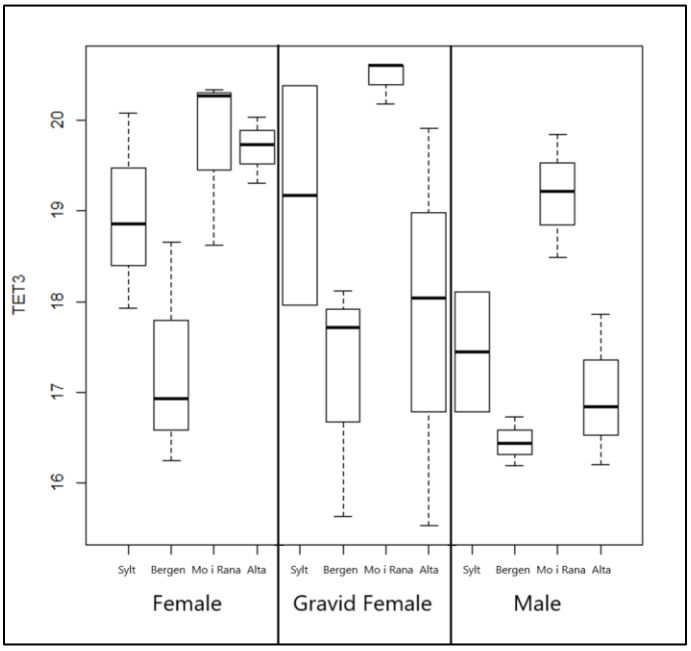

Figure 8.12. Box plot of median (and range) TET3 expression averaged over pectoral muscle for all sexes for each of the four sampled populations.

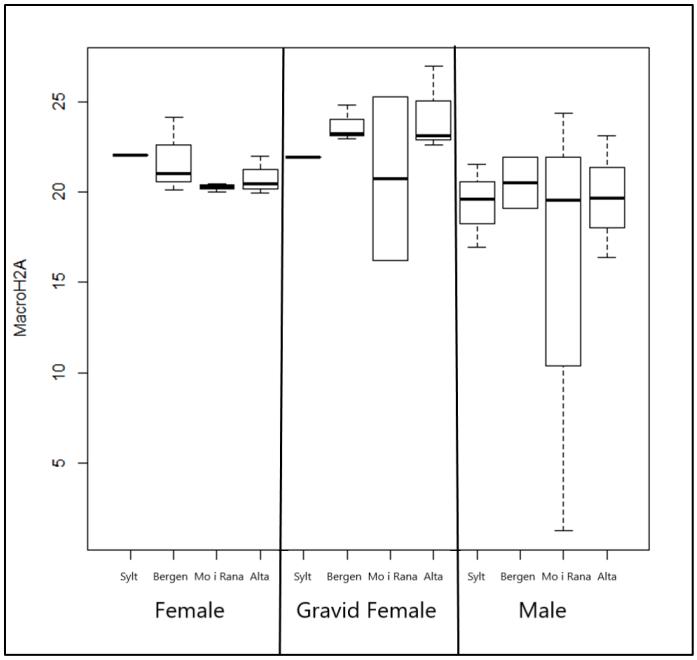

Figure 8.13. Box plot of median (and range) MacroH2A expression averaged over gonads for all sexes for each of the four sampled populations.

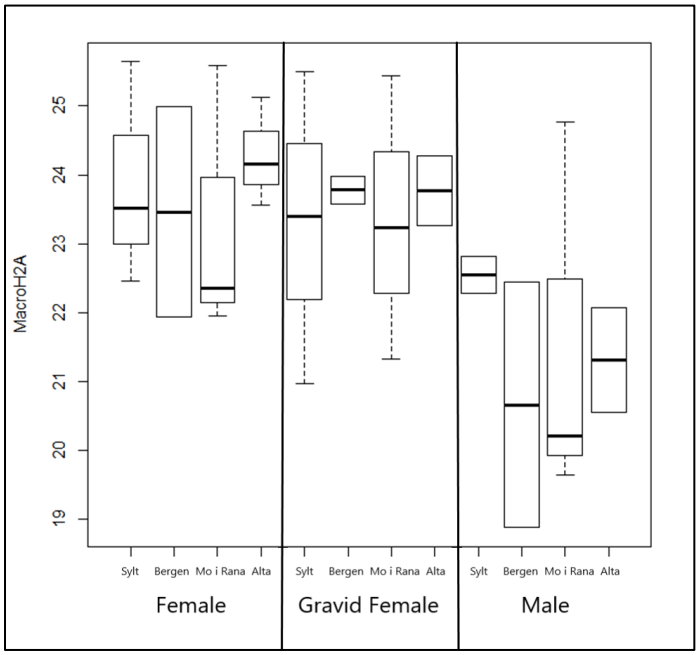

Figure 8.14. Box plot of median (and range) MacroH2A expression averaged over pectoral muscle for all sexes for each of the four sampled populations.

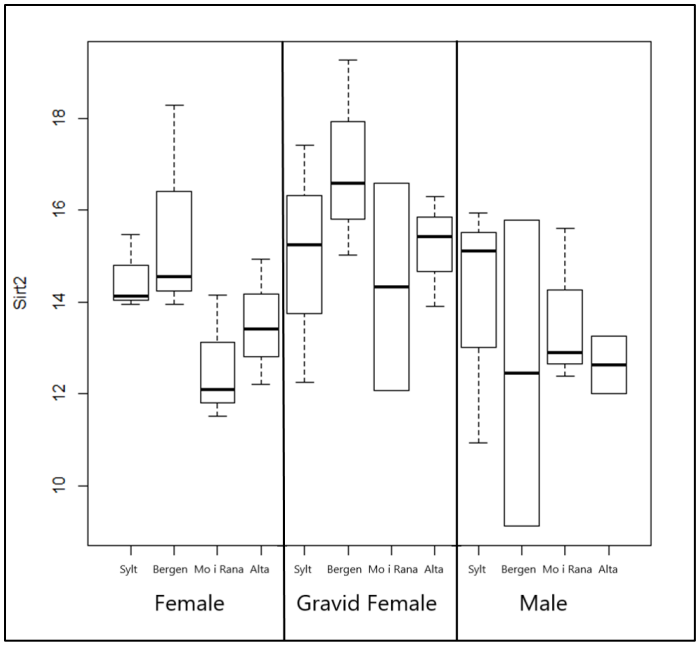

Figure 8.15. Box plot of median (and range) Sirt2 expression averaged over gonads for all sexes for each of the four sampled populations.

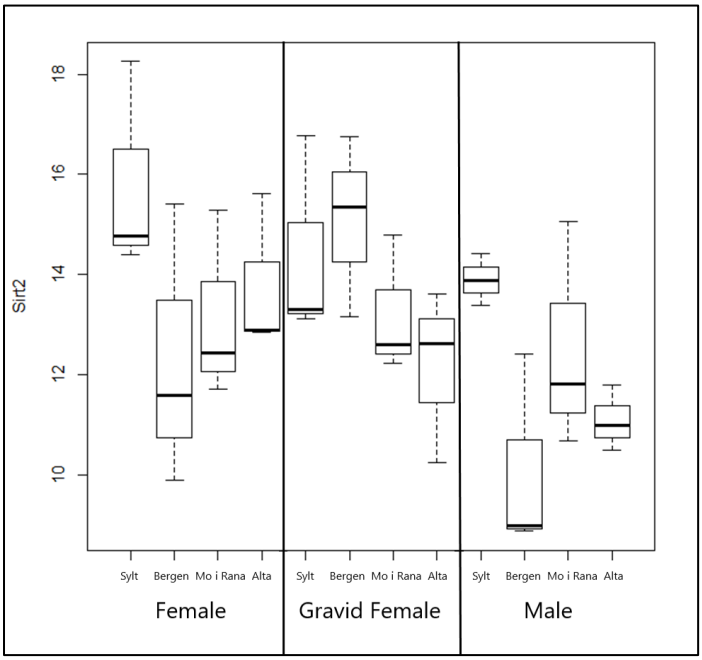

Figure 8.16. Box plot of median (and range) Sirt2 expression averaged over pectoral muscle for all sexes for each of the four sampled populations.

8.4 Target Gene Sequences

Table 8.6. Target Gene Sequences

Target Gene	Gene Sequence (5’ -> 3’)
DNMT1_1 (F)	ACAGCCAACCATCATGTCAA
DNMT1_1 (R)	AGTCGCCTCTGCATCATCTT
DNMT3ab_2 (F)	AAATCCTTTACGGAGGCTCT
DNMT3ab_2 (R)	GGAGGCTCTAAACCCTTTGG
TET1_2 (F)	TACAACCAGAGCACCAGCAG
TET1_2 (R)	CTGCTGGTGCTCTGGTTGTA
TET3_1 (F)	CTCCTAGCCCTCAGCCAAAT
TET3_1 (R)	CAGGATTGCTGTGCTTCAAA
MacroH2A_1 (F)	CGATCGAAGAGCAAGAAACC
MacroH2A_1 (R)	TGGTACGGACTCGTTGTCTG
Sirtuin2_1 (F)	TGCAGGAGACACAGAGATGG
Sirtuin2_1 (R)	GAGTCAGCTCGTCCAGAACC